UCLA
UCLA Electronic Theses and Dissertations

Title

New Methods for Lentiviral-Based Hematopoietic Stem Cell Gene Therapy

Permalink

https://escholarship.org/uc/item/2tx15553

Author

Masiuk, Katelyn

Publication Date

2019

Peer reviewed|Thesis/dissertation

UNIVERSITY OF CALIFORNIA

Los Angeles

New Methods for Lentiviral-Based Hematopoietic Stem Cell Gene Therapy

A dissertation submitted in partial satisfaction of the requirements for the

degree Doctor of Philosophy

in Molecular Biology

by

Katelyn Masiuk

2019

ABSTRACT OF THE DISSERTATION

New Methods for Lentiviral-Based Hematopoietic Stem Cell Gene Therapy

by

Katelyn Masiuk

Doctor of Philosophy in Molecular Biology

University of California, Los Angeles, 2016

Professor Donald Barry Kohn, Chair

ABSTRACT

Hematopoietic stem cell (HSC) transplant with gene therapy has recently emerged as a successful clinical treatment of a number of previously incurable genetic blood diseases. This approach aims to permanently fix genetic defects in HSCs, a rare and specialized type of cell with the unique ability to regenerate the entire blood system throughout a patient's lifetime. In this approach, bone marrow (BM) or mobilized peripheral blood (mPB) is collected from a patient, enriched for HSCs, transduced with an engineered lentiviral vector (LV) encoding the correct genetic sequence, and transplanted back into the patient. After transplant, modified HSCs engraft in the BM and produce healthy blood cells throughout the patient's lifetime.

While the last decade of research has yielded major advances including successful Phase I/II gene therapy clinical trials, clinical and commercial scaling of this technology to a broader range of patients and diseases has revealed a number of hurdles. One major limitation is the great expense and difficulty of producing clinical-grade LV, which I address in Chapters 2 and 3 by presenting two methods that improve the efficiency of LV transduction of HSC. In Chapter 4, I demonstrate the successful application of a new LV gene therapy for an autoimmune blood disease.

Chapter 2 presents a method to enhance the enrichment of HSCs from the heterogeneous cell population obtained from the collection of bone marrow cells, addressing a critical limitation in creating cost-effective, clinical-grade LV vector. This method utilizes immunomagnetic beads to purify CD34+CD38- cells, a population highly enriched for HSCs beyond standard CD34+ selection. Using immune-deficient xenograft models, we demonstrate that enrichment of CD34+CD38- cells reduces gene therapy culture scale and lentiviral vector requirements by ~10-fold while still maintaining the long-term gene-marked engraftment required for clinical benefit. Therefore, this strategy represents an easily translatable method which can conserve valuable clinical grade LV preparations and could lower the cost per patient, or allow for the treatment of a greater number of patients.

Chapter 3 presents a method to further improve HSC transduction efficiency with the use of two compounds: Prostaglandin E2 (PGE2) and poloxamer synperonic F108 (PS-F108). While transduction enhancement with each individual compound has previously been reported, the combination of these compounds leads to a synergistic and marked improvement in LV transduction of HSCs using a globin LV. Remarkably, this synergistic combination achieved a 6-fold improvement in gene transfer to long-term engrafting HSCs while using a LV dose 10-fold lower than the dose in our current clinical protocol. Thus this strategy has two major advantages: it reduces the amount of viral particles required to transduce HSCs, and also allows for better gene transfer and ultimate globin transgene expression, which is critical to improving clinical efficacy.

Finally, chapter 4 demonstrates the effectiveness of a newly engineered LV for the treatment of a severe form of genetic autoimmunity called IPEX syndrome. IPEX is caused by mutations in FoxP3, the key lineage-determining transcription factor required for the development and function of regulatory T cells (Treg cells). We developed a new LV using endogenous human FOXP3 regulatory elements to restore FoxP3 expression in a developmentally appropriate manner. We use this LV to transduce HSCs and restore functional Treg development in a mouse model of FoxP3 deficiency and successfully rescue

the autoimmune defects associated with this phenotype. These findings demonstrate preclinical efficacy for the treatment of IPEX patients by autologous HSC transplant and may provide further insight into new cell therapies for autoimmunity.

Collectively, the work described here advances the field of gene therapy by improving the efficiency of the manufacturing process and expanding the range of diseases which can be treated by this method.

The dissertation for Katelyn Masiuk is approved.

Gay M. Crooks

John P. Chute

Dinesh Rao

Jerome Zack

Donald Barry Kohn, Committee Chair

University of California, Los Angeles

2019

DEDICATION

This thesis is dedicated to two amazing women who have shaped my path:

My mother, Jan Masiuk, who has taught me that success in life is measured in many ways

and

Dr. Lauren Markell, the saint who taught me how to pipette

TABLE OF CONTENTS

LIST OF FIGURES AND TABLES

Chapter 4

ACKNOWLEDGEMENTS

I would first like to acknowledge my mentor, Don Kohn. His constant support, patience, encouragement, and sense of humor have made the seemingly daunting task of completing a PhD a truly remarkable experience that I would do all over again in a heartbeat. Don's incredible scientific career has spanned the entire development of hematopoietic stem cell gene therapy - from the early development of cell culture and viral production techniques to the very first gene therapy clinical trials. Most recently, he has lead successful clinical trials to cure dozens of "bubble babies" with ADA-SCID, representing a true clinical victory resulting from decades of science. It has not been lost on me how lucky I have been to be in the lab during this exciting time. It is my great hope that our first cured sickle patient is right around the corner!

Being a part of this process has been truly inspiring and has opened my eyes to the remarkable things that can be achieved through a career as a physician scientist. In addition to Don's direct mentorship, his dedication to his patients and passion for science is infectious, and has served as the foundation for the incredible team of talented, enthusiastic scientists who are inspired to work for him. I consider myself very privileged to have worked as a member of this incredible team. I never dreamed a PhD could be so enjoyable.

I would also like to acknowledge my other key mentor, Dr. Roger Hollis, for being my day-to-day resource in the lab. Roger has served as a tremendous wealth of knowledge on everything related to lentiviral vectors, and also as an endless source of laughs (and candy!) that brighten my day. I sincerely appreciate all of the help he has provided in guiding my projects and helping me to personally and professionally navigate my PhD journey.

all of the tremendous technical support and expertise in the lab, I made it through a PhD in the Kohn lab without ever cloning or packaging a vector (shhh, don't tell Don).

I will always be indebted to Felicia Codrea and Jessica Scholes at the FACS core for training me in the secret arts of flow cytometry (my favorite lab technique!), and for their continued help with all of my experiments. They are both so talented and truly stellar at what they do, and I greatly appreciate how hard they work to keep those fickle lasers and everybody's experiments running.

My MD/PhD classmates – John Thompson, Michael Liu, Shivani Thaker, Ernest Lee, Alex Sun, and Sophie Lewis – Thanks for serving as a constant source of support throughout all of the struggles that accompany pursuing such a daunting career path. I am sure there will be many more to come and I am lucky to have you guys by my side. You are some of the most brilliant people I have ever met, and even when we try to relax and have some drinks, I can't help but have the nerdiest conversations with you. I am truly grateful for your wonderful friendship and excited to have such talented colleagues in such a diverse array of clinical specialties.

To my mom and dad – Jan and Mike Masiuk - I wouldn't be where I am on this path without such incredible and supportive parents. You have always emphasized the importance of education, let me know that it's ok to march to the beat of my own drum, and have never let me doubt myself. Thanks for letting me hone the art of crafting carefully worded arguments when I was 14 (ha!) - it came in very useful when writing reviewers responses. It has been hard to move across the country from you, but I appreciate all of the phone calls and visits and how truly interested and engaged you are in my work.

And lastly, I'd like to thank my perfect husband Ted Present, who has supported my journey in every single way. Thanks for always celebrating my successes (and commiserating my failures) with a cocktail, for picking me up late at lab with sushi and chocolate, for listening to endless iterations of my presentations, removing excess verbiage from my grant proposals (be concise!), enduring cringe-worthy

personification of immune cells, and always encouraging me to strive for the best. You are a talented, enthusiastic scientist and you inspire my own passion for the work that I do - I can't wait to see where life takes us next!

EDUCATION

2012 - present	**David Geffen School of Medicine at UCLA**, Los Angeles, CA M.D. candidate, expected date of completion: June 2021 USMLE Step 1 Exam: Pass - 264 (June 2014)
2014 - present	**UCLA Molecular Biology Institute**, Los Angeles, CA Ph.D. candidate, expected date of completion: May 2019 Cumulative GPA: 3.83
2007 - 2011	**The Pennsylvania State University**, *Schreyer Honors College*, University Park, PA B.S. Biochemistry and Molecular Biology 2011, Valedictorian Cumulative GPA: 3.96

HONORS AND AWARDS

2018	Travel Award - European Society of Gene and Cellular Therapy
2018	Travel Award - Keystone Symposium: Emerging Cellular Therapeutics
2017-2018	Whitcome Fellowship in Molecular Biology, UCLA
2017	Abstract Achievement Award - 60th Annual American Society of Hematology
2016	Abstract Achievement Award - 59th Annual American Society of Hematology
2011	Wedler Award for Most Outstanding Honors Thesis in Biochemistry and Molecular Biology, The Pennsylvania State University
2007-2011	Braddock Scholar (full scholarship), The Pennsylvania State University
2007-2011	Schreyer Academic Excellence Scholarship, The Pennsylvania State University
2011	1st Place Abstract Award, Dermal Toxicology - Society of Toxicology
2010	DAAD (German Academic Exchange Service) Research Fellowship
2007	National Merit Scholar

PUBLICATIONS

Masiuk, KE, Laborada, J, Roncarolo, MG, Hollis, RP and Kohn, DB. Lentiviral Gene Therapy in HSCs Restores Lineage-Specific Foxp3 Expression and Suppresses Autoimmunity in a Mouse Model of IPEX Syndrome. Cell Stem Cell, 2019.

Masiuk KE, Campo-Fernandez B, Hollis RP, Kohn DB. PGE2 and Poloxamer-F108 Enhance Transduction of Human Hematopoietic Stem and Progenitor Cells with a β-Globin Lentiviral Vector. *Molecular Therapy Methods and Clinical Development*, in press, 2019.

Masiuk KE, Brown D, Laborada J, Hollis RP, Urbinati F, Kohn DB. Improving Gene Therapy Efficiency through the Enrichment of Human Hematopoietic Stem Cells. Mol Ther. 25(9):2163-2175, 2017.

Urbinati, F, Campo Fernandez, B, **Masiuk, KE**, Poletti, V, Hollis, RP, Koziol, C, Kaufman, ML, Brown, D, Mavilio, F and Kohn, DB Gene Therapy for Sickle Cell Disease: A Lentiviral Vector Comparison Study. Human gene therapy, 29(10), 1153-1166, 2018

Baldwin K, Urbinati F, Romero Z, Campo-Fernandez B, Kaufman ML, Cooper AR, **Masiuk K**, Hollis RP, and Kohn DB. Enrichment of Human Hematopoietic Stem/Progenitor Cells Facilitates Transduction for Stem Cell Gene Therapy. Stem Cells *33*(5), 1532-1542, 2015.

Padmakumar V, **Masiuk KE**, Luger D, Lee C, Coppola V, Tessarollo L, Hoover SB, Karavanova I, Buonanno A, Simpson RM, Yuspa SH. Detection of differential fetal and adult expression of chloride intracellular channel 4 (CLIC4) protein by analysis of a green fluorescent protein knock-in mouse line. BMC Developmental Biology 14.1: 24, 2014.

Padmakumar VC, Speer K, Pal-Ghosh S, **Masiuk KE**, Ryscavage A, Dengler SL, Hwang S, Edwards JC, Coppola V, Tessarollo L, Stepp MA, Yuspa SH. Spontaneous skin erosions and reduced skin and corneal wound healing characterize CLIC4(NULL) mice. Am J Pathol. 181(1):74-84, 2012.

Mordasky Markell L, **Masiuk KE**, Blazanin N, Glick AB. Pharmacological inhibition of ALK5 causes a cornification response in mouse keratinocytes expressing oncogenic HRas. Mol Cancer Res. 9:746, 2011.

Mordasky Markell L, Pérez-Lorenzo R, **Masiuk KE**, Kennett MJ, Glick AB. Use of a TGFbeta type I receptor inhibitor in mouse skin carcinogenesis reveals a dual role for TGFbeta signaling in tumor promotion and progression. Carcinogenesis. 31(12):2127-35, 2010.

ABSTRACTS

Masiuk, KE, Hollis, RP, Kohn, DB and Campo-Fernandez, B. (2018) dmPGE2 and poloxamer-F108 enhance transduction of human hematopoietic stem and progenitor cells with a beta-globin lentiviral vector. Human Gene Therapy 29(12) A36-A36. Presented at the European Society of Gene and Cellular Therapy 2018, Laussanne, Switzerland
- *Recipient of Abstract Achievement Award*

Masiuk, KE, Laborada, JL, Hollis, RP, Kohn DB. (2018) Hematopoietic Stem Cell Gene Therapy for IPEX Syndrome. Selected for oral presentation at Keystone Symposium on Emerging Cellular Therapeutics – T cells and Beyond, Keystone, Colorado.
- *Recipient of Abstract Achievement Award*

Masiuk, KE, Laborada, JL, Hollis, RP, Kohn DB. (2017) Development of a Treg Lineage Specific Lentiviral Vector for the Treatment of IPEX Syndrome. Blood 130:528. Selected for oral presentation at American Society of Hematology 2017, Atlanta, GA.

- *Recipient of Abstract Achievement Award*

Masiuk, KE, Brown, D, Urbinati, F, Hollis, RP, & Kohn, DB. (2016) Enrichment of Hematopoietic Stem Cells Using Immunomagnetic Beads to Facilitate Gene Therapy. Blood, 128(22), 2313. Presented at American Society of Hematology 2016, San Deigo, CA.
- *Recipient of Abstract Achievement Award*

Masiuk KE, Padmakumar VC, Coppola V, Tessarollo L, Yuspa SH. (2012) Skin erosions and extramedularry hematopoeisis in CLIC4-null mice. NIH Intramural Research Festival, Bethesda, MD.

Masiuk KE, Mordasky Markell L, Blazanin N, Glick AB. (2011) Pharmacological inhibition of the TGFβ type I receptor induces premalignant keratinocyte terminal differentiation. The Toxicologist 104 (1): # 222. Presented at 2011 Society of Toxicology Annual Meeting in Washington, D.C.
- *Recipient of Abstract Achievement Award*

Mordasky Markell L, Pérez-Lorenzo R, **Masiuk KE**, Glick AB. (2010) Use of a TGFb1 type I receptor inhibitor in mouse skin carcinogenesis reveals a dual role for TGFb1 signaling in tumor promotion and progression. International Skin Carcinogenesis Conference. State College, PA.

Mordasky Markell L, Pérez-Lorenzo R, **Masiuk KE**, Kwon H, Glick AB. (2010) Pharmacological inhibition of TGFβ1 signaling enhances malignant progression of chemically induced skin cancers through changes in inflammatory response. The Toxicologist 103 (1): # 671.

Chapter 1: Introduction

An overview of current techniques and limitations in hematopoietic stem cell gene therapy

Hematopoietic stem cells and blood cell production

Hematopoietic stem cells (HSCs) are rare cells that reside in the bone marrow and are tasked with the daily regeneration of billions of red and white blood cells produced throughout our lifetime. A healthy blood system produces red blood cells to carry oxygen, white blood cells to fight infections, and platelets to aid in blood clotting. However, a wide range of genetic mutations affect various cell types in the blood system, which impair these functions and result in severe disease. Thus, the overall goal of the field of hematopoietic stem cell gene therapy and the work outlined in this thesis is to correct genetic defects in patients' HSCs and restore proper functioning of the blood system.

As HSCs develop into mature blood cells, they go through many stages of maturation (Figure 1-1). An important distinction can be made between a hematopoietic stem and progenitor cell (HSC and HPC), which represent different phases of development. HSCs represent the earliest phase of development, can divide indefinitely (throughout the lifespan of an organism), and are capable of giving rise to all lineages of blood cells. HSCs divide very slowly, and can either self-renew (give rise to new stem cells), or differentiate into HPCs. HPCs divide rapidly in order to produce the high output of mature blood cells made in the body each day, yet these cells have a short lifespan (months to years). Because true HSCs are rare (less than 1 in 10,000 bone marrow cells), they cannot be directly isolated from the bone marrow. Thus the population of cells collected and enriched from the bone marrow to be used for transplant is a heterogenous mix referred to as hematopoietic stem and progenitor cells (HSPCs). However, modification and engraftment of true long-term HSCs is required for a durable clinical benefit with gene therapy.
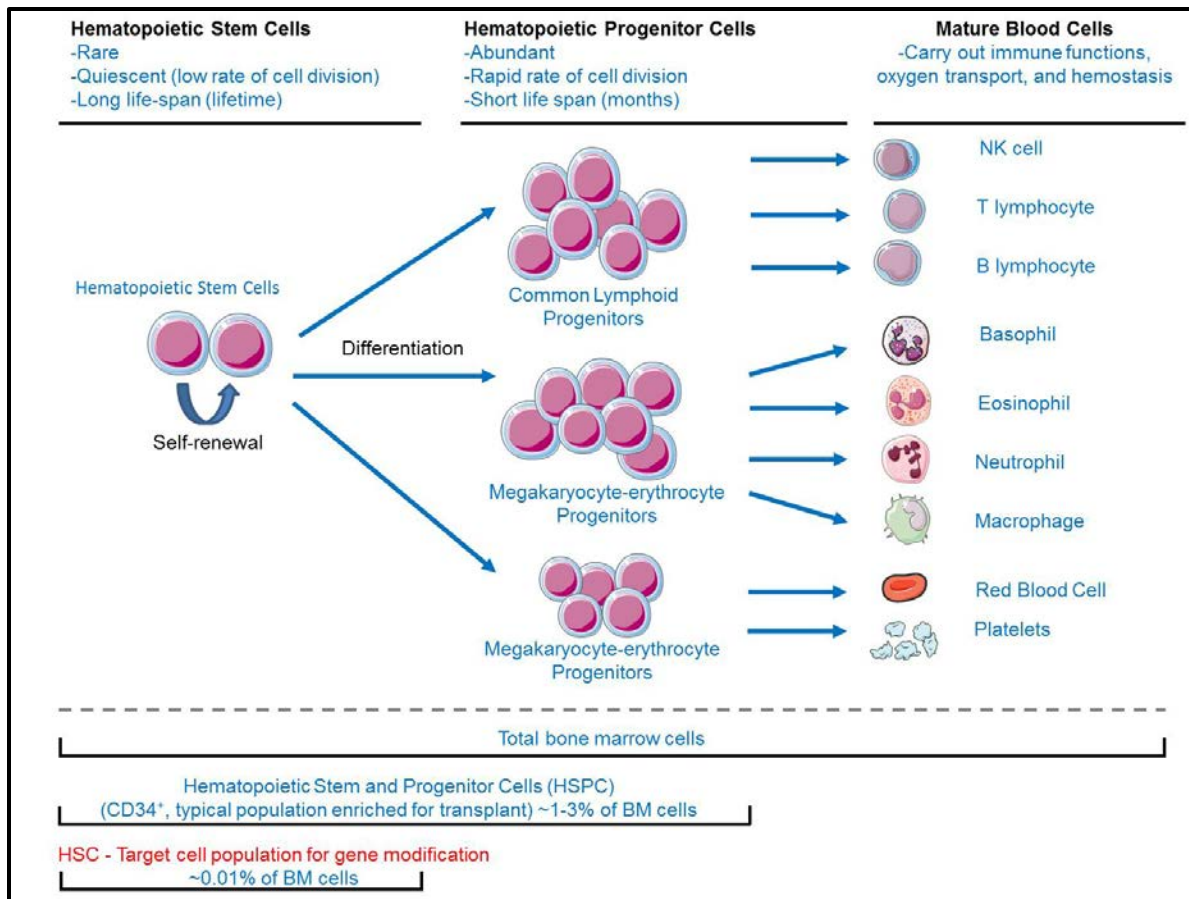
Figure 1-1: Hierarchy of hematopoietic stem and progenitor cell populations in the bone marrow

Hematopoietic stem cell transplant for genetic blood diseases – past and future

A number of genetic diseases which affect the blood system can be treated by replacing defective HSCs with a transplant of healthy HSCs. When donor HSCs come from an outside donor, this process is referred to as an allogeneic HSC transplant. This procedure was first successfully performed in 1968 for the treatment of Wiskott Aldrich Syndrome[1,2], and has since been used in a number of other hematologic diseases summarized in table 1-1.

Primary immune deficiencies	
ADA-deficient severe combined immune deficiency	X-linked severe combined immune deficiency
other genetic forms of SCID (Artemis, Rag1/2).	chronic granulomatous disease
leukocyte adhesion deficiency	Wiskott-Aldrich Syndrome
hemophagocytic lymphohistiocytosis	X-linked hyper IgM syndrome
X-linked lymphoproliferative disease	X-linked Agammaglobulinemia
common variable immunodeficiency	IPEX Syndrome
Hemoglobinopathies	
sickle cell disease	beta-thalassemia
Storage and metabolic disorders	
mucopolysaccharidoses (I-VII)	Gaucher Disease and other lipidoses
X-linked Adrenoleukodystrophy	Fanconi anemia
osteopetrosis	metachromatic leukodystrophy
Congenital cytopenias and stem cell defects	
Kostmann's Syndrome	Schwachman-Diamond Syndrome

Table 1-1: List of genetic blood diseases treated with allogeneic HSPC. Adapted from Morgan, Gray, Lomova, & Kohn, 2017

In an allogeneic HSCT, HSPCs are first collected from the bone marrow or blood of an immunologically matched donor. The recipient is then conditioned using chemotherapy or radiation in order to eliminate their own HSPCs and to make room for the incoming donor HSPCs. The donor HSPC graft is then infused intravenously into the patient's bloodstream. HSPCs in the blood stream respond to a number of biochemical signals that direct them towards regions of the bone marrow composed of supportive stromal cells called the stem cell "niche." Following engraftment in the niche, short-term HPCs will rapidly replace the ablated blood system for the first few weeks to months, and then are themselves eventually replaced by the engrafted long-term HSCs. While a patient is regenerating the immune system during the first few weeks, they are highly susceptible to infection, anemia, and bleeding, and may require intensive medical support until their blood system fully recovers.
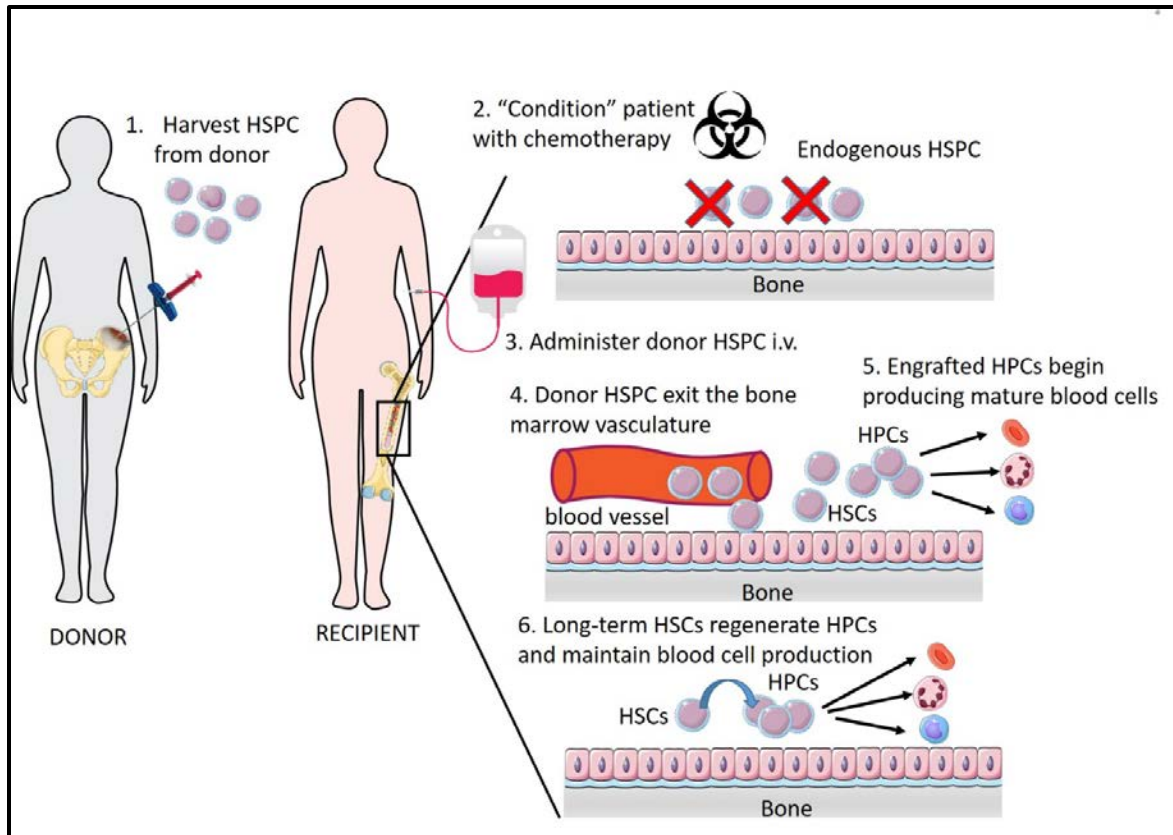
Figure 1-2: Allogeneic HSC transplant

While allogeneic HSCT has been successful for a wide range of genetic blood diseases, there are inherent limitations which stem from the mismatch between the donor and recipient immune systems. The first is the risk of graft rejection, which occurs when T cells from the recipient immune system recognize the donor cells as foreign invaders and subsequently destroy the incoming cells. As the patient has previously had their own HSPCs ablated with chemotherapy or radiation, failure of the incoming donor HSPCs to engraft can be a very serious and often fatal outcome. The second major immunologic complication is the risk of graft-versus host disease, which occurs when mature immune cells in the donor population recognize the recipient's body as "foreign" and attack various organs, including the skin, gastrointestinal tract, and liver. Thus in order to minimize these adverse outcomes, the field of transplant immunology has evolved to carefully select immunologically compatible donors and

recipients, and further utilizes immunosuppressive drugs to minimize the risk of immunologic transplant complications. Even while using immunosuppressive drugs and an immunologically matched donor, the risk of serious immunologic transplant complications is always present. The most limiting factor for allogenic HSCT, however, is the lack of donor availability; because such close immunologic matching is required, the majority of patients with blood diseases simply do not have a matched donor available, which precludes them from undergoing this potentially curative option.

A preferable approach made possible by the field of gene therapy is autologous HSC transplant (Figure 1-3). Rather than using an outside donor as a source of healthy HSCs, HSCs are harvested directly from the patient and the underlying genetic defect is fixed in the patients' own stem cells prior to transplant back into the patient. This approach avoids the immunologic complications associated with allogeneic transplant and also broadens the range of patients who are able to receive treatment, as each patient can serve as their own donor. Additionally, less aggressive conditioning regimens can be used which can make the post-transplant recovery period safer in autologous transplant.
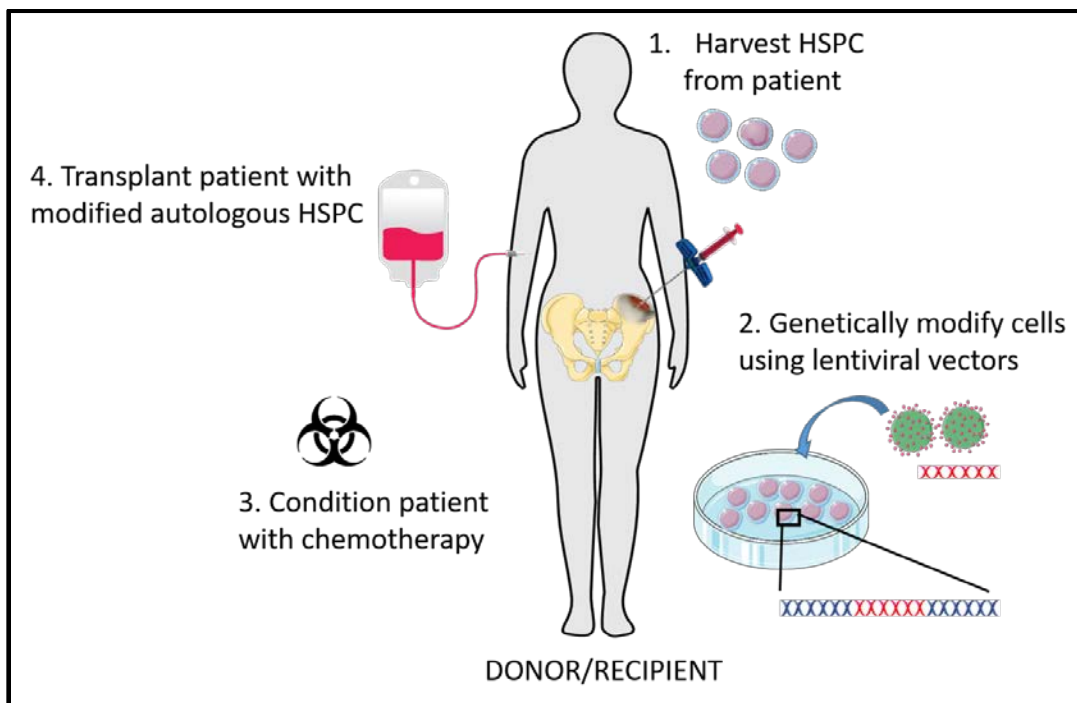
Figure 1-3: Autologous HSC transplant with gene therapy

Collection and enrichment of hematopoietic stem cells

HSCs residing in the bone marrow can be collected from a patient by two major methods. The first is aspiration of cells from the bone marrow, which is typically performed as a surgical procedure under general anesthesia. The second method involves mobilizing the cells from the bone marrow to the blood stream using drugs (such as Granulocyte Colony Stimulating Factor (G-CSF) and/or Plerixafor) and collecting the cells from the blood using leukapheresis.

Once the cell product has been obtained from the patient, this collection of cells represents a heterogeneous mix of blood cells at various stages of development. However, only a very small fraction of the collected product represents true HSCs capable of engrafting in a patient and producing blood cells throughout a patient's lifetime (Figure 1-1). These HSCs must be enriched from the total harvest of collected cells, as it would be prohibitively inefficient and costly to culture and modify all harvested cells with limited engraftment potential.

Historically, HSCs have been enriched from the total cell harvest by selecting for cells which express the surface marker CD34. CD34 is expressed early in hematopoietic development, and is expressed on both HSCs and HPCs (Figure 1-1). Many clinical gene therapy protocols enrich CD34+ cells using immunomagnetic beads. Harvested cell products are labeled with magnetic beads linked to antibodies which bind CD34, followed by isolation of these cells using a magnetic column. This technology is available in a number of GMP-grade cell enrichment systems for clinical use.

While CD34 enrichment is an effective way to isolate HSPC from whole bone marrow or mobilized peripheral blood and allows for a ~30-100-fold reduction in the total cell number, this enrichment may still be considered inefficient in a gene therapy setting, as the majority of the CD34+ cells are short-term HPCs. Only a small fraction of CD34+ cells (<1 in 100) represent true HSCs with long-term engraftment potential. Therefore, LV transduction of total CD34+ cells may represent a wasteful use of valuable LV preparations, as many of the cells treated with LV will only produce blood cells for

weeks to months after transplant. A more efficient use of LV would only modify long-term HSCs, which

will eventually replace short-term HPC and take over long-term blood cell production. In chapter 2, we

demonstrate an immunomagnetic bead (IB)-based method to purify CD34+CD38- cells, a population

~10-fold enriched for HSCs beyond standard CD34+ selection. This strategy may serve as a valuable tool

to preserve valuable LV preparations and conduct gene therapy more efficiently.

Genetic Modification of HSC

Once HSCs have been harvested from a patient and isolated by either traditional CD34 selection

or by improved HSC enrichment methods, they must be genetically modified in order to correct the

underlying defect. Currently, one of the most efficient and least toxic ways to modify HSC genomes is

through transduction with a 3rd generation self-inactivating (SIN) LV [4]. This virus system is based on the

parental HIV virus and has removed the endogenous enhancer/promoter from the Long Terminal

Repeat (LTR) [5,6], creating a safer, self-inactivating vector that cannot transcribe its own genome to

replicate after transduction. This system capitalizes on the unique ability of LVs to efficiently infect

human cells and integrate their DNA into a cell's genome. This process represents a permanent

modification that will be inherited by daughter cells after all future cell divisions.

The first successful applications of these LVs in gene therapy trials used strong, constitutively

active promoters to drive high levels of transgene expression in stem cells and all daughter blood cell

lineages. An example of this application is the treatment of adenosine deaminase (ADA) deficiency [7,8],

where a broad range of ADA expression throughout the hematopoietic system was shown to be safe and

sufficient to correct the disease.

However, for other diseases, strong gene promotion and ubiquitous expression can problematic.

One example is restoration of FoxP3 expression for the treatment of IPEX Syndrome (Chapter 4). FoxP3

is a transcription factor which plays a key role in cell fate decisions, thus we found that inappropriate

FoxP3 expression throughout the hematopoietic system was detrimental to normal hematopoietic development and long-term engraftment.

In order to achieve more precise, lineage-specific expression, LV can be designed using regulatory elements such as promoters and enhancers from the endogenous gene. However, a major challenge underlying this type of LV design is the trade-off between including a number of large, endogenous regulatory sequences and increasing LV genome size. Larger LV genomes typically exhibit reduced titers and decreased transduction efficiency, thus making it difficult to achieve therapeutic correction of HSC. This has been readily apparent in clinical efforts to treat hemoglobinopathies, the most common genetic blood disorders. The LVs used in these trials utilize large elements of the endogenous β-globin locus control region (LCR) to drive erythroid-specific expression of a β-globin transgene in mature erythrocytes [9,10]. Clinical scale viral production of globin LVs has often resulted in poor titers and gene transfer to primitive HSCs, often failing to achieve sufficiently high copy numbers to correct the disease [11].

For example, in our clinical trial for sickle cell disease, treatment of a single patient under our current clinical protocol required the production of >30L of raw viral supernatant, required 6-12 months for sourcing, production, and validation, and cost $600,000. Ultimately, using the entire batch of LV to treat the patients HSC resulted in suboptimal gene transfer (average 0.3 vector genomes/cell).

Therefore, new methods which improve the transduction efficiency of large LV such as globin LV are critical to the future success of these clinical trials. In part, the strategy of improving HSC enrichment using CD34+CD38- selection (Chapter 2) may improve this problem by allowing clinical scale LV products to be used more efficiently. Furthermore, in Chapter 3, we dramatically improve LV transduction efficiency through the use of transduction enhancing compounds, allowing us to achieve therapeutic levels of gene correction with 10-fold less LV. Essentially, we have found that there are no bad LVs, just LVs without transduction enhancers.

In summary, the work in this thesis has made important improvements to clinical gene therapy and may pave the way to bring this technology to a greater number of patients with hematologic diseases.

REFERENCES

1.	FritzH. Bach M.D. Harvard, RichardJ. Albertini M.D. Wisconsin , Patricia Joo M.D. Wisconsin , JamesL. Anderson M.D. Wisconsin MBMDM. Bone marrow transplantation in a patient with the Wiskott-Aldrich Syndrome. *Lancet*. 1968;292(7583):1364-1366.

2.	Gatti RA, Meuwissen HJ, Allen HD, Hong R, Good RA. Immunological reconstitution of sex-linked lymphopenic immunological deficiency. *Lancet (London, England)*. 1968;2(7583):1366-1369.

3.	Morgan RA, Gray D, Lomova A, Kohn DB. Hematopoietic Stem Cell Gene Therapy: Progress and Lessons Learned. *Cell Stem Cell*. 2017;21(5):574-590.

4.	Naldini L, Blomer U, Gallay P, et al. In Vivo Gene Delivery and Stable Transduction of Nondividing Cells by a Lentiviral Vector. *Science (80-)*. 1996;272(5259):263-267.

5.	Dull T, Zufferey R, Kelly M, et al. A third-generation lentivirus vector with a conditional packaging system. *J Virol*. 1998;72(11):8463-8471.

6.	Zufferey R, Dull T, Mandel RJ, et al. Self-inactivating lentivirus vector for safe and efficient in vivo gene delivery. *J Virol*. 1998;72(12):9873-9880.

7.	Aiuti A, Cattaneo F, Galimberti S, et al. Gene therapy for immunodeficiency due to adenosine deaminase deficiency. *N Engl J Med*. 2009;360(5):447-458.

8.	Candotti F, Shaw KL, Muul L, et al. Gene therapy for adenosine deaminase-deficient severe combined immune deficiency: clinical comparison of retroviral vectors and treatment plans. *Blood*. 2012;120(18):3635-3646.

9.	Romero Z, Urbinati F, Geiger S, et al. β-globin gene transfer to human bone marrow for sickle cell disease. *J Clin Invest*. 2013;123(8):3317-3330.

10.	Negre O, Bartholomae C, Beuzard Y, et al. Preclinical evaluation of efficacy and safety of an improved lentiviral vector for the treatment of β-thalassemia and sickle cell disease. *Curr Gene Ther*. 2015;15(1):64-81.

11.	Kanter J, Walters MC, Hsieh MM, et al. Interim Results from a Phase 1/2 Clinical Study of Lentiglobin Gene Therapy for Severe Sickle Cell Disease. *Blood*. 2016;128(22):1176 LP-1176.

Chapter 2:

Improving Gene Therapy Efficiency through the Enrichment of Human Hematopoietic Stem Cells

Original Article

Improving Gene Therapy Efficiency through the Enrichment of Human Hematopoietic Stem Cells

Katelyn E. Masiuk,[1] Devin Brown,[1] Jennifer Laborada,[1] Roger P. Hollis,[1] Fabrizia Urbinati,[1] and Donald B. Kohn[1,2,3]

[1]Department of Microbiology, Immunology & Molecular Genetics, University of California, Los Angeles, Los Angeles, CA 90095, USA; [2]Department of Pediatrics, David Geffen School of Medicine, University of California, Los Angeles, Los Angeles, CA 90095, USA; [3]Department of Molecular & Medical Pharmacology, University of California, Los Angeles, Los Angeles, CA 90095, USA

Lentiviral vector (LV)-based hematopoietic stem cell (HSC) gene therapy is becoming a promising clinical strategy for the treatment of genetic blood diseases. However, the current approach of modifying 1×10^8 to 1×10^9 CD34$^+$ cells per patient requires large amounts of LV, which is expensive and technically challenging to produce at clinical scale. Modification of bulk CD34$^+$ cells uses LV inefficiently, because the majority of CD34$^+$ cells are short-term progenitors with a limited post-transplant lifespan. Here, we utilized a clinically relevant, immunomagnetic bead (IB)-based method to purify CD34$^+$ CD38$^-$ cells from human bone marrow (BM) and mobilized peripheral blood (mPB). IB purification of CD34$^+$CD38$^-$ cells enriched severe combined immune deficiency (SCID) repopulating cell (SRC) frequency an additional 12-fold beyond standard CD34$^+$ purification and did not affect gene marking of long-term HSCs. Transplant of purified CD34$^+$CD38$^-$ cells led to delayed myeloid reconstitution, which could be rescued by the addition of non-transduced CD38$^+$ cells. Importantly, LV modification and transplantation of IB-purified CD34$^+$ CD38$^-$ cells/non-modified CD38$^+$ cells into immune-deficient mice achieved long-term gene-marked engraftment comparable with modification of bulk CD34$^+$ cells, while utilizing ~7-fold less LV. Thus, we demonstrate a translatable method to improve the clinical and commercial viability of gene therapy for genetic blood cell diseases.

INTRODUCTION

Lentiviral vector (LV)-based gene modification of autologous hematopoietic stem cells (HSCs) has demonstrated remarkable success for the treatment of genetic blood diseases.[1–6] In this approach, bone marrow (BM) or mobilized peripheral blood (mPB) is collected from a patient, enriched for HSCs, transduced with LV encoding the correct genetic sequence, and transplanted back into the patient. After transplant, HSCs engraft in the BM and produce mature, gene-corrected hematopoietic cells ideally throughout the patient's lifetime. New clinical trials using anti-sickling β-globin vectors show promising early results in the treatment of sickle cell disease (SCD), the most common genetic blood disorder affecting millions of people.[7] However, broad use of gene ther-

apy will require an unprecedented amount of clinical-grade vector production, a process that is currently limited by high cost and commercial manufacturing capacity. Currently, production and clinical validation of β-globin vector for a single patient may require 20–40 L of viral supernatant and cost in the range of $250,000–$500,000. Therefore, new methods that reduce the amount of LV required per patient are needed to make gene therapy clinically and commercially feasible.

One strategy to reduce LV requirements is to improve enrichment of HSCs before transduction. Current clinical HSC enrichment protocols use immunomagnetic beads (IBs) to select for cells expressing the surface marker CD34 prior to LV transduction. This method is inefficient in a gene therapy setting, because the majority of CD34$^+$ cells are short-term progenitor cells with a limited post-transplant lifespan. Further isolation of HSCs from short-term progenitors could improve LV economy by only transducing cells that can endure for the lifetime of the patient. We postulated that purifying CD34$^+$ CD38$^-$ cells would further enrich for HSCs, reduce the absolute number of cells to be transduced with LV, and reduce the total LV dose required per patient. Importantly, these benefits could be achieved while still retaining the target HSCs required for long-term clinical benefit after transplantation.

To date, little is known about clinical transplantation of highly purified HSCs. A small number of clinical trials have shown successful transplantation of CD34$^+$CD90$^+$ cells,[8–10] which represented ~50% of total CD34$^+$ cells. In contrast, CD34$^+$CD38$^-$ cells are highly enriched for HSCs and represent ~5%–10% of CD34$^+$ cells. While a large body of work has characterized the repopulation capacity of CD34$^+$CD38$^-$ cells, the majority of this work has been performed using fluorescence-activated cell sorting (FACS)-purified cord blood

(CB). In contrast with FACS purification, IB-based cell sorting is currently available in Good Manufacturing Practice (GMP)-grade platforms with the capacity to purify large cell numbers quickly with high recovery. Here, we investigate an IB-based method to purify CD34$^+$CD38$^-$ cells from human BM and mPB samples with focus on practical implementation of our findings to current clinical gene therapy trials. We demonstrate the capacity of this method to reduce LV dose by ~5- to 10-fold while maintaining early post-transplant recovery and long-term engraftment of gene-modified cells. These findings have the potential to reduce the total LV required per patient and improve the clinical and commercial viability of gene therapy for genetic blood cell diseases.

RESULTS

More Than 90% of CD34$^+$ Long-Term Repopulating Activity Is Contained within the Lowest 6% of CD38 Expression

Translating CD34$^+$CD38$^-$ purification to the clinic will require efficient HSC recovery to sustain engraftment of gene-corrected cells after transplant. In order to identify a target cell population to purify for gene therapy, we first sought to determine which subsets of BM CD34$^+$ cells are capable of long-term engraftment after ex vivo culture required for LV transduction. We performed a competitive transplant assay in immune-deficient non-obese diabetic (NOD)/severe combined immune deficiency (SCID)/gamma (NSG) mice utilizing CD34$^+$ cells with varying levels of CD38 expression (Figure 1A). IB-purified CD34$^+$ BM cells were sorted by FACS to obtain three different cell populations with increasing, constant percentiles of CD38 expression (e.g., 6% intervals: 0%–6%, 6%–12%, and 12%–18% of CD38 expression). Each fraction of sorted cells was pre-stimulated with cytokines (interleukin-3 [IL-3], stem cell factor [SCF], fms-related tyrosine kinase 3 [Flt3]-ligand, and thrombopoietin) for 24 hr and then transduced for an additional 24 hr with one of three fluorescent LVs: CCL-ubiquitin C (UBC)-mCitrine, CCL-UBC-mStrawberry, or CCL-UBC-mCerulean. Following transduction, 15,000 cells from each of three differentially labeled CD38 intervals were competitively co-transplanted into sub-lethally irradiated NSG mice. Fluorescent reporter gene color choice for each sorted fraction was rotated to account for potential differences in transduction efficiency among vectors (Figure S1).

At 16–18 weeks post-transplantation, engrafted hCD45$^+$ cells in NSG BM were analyzed by flow cytometry for mCitrine, mStrawberry, and mCerulean expression to determine the long-term engraftment potential of each initially sorted population. Two separate transplants were performed using different intervals of CD38 expression (Figure 1B). In transplant 1, >90% of hCD45$^+$ cells present in the BM were derived from CD34$^+$CD38$^{0\%-6\%}$ cells, whereas <10% of hCD45$^+$ cells were derived from CD34$^+$CD38$^{6\%-12\%}$ and CD34$^+$CD38$^{12\%-18\%}$ cells. In transplant 2, 54% of hCD45$^+$ cells were derived from CD34$^+$CD38$^{0\%-3\%}$ cells, with an additional 40% of hCD45$^+$ cells derived from the CD34$^+$CD38$^{3\%-6\%}$ fraction. For each transplant, the observed patterns were consistent in myeloid (CD33$^+$), lymphoid (CD19$^+$), and hematopoietic stem and progenitor cells (HSPCs) (CD34$^+$) lineages.

Collectively, these results suggest that after ex vivo culture and LV transduction, the majority of long-term repopulating activity in CD34$^+$ adult BM cells is contained within the lowest 6% of CD38 expression. Furthermore, while the CD34$^+$CD38$^{0\%-3\%}$ fraction is highly enriched for long-term HSCs, the CD34$^+$CD38$^{3\%-6\%}$ also contains a substantial proportion of long-term HSCs; thus, purification beyond the lowest 6% of CD38 expression may lead to HSC loss. Based on these results, we defined "CD34$^+$CD38$^-$ cells" as the lowest 6% of CD38 expression for subsequent experiments tracking phenotypic HSC recovery.

Titration of CD38 Magnetic Labeling Optimizes Recovery and Purity of CD34$^+$CD38$^-$ Cells

We next sought to optimize a clinically relevant, IB-based method to purify CD34$^+$CD38$^-$ cells. We chose to first deplete CD38$^+$ cells and subsequently select CD34$^+$ cells. CD38 magnetic labeling was performed using a primary anti-CD38-phycoerythrin (PE)-conjugated antibody followed by incubation with anti-PE magnetic beads. Unlabeled CD38$^-$ cells can be relabeled with CD34 beads, thereby preventing the necessity of a bead removal step. CD34$^+$ cells exhibit a gradient pattern of CD38 expression rather than discrete positive and negative populations. We found that the proportion of cells separated into CD38$^-$ and CD38$^+$ fractions could be adjusted by varying the intensity of CD38 magnetic labeling with different concentrations of magnetic beads (Figure 2). Mononuclear cells (MNCs) from CB, BM, and mPB were separated into CD38$^-$ and CD38$^+$ fractions using three different concentrations of anti-PE beads. Strong magnetic labeling (anti-PE beads 1:5) greatly enriched for CD34$^+$CD38$^-$ cells (13-, 16-, and 15-fold for CB, BM, and mPB, respectively), but resulted in low recovery of CD34$^+$CD38$^-$ cells (50%, 19%, and 59% for CB, BM, and mPB). Weak magnetic labeling (anti-PE beads 1:25) resulted in high recovery of CD34$^+$CD38$^-$ cells (93%, 67%, and 96% for CB, BM, and mPB, respectively) but reduced enrichment of CD34$^+$CD38$^-$ cells (4.6-, 10.3-, and 4.7-fold for CB, BM, and mPB). Thus, there is a tradeoff between recovery and fold-enrichment of CD34$^+$CD38$^-$ cells that can be optimized by altering the strength of CD38 magnetic labeling. Here, we observe that anti-PE bead concentrations of 1:10 for mPB and >1:25 for BM (1:40 was used in all subsequent experiments) can optimize both enrichment and recovery of CD34$^+$CD38$^-$ cells.

Co-depletion of CD15$^+$ and CD38$^+$ Cells Increases the Purity of Isolated CD34$^+$CD38$^-$ Cells

In BM and CB, we observed that CD38 depletion followed by CD34 selection led to a final cell product with <50% CD34$^+$ cells because of contamination of CD15$^+$ granulocytes (Figure 3A, top). Similar absolute numbers of granulocytes were isolated by CD34$^+$ or CD34$^+$ CD38$^-$ purification (Figure 3B), suggesting that the CD38 depletion step does not increase non-specific granulocyte selection. To obtain more highly purified CD34$^+$CD38$^-$ cells, we included a CD15 magnetic bead during the CD38 depletion step, allowing us to simultaneously co-deplete CD38$^+$ cells and CD15$^+$ granulocytes prior to CD34 selection (Figure 3C). In BM, addition of a CD15 bead increased purity of CD34$^+$CD38$^-$ cells from 24.5% of total cells to
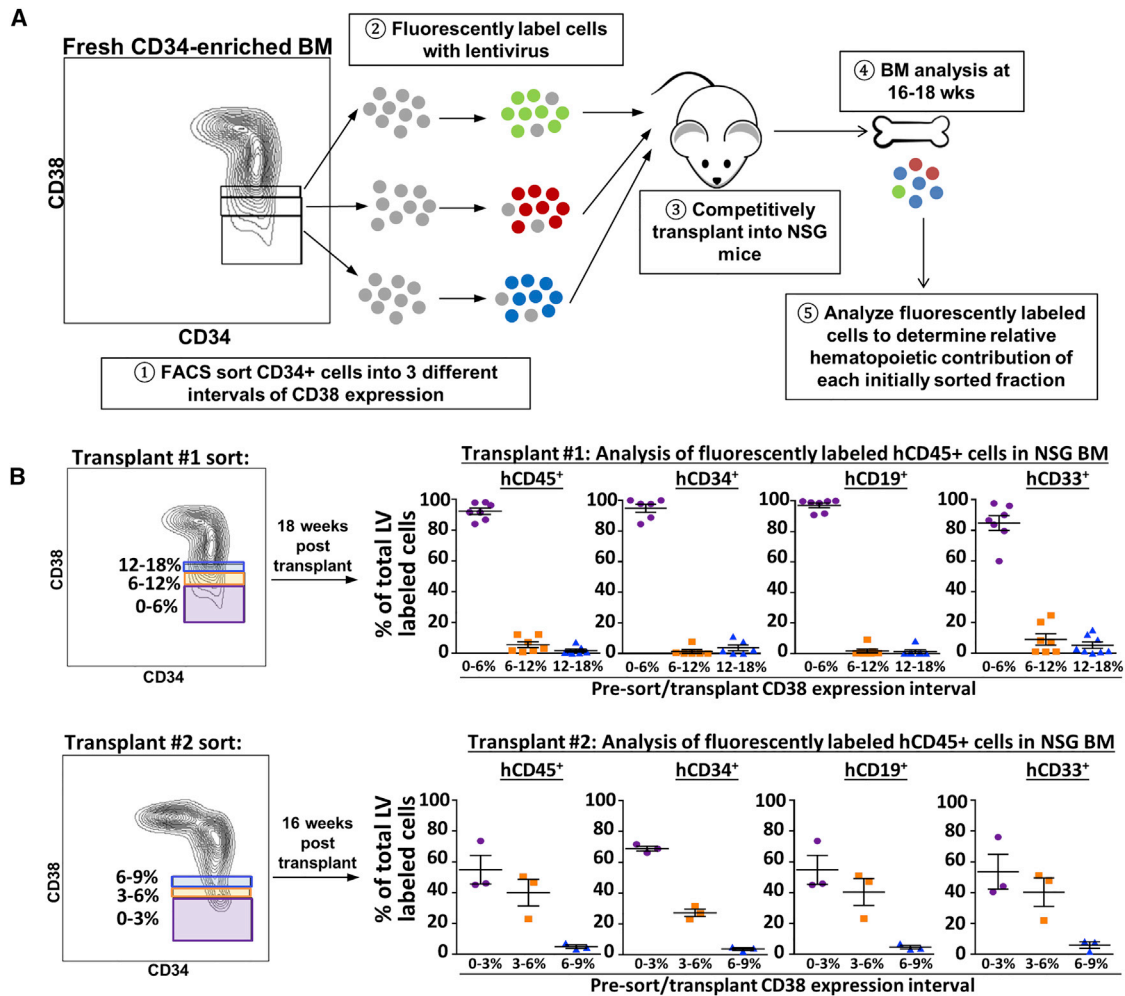
Figure 1. Long-Term Repopulating Activity of CD34$^+$CD38$^-$ Subsets

(A) Experimental setup. (1) FACS sort: BM cells were magnetically enriched for CD34 and sorted by FACS into distinct populations of increasing CD38 expression. Each gate contains an equivalent number of cells. (2) LV transduction: Cells from each interval were transduced with one of three LVs expressing the fluorescent proteins mCitrine, mStrawberry, or mCerulean. (3) Transplant: A combination of cells from each sorted interval (each differentially labeled) were combined and competitively transplanted into sub-lethally irradiated NSG mice. Each mouse received an equal number of cells from each sorted fraction. (4) BM analysis: NSG BM was analyzed at 16–18 weeks for the presence of fluorescently labeled hCD45$^+$ cells. (5) Fluorescently labeled hCD45$^+$ cells engrafted in the NSG BM were analyzed for their relative contribution to human hematopoiesis. (B) Relative abundance of labeled cells in NSG BM. Two separate transplants were performed using different intervals of CD38 expression (top and bottom). Initial sort for CD38 expression is shown in the left panels. At 16–18 weeks post-transplant, fluorescent, LV-labeled hCD45$^+$, hCD34$^+$, hCD19$^+$, and hCD33$^+$ cells were analyzed. y axis represents the relative frequency of each sorted and/or labeled CD38 fraction as a percent of all fluorescently labeled cells. Bars represent mean ± SEM. n = 7 mice for transplant 1; n = 3 mice for transplant 2.

70.5% of total cells, thus further reducing total number of cells isolated prior to transduction. Based on these findings, all subsequent CD34$^+$CD38$^-$ purifications were performed using CD38/CD15 co-depletion.

Optimized CD34$^+$CD38$^-$ Dual IB Purification Enriches CD34$^+$CD38$^-$ Cells with High Recovery and Results in Efficient HSC Gene Marking

We next compared the optimized CD34$^+$CD38$^-$ IB purification strategy with standard CD34$^+$ selection in multiple BM and mPB samples

from healthy donors. For each sample analyzed, two identical fractions of MNCs were purified by either CD34$^+$ single-step IB purification or CD34$^+$CD38$^-$ dual IB purification. The total cell product obtained after purification by each method was analyzed by flow cytometry and counting beads to determine absolute CD34$^+$CD38$^-$ cell counts (Figures 4A and 4B; Figure S2). In BM, CD34$^+$CD38$^-$ dual IB purification of starting MNCs recovered a median 62.5% (range 57.2%–65.6%) of phenotypically defined CD34$^+$CD38$^-$ cells, whereas standard CD34 selection recovered a median of 93.1% (range 80%–95.6%) of CD34$^+$CD38$^-$ cells. CD34$^+$CD38$^-$ dual IB purification
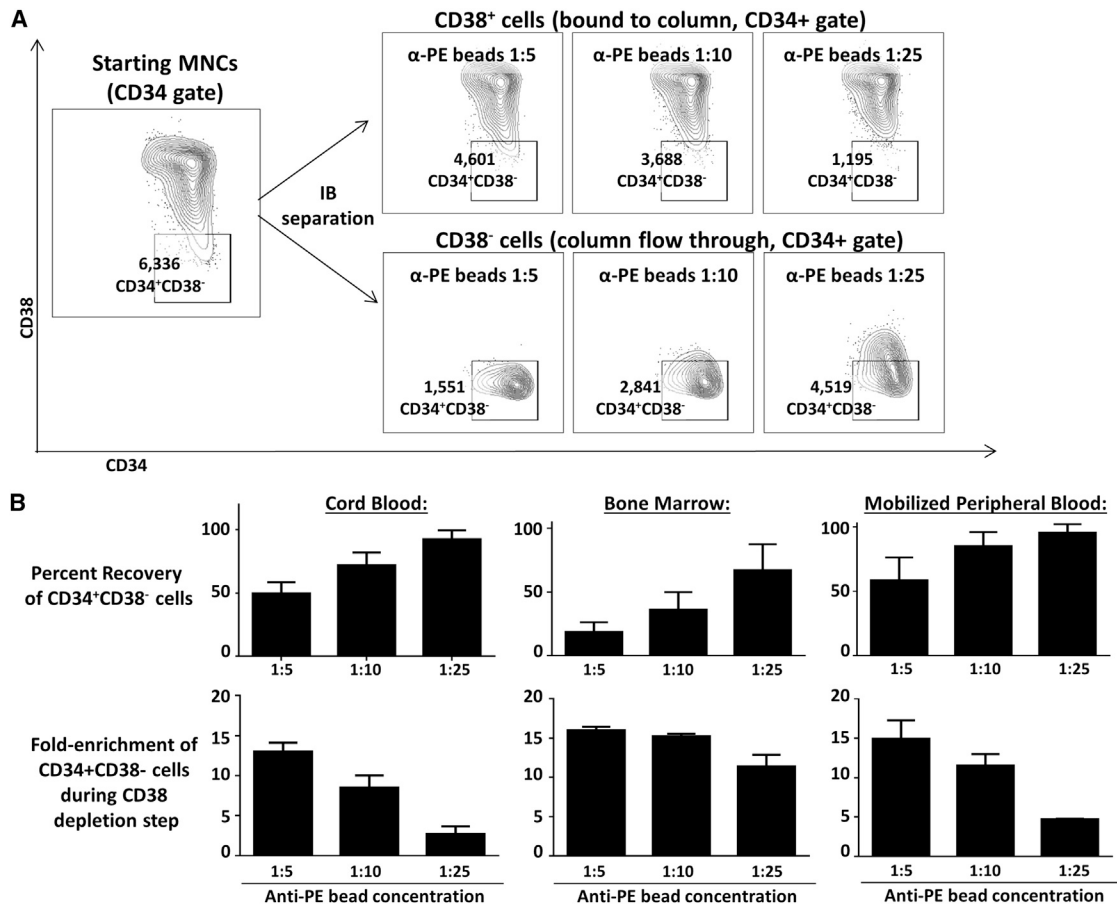
Figure 2. Titration of CD38 Immunomagnetic Labeling Influences Recovery and Enrichment of CD34⁺CD38⁻ Cells

(A) CD38 depletion of BM mononuclear cells (MNCs) using three different concentrations of anti-PE beads (one representative experiment is shown). Plots are gated to show CD34⁺ cells present in starting MNCs (far left), and after column separation into CD38⁺ (top) and CD38⁻ (bottom) fractions. Gates show CD34⁺CD38⁻ cells (defined as the lowest 6% of CD38 expression) and list absolute counts of CD34⁺CD38⁻ cells in each population. (B) Efficiency of CD38 depletion step at different PE bead concentrations. Bar graphs show "percent recovery" and "fold-enrichment" of CD34⁺CD38⁻ cells before and after CD38 depletion using three different anti-PE bead concentrations. Bars represent mean ± SEM. Data represent three independent experiments each for CB, BM, and mPB.

enriched for CD34⁺CD38⁻ cells an additional 8.7-fold (range 4.8–12) beyond standard CD34⁺ purification. Similar results were achieved in mPB, with a median CD34⁺CD38⁻ recovery of 75.1% (range 58.4%–91.0%) by dual CD34⁺CD38⁻ purification and 87.9% (range 83.7%–93.2%) by standard CD34 selection. CD34⁺CD38⁻ dual IB purification enriched for CD34⁺CD38⁻ cells an additional 12-fold (range 8.7–13.2) beyond standard CD34⁺ purification.

To further assess recovery of functional HSCs, we transplanted cells from each purified population into NSG mice at limiting doses. Limiting dilution analysis of CCL-UBC-mCitrine LV-transduced cells demonstrated a 12-fold enrichment of SCID repopulating cell (SRC) frequency within CD34⁺CD38⁻ cells (1 in 2,314 cells; 95% confidence interval: 1/1,241–1/4,314) compared with CD34⁺ cells (1 in 28,248 cells; 95% confidence interval: 1/14,701–1/54,278) (Figure 4C; Figure S3). Analysis of long-term (>16 week) engrafted hCD45⁺ cells in NSG BM revealed no significant difference in average vector copy

number per human cell between groups, suggesting that the dual CD34⁺CD38⁻ IB purification method allows for efficient transduction of HSCs while using less cells and LV (Figure 4D).

CD34⁺CD38⁻ Cells Show Delayed Myeloid Recovery that Can Be Rescued by Increasing Cell Dose or Adding Back Non-transduced CD38⁺ Cells

Purifying CD34⁺CD38⁻ cells may provide the advantage of utilizing less LV to transduce HSCs. However, transplanting a smaller population of quiescent, stem-enriched cells may cause delayed recovery of neutrophils and leave a patient susceptible to infection early after transplant. Therefore, we compared the early myeloid potential of IB-purified CD34⁺ and CD34⁺CD38⁻ cells. Here, we transplanted purified cells into the NSG-SGM3 mouse model,[11] an immune-deficient mouse model that supports human myelopoiesis through constitutive expression of human cytokines IL-3, granulocyte-macrophage colony-stimulating factor (GM-CSF), and SCF. In order to
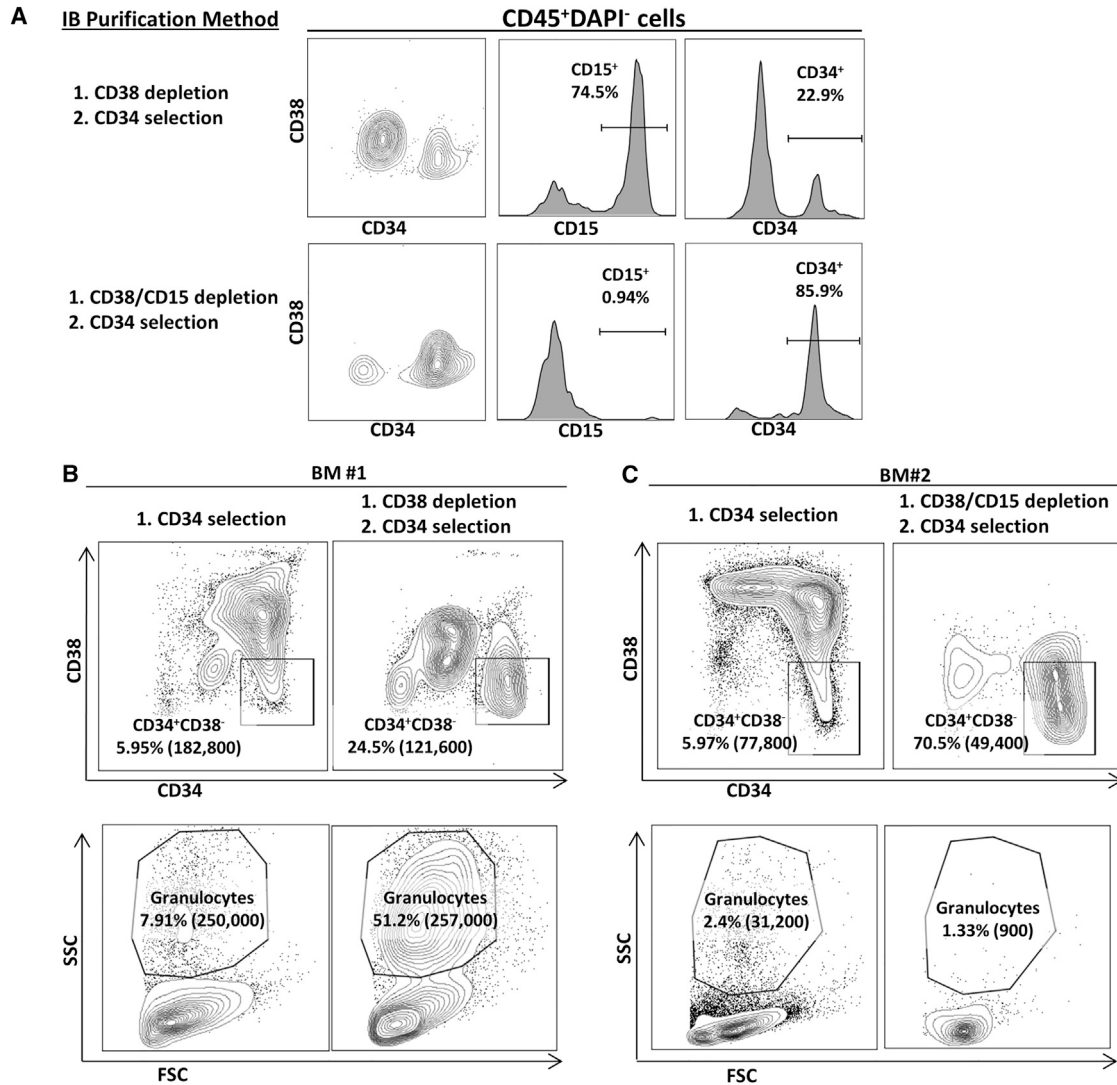
Figure 3. Co-depletion of CD15$^+$ and CD38$^+$ Cells Increases CD34$^+$CD38$^-$ Purity

(A) CD34$^+$CD38$^-$ cells were purified from CB MNCs using one of two methods: CD38 depletion followed by CD34 selection (top) or CD38/CD15 co-depletion followed by CD34 selection (bottom). Leftmost FACS plot shows CD34 and CD38 staining of all viable leukocytes (CD45$^+$DAPI$^-$) isolated by either method. Histograms indicate the percentage of CD15$^+$ and CD34$^+$ cells within total viable leukocytes isolated by each method. (B) IB purification of BM 1 (no CD15 co-depletion). Left panel shows CD34 purification, and right panel shows parallel CD34$^+$CD38$^-$ purification (using CD38 depletion only). FACS plots show viable leukocytes (CD45$^+$DAPI$^-$) isolated by each method. Gates show CD34$^+$CD38$^-$ cells (top) and granulocytes (defined by high side scatter [SSC], bottom) purified by each method. Absolute cell counts are listed in parentheses. (C) IB purification of BM 2 (with CD15 co-depletion). Left panel shows CD34 purification, and right panel shows parallel CD34$^+$CD38$^-$ purification (using CD38/CD15 co-depletion). FACS plots show viable leukocytes (CD45$^+$DAPI$^-$) isolated by each method. Gates show CD34$^+$CD38$^-$ cells (top) and granulocytes (defined by high SSC, bottom) purified by each method. Absolute cell counts are listed in parentheses.

reflect a clinically relevant scenario, transplanted cell doses for each group represented the total cells obtained from IB purification of a standard volume of marrow (marrow equivalent [ME]). 1 marrow equivalent of CD34$^+$CD38$^-$ cells showed decreased early production of circulating human myeloid cells as compared with 1 marrow equivalent of CD34$^+$ cells (Figure 5A). 2.5 marrow equivalent of CD34$^+$ CD38$^-$ cells achieved myeloid reconstitution comparable with 1 marrow equivalent of CD34$^+$ cells, whereas 6 marrow equivalent of

CD34$^+$CD38$^-$ cells resulted in myeloid reconstitution ~3-fold higher than 1 marrow equivalent of CD34$^+$ cells. These results demonstrate that dual IB-purified CD34$^+$CD38$^-$ cells are capable of early myeloid reconstitution, but contain less early myeloid potential than CD34$^+$ cells purified from an equivalent volume of BM.

We next investigated whether co-transplanting non-transduced CD38$^+$ cells (obtained during IB depletion of MNCs) alongside
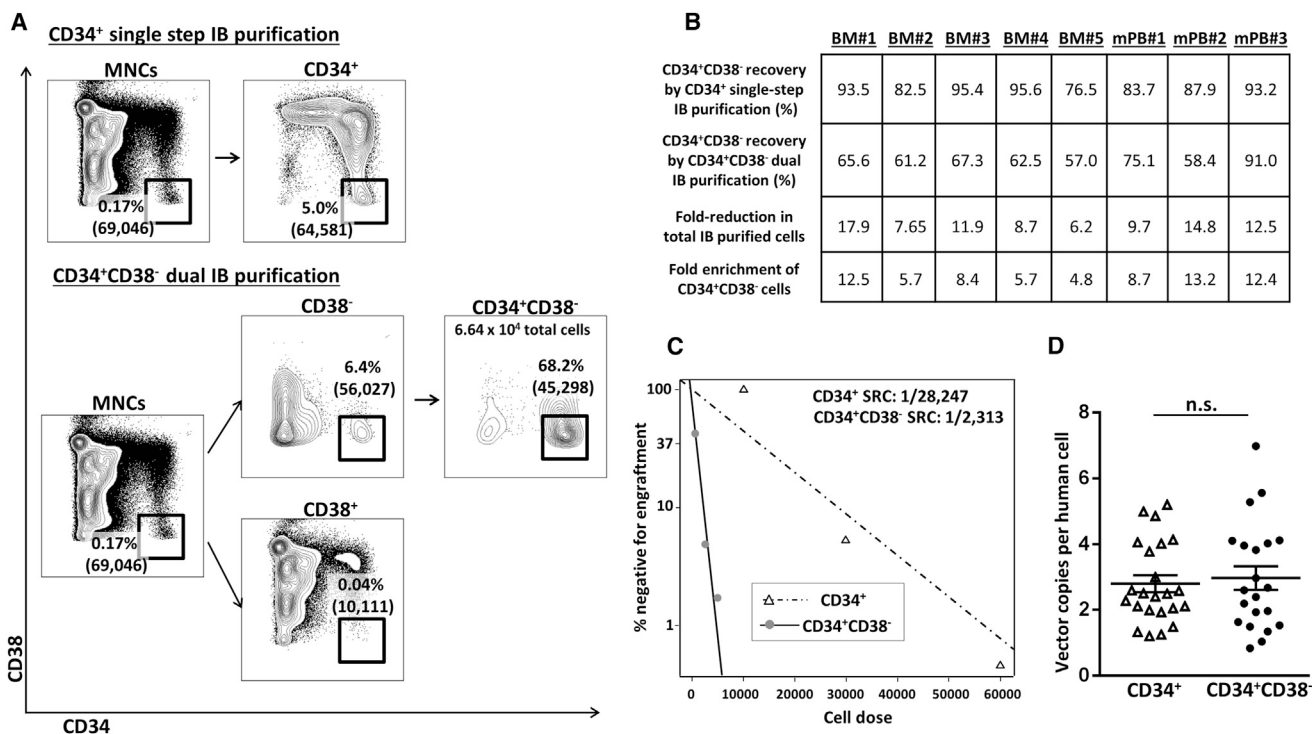
Figure 4. Comparison of CD34$^+$ Single-Step IB Purification versus CD34$^+$CD38$^-$ Dual IB Purification

(A) Comparison of a single representative BM sample purified in parallel by either CD34$^+$ single-step IB purification (top) or CD34$^+$CD38$^-$ dual IB purification (bottom). Gates show CD34$^+$CD38$^-$ cells (defined as the lowest 6% of CD38 expression) with absolute cell counts listed in parentheses. (B) Recovery and enrichment of CD34$^+$CD38$^-$ cells obtained from IB purification of BM and mPB MNCs. 5 BM samples and 3 mPB sample from independent donors were purified in parallel by either CD34$^+$ single-step IB purification or CD34$^+$CD38$^-$ dual IB purification. For each sample, CD34$^+$CD38$^-$ cells were defined as those with the lowest 6% of CD38 expression within CD34$^+$ cells. Recovery indicates the percentage of CD34$^+$CD38$^-$ cells recovered after purification from starting MNCs, and it is calculated for both CD34$^+$ single-step (row 1) and CD34$^+$CD38$^-$ dual IB purification (row 2). Fold-reduction (row 3) indicates the reduction in the total number of cells purified by CD34$^+$CD38$^-$ dual IB selection as compared with standard CD34 selection. This represents the clinically relevant reduction in the number of cells to be transduced and concordant vector dose reduction. Fold-enrichment (row 4) represents the enrichment of CD34$^+$CD38$^-$ cells as a percentage of total cells obtained by CD34$^+$CD38$^-$ dual IB purification compared with standard CD34$^+$ IB purification. (Figure S2 shows absolute cell counts for each IB-purified fraction.) (C) Poisson statistical analysis of limiting dilution NSG xenotransplant assay of IB-purified BM. Plots demonstrate SRC frequency of CCL-UBC-mCitrine transduced CD34$^+$ or CD34$^+$CD38$^-$ IB-purified cells (n = 5–7 mice transplanted at each cell dose per condition; see Figure S3 for individual values). y axis shows the percentage of recipient NSG mice containing <0.015% hCD45$^+$ cells (non-engrafted) in the BM at 16 weeks post-transplantation versus the number of cells injected per mouse (x axis). (D) In vivo VCN analysis. NSG mice were transplanted with IB-purified CD34$^+$ or CD34$^+$CD38$^-$ cells transduced with CCL-UBC-mCitrine LV. 16 weeks post-transplant, engrafted human cells in NSG BM were analyzed for VCN by digital droplet polymerase chain reaction (ddPCR). Data represent three independent experiments performed using BM from independent donors; n = 21–23 mice/group. n.s., not significant. Bars represent mean ± SEM.

transduced CD34$^+$CD38$^-$ cells could produce early hematopoietic recovery comparable with CD34$^+$ cells. In order to avoid xenogeneic graft-versus-host disease (GVHD) in recipient mice receiving CD38$^+$ cells, we purified CD34$^+$, CD34$^+$CD38$^-$, and CD38$^+$ populations from CD3-depleted BM MNCs (Figure 5B). IB-purified CD34$^+$ or CD34$^+$CD38$^-$ cells were transduced with CCL-UBC-mCitrine LV, whereas CD38$^+$ cells were cultured in parallel transduction conditions without LV. NSG-SGM3 mice received 1 marrow equivalent of the grafts depicted in Figure 5B: (1) CD34$^+$ cells (+mCitrine LV), (2) CD34$^+$CD38$^-$ cells (+mCitrine LV), (3) CD34$^+$CD38$^-$ cells (+mCitrine LV) + CD38$^+$ cells (non-transduced), or (4) CD38$^+$ cells (non-transduced). Irradiated CD34$^-$ cells were added as needed so that each mouse received the same number of total cells (Table S1).

Two transplants were performed using BM from independent donors. Transplant 1 used highly purified CD34$^+$CD38$^-$ cells (~1% of total CD34$^+$ cells), and transplant 2 used more moderately purified CD34$^+$CD38$^-$ cells (~12% of total CD34$^+$ cells) (Figure 5C). In transplant 1, mice receiving CD34$^+$CD38$^-$ cells showed significantly reduced levels of circulating human neutrophils at 3 weeks compared with mice transplanted with CD34$^+$ cells. The addition of non-transduced CD38$^+$ cells to the graft significantly increased circulating neutrophil levels. The same pattern was observed in transplant 2, but it did not reach significance when using more moderately purified CD34$^+$CD38$^-$ cells. Thus, when compared with CD34$^+$ cells, moderately purified CD34$^+$CD38$^-$ cells (~12% of total CD34$^+$ cells) do not show as great of an early myeloid deficit when compared with stringently purified CD34$^+$CD38$^-$ cells (~1% of total CD34$^+$ cells). These results
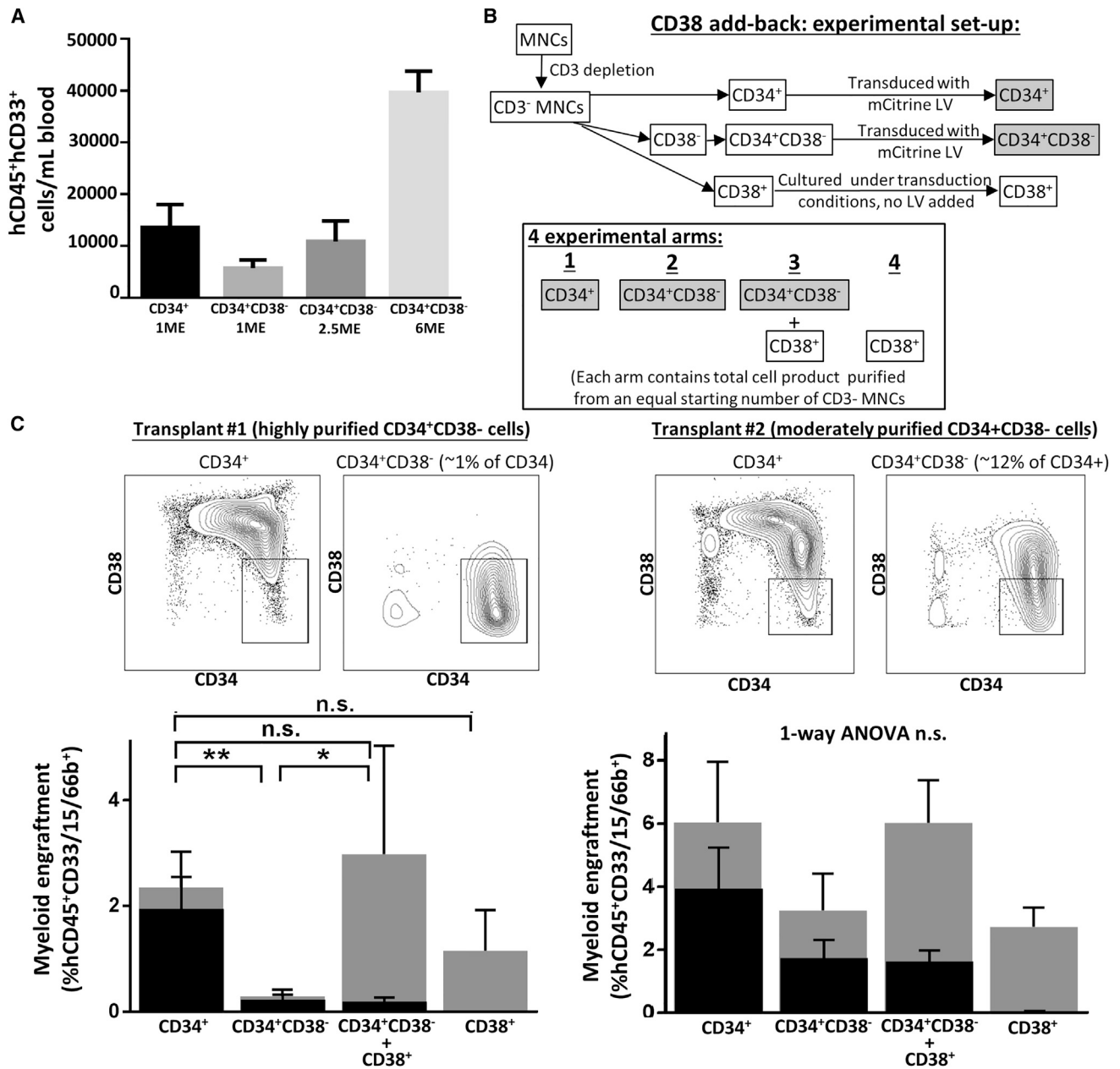
Figure 5. Early Myeloid Potential of IB-Purified CD34$^+$ and CD34$^+$CD38$^-$ Cells

(A) Early myeloid engraftment of CD34$^+$ and CD34$^+$CD38$^-$ IB-purified cells. Peripheral blood hCD45$^+$hCD33$^+$ cells per milliliter was quantified at 4 weeks from NSG-SGM3 mice transplanted with CD34$^+$ cells or increasing doses of CD34$^+$CD38$^-$ cells IB-purified from BM. Cell doses for each group reflect the total cells obtained from IB purification from a standard volume of marrow (marrow equivalent). n = 3 mice/group. Bars represent mean ± SEM. (B) CD38 add-back experimental setup. BM MNCs were IB-depleted of CD3$^+$ T cells to avoid xenogeneic graft-versus-host disease. CD3$^-$ cells were further purified to obtain CD34$^+$, CD34$^+$CD38$^-$, or CD38$^+$ populations. CD34$^+$ and CD34$^+$CD38$^-$ cells were transduced with a CCL-UBC-mCitrine LV, while CD38$^+$ cells were cultured in parallel without the addition of LV. 4 experimental arms were transplanted, with each mouse receiving 1 marrow equivalent of the pictured graft. Gray boxes represent UBC-mCitrine transduced populations; white boxes represent non-transduced populations. (C) Early myeloid engraftment of IB-purified cells in NSG-SGM3 mice. Two transplants were performed using the four arms described in (B). Flow plots show CD34$^+$ or CD34$^+$CD38$^-$ IB-purified cells prior to transplant (left: highly purified CD34$^+$CD38$^-$ cells; right: moderately purified CD34$^+$CD38$^-$ cells). Bar graphs represent mean ± SEM of myeloid engraftment in peripheral blood. Gray bars represent total myeloid engraftment, and overlay of black bars represents gene-marked (mCitrine$^+$) myeloid engraftment. Myeloid engraftment is expressed as the percent of hCD45$^+$CD33$^+$/CD66b$^+$/CD15$^+$ cells out of total CD45$^+$ (human and murine) cells. Each graph represents one experiment performed using BM from independent donors with n = 4–5 mice/arm. *p < 0.05, **p < 0.01. n.s., not significant.

19

are consistent with the retention of CD38^{low} myeloid progenitors within the CD34^{+}CD38^{-} fraction when using a more moderate purification strategy (~12% of total CD34^{+} cells). In both transplants, the majority of human neutrophils present at 3 weeks in arm 3 were mCitrine^{-}, confirming that these cells derive from non-transduced CD38^{+} cells. In the NSG model, we observed a similar defect in early myelopoiesis from transplanted CD34^{+}CD38^{-} cells and rescue by the add-back of CD38^{+} cells (Figure S4), suggesting that these results are not unique to the NSG-SGM3 model. Collectively, these data show that addition of cultured, non-transduced CD38^{+} cells can restore early myeloid engraftment when added to transduced CD34^{+}CD38^{-} cells.

Addition of CD38^{+} Cells Enhances Long-Term Engraftment of Gene-Modified HSCs

We next assessed the effect of adding back non-transduced CD38^{+} cells on long-term gene-marked engraftment. Here, we transplanted IB-purified CD34^{+}, CD34^{+}CD38^{-}, and CD38^{+} cells into NSG mice using the same four experimental arms depicted in Figure 5B. To reflect a clinically relevant scenario, each mouse received the total cell product purified from a set volume of BM. At 16 weeks post-transplant, recipients of CD34^{+}CD38^{-} cells showed decreased engraftment of total (hCD45^{+}) and gene-marked (mCitrine^{+} hCD45^{+}) cells as compared with recipients of CD34^{+} cells (Figure 6A). Addition of non-transduced CD38^{+} cells to the graft of transduced CD34^{+}CD38^{-} cells significantly increased engraftment of gene-marked (hCD45^{+}mCitrine^{+}) cells to levels achieved by CD34^{+} cell transplants. Importantly, this was accomplished using 6.2- and 7.8-fold less LV (in two independent experiments) compared with the volumes required to transduce bulk CD34^{+} cells. All transplanted arms showed similar lineage distribution, with the exception of mice transplanted with CD38^{+} cells alone, which showed a significant myeloid bias in engrafted cells (Figure 6B). PB analysis showed comparable engraftment of total hCD45^{+} cells at all time points after transplant of transduced CD34^{+} cells or transduced CD34^{+}CD38^{-} cells co-transplanted with non-transduced CD38^{+} cells (Figure 6C, left). At early time points (3–12 weeks), transduced CD34^{+} cells showed higher levels of gene-marked (mCitrine^{+}) engraftment than transduced CD34^{+}CD38^{-} cells co-transplanted with non-transduced CD38^{+} cells (Figure 6C, right). However, after 12 weeks, we observed equivalent levels of gene-marked engraftment in these two groups. These data suggest that non-transduced CD38^{+} cells drive early hematopoiesis (3–12 weeks), while gene-marked CD34^{+}CD38^{-} cells take over hematopoiesis 12 weeks after transplant.

DISCUSSION

We have demonstrated a clinically relevant, IB-based method for purifying CD34^{+}CD38^{-} cells from CB, mPB, and BM (Figure 7). We further show that modification of CD34^{+}CD38^{-} cells with a reduced LV dose coupled with co-transplantation with non-modified CD38^{+} cells produced early myeloid reconstitution and long-term engraftment of gene-marked cells comparable with traditional methods of modifying bulk CD34^{+} cells.

The strategy explored here is broadly applicable to a number of HSC-based gene therapy applications and may be especially useful in gene therapy for hemoglobinopathies, where clinical-scale LV production has proven difficult because of the large size and complexity of the human β-globin gene expression cassette. We estimate that the additional cost to purify 1×10^{10} total BM or mPB cells beyond standard CD34^{+} IB purification is ~$10,000 per patient (based on the cost of commercially available CD38 antibody, CD15 antibody, and anti-biotin beads). Therefore, the per-patient cost of improving stem cell enrichment is highly cost-efficient compared with current vector production costs (~$500,000 per patient). Furthermore, this strategy may improve efficiency in clinical-scale HSC gene-editing applications such as CRISPR/Cas9.

While a number of in vivo repopulating studies have shown that HSCs are enriched within the CD34^{+}CD38^{-} fraction,[12–16] we sought to more thoroughly define a target population to isolate for gene modification. The majority of prior work has evaluated the engraftment capacity of FACS-sorted/uncultured cells, whereas current gene therapy protocols require a period of ex vivo culture that likely alters repopulating capacity. Additionally, prior work has used variable definitions for CD34^{+}CD38^{-} cells ranging from the lowest 1% to 30% of CD38 expression. Some work has also suggested that a CD34^{+}CD38^{low} fraction contains long-term repopulating activity.[14,16] Here, we find that within freshly isolated BM CD34^{+} cells, only the lowest 6% of CD38 expression is capable of long-term NSG repopulation after LV transduction/ex vivo culture. Thus, purifying CD34^{+} cells based on CD38 expression alone could lead to a theoretical ~16-fold enrichment of long-term repopulating activity.

High individual donor variability in CD38 expression could be a potential hurdle to clinical translation. Because the lowest 6% of CD38 expression may not encompass >90% of HSCs for every individual, a conservative cutoff for CD38 expression may increase the chance of retaining HSCs. Our results show that the level of CD38 expression retained within the CD38^{+} and CD38^{-} populations can be adjusted by titration of magnetic beads, thereby achieving optimal recovery of CD34^{+}CD38^{-} cells while also maximizing HSC enrichment. Clinical scale-up to GMP-grade IB sorting systems will likely require additional titration of CD38 magnetic labeling specific to the system parameters (magnetic field strength, column flow rate, etc.).

In the dual CD34^{+}CD38^{-} IB protocol, we found that CD38^{+}/CD15^{+} co-depletion increased purity of CD34^{+}CD38^{-} cells by preventing the non-specific enrichment of CD15^{+} granulocytes. Due to the relative rarity of CD34^{+}CD38^{-} cells (~0.1%–0.3% of MNCs), non-specific enrichment of granulocytes can represent >50% of total cells after CD34^{+}CD38^{-} purification. In contrast, CD34^{+} cells are ~10 times more abundant than CD34^{+}CD38^{-} cells (~1%–3% of MNCs); thus, the relative contribution of granulocytes is minor in CD34^{+} purified cells (<10%). Because clinical vector doses are calculated on a per-cell basis, contaminating granulocytes present in CD34^{+} CD38^{-} purified populations could reduce vector MOI and limit the

20
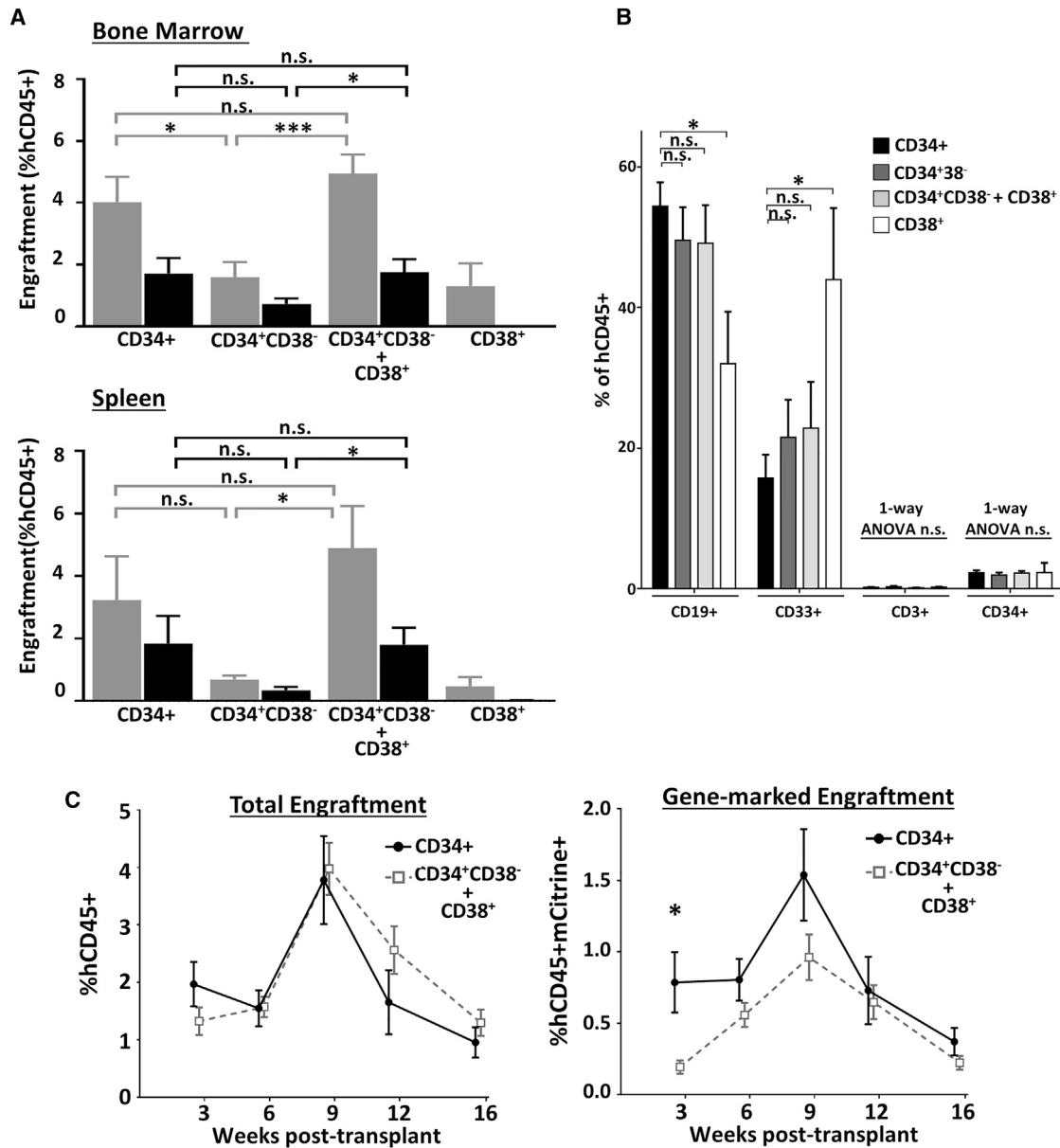
Figure 6. Long-Term Engraftment of IB-Purified Cells

(A) Long-term engraftment of IB-purified cells in NSG BM (top) or spleen (bottom) 16 weeks post-transplant. Gray bars represent mean ± SEM of total human engraftment (% hCD45+); black bars represent gene-marked engraftment (%hCD45+mCitrine+). Engraftment is expressed as the percent of hCD45+ or hCD45+mCitrine+ cells out of total CD45+ (human and murine) cells. Data represent two experiments using BM from independent donors with a total of eight to nine mice per arm. (B) Lineage analysis of total hCD45+ in NSG BM 16 weeks post-transplant. Bars show mean ± SEM of each lineage (CD19+ B cells, CD33+ myeloid cells, CD3+ T cells, and CD34+ HSPCs) expressed as percent of total hCD45+ cells. Data represent two experiments using BM from independent donors with a total of eight to nine mice per arm. (C) PB engraftment over time after transplant of CCL-UBC-mCitrine transduced CD34+ cells (filled circles) or CCL-UBC-mCitrine transduced CD34+CD38− cells combined with non-transduced CD38+ cells (open squares). Left panel shows total PB engraftment (%hCD45+); right panel shows gene-marked engraftment (%hCD45+mCitrine+). *p < 0.05, ***p < 0.001. n.s., not significant.

vector dose reduction achieved by CD34+CD38− IB purification. Furthermore, cryopreservation of a granulocyte-rich cell population could potentially lead to poor cell recovery upon thawing because of granulocyte death and/or clumping.

Application of the optimized CD34+CD38− dual IB method to samples of healthy BM and mPB achieved ~75% recovery and ~10-fold enrichment of phenotypically defined CD34+CD38− cells in mPB, and ~60% recovery and ~5-10-fold enrichment in BM. In BM,

Clinical Cell Processing Pathway
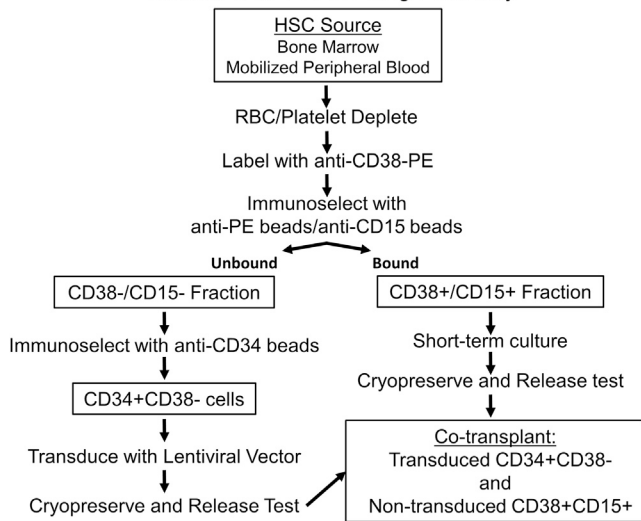
Figure 7. Proposed Clinical Cell Processing Pathway
BM or mPB will be RBC/platelet depleted, followed by labeling with CD38-PE, anti-PE beads, and anti-CD15 beads. The CD38$^+$/CD15$^+$ fraction (bound to the column) will undergo short-term culture followed by cryopreservation and release testing. The CD38$^-$/CD15$^-$ fraction (column flow-through) will be labeled with anti-CD34 beads, followed by selection of CD34$^+$CD38$^-$ cells. CD34$^+$CD38$^-$ cells will undergo transduction with LV followed by cryopreservation and release testing. After successful release testing, transduced CD34$^+$CD38$^-$ cells and non-transduced CD38$^+$/CD15$^+$ cells will be thawed and co-transplanted into a conditioned patient.

CD34$^+$CD38$^-$ purification results in a 12-fold enrichment of SRC beyond standard CD34$^+$ selection. We observed no difference in transduction efficiency of IB-purified CD34$^+$CD38$^-$ or CD34$^+$ cells when evaluated by vector copy number (VCN) analysis of long-term NSG-engrafted human cells. This is in contrast with our lab's previous demonstration that highly purified (FACS-sorted) CB CD34$^+$CD38$^-$ cells demonstrate enhanced transduction in vitro compared with CD34$^+$ cells.[17] This discrepancy could be because of differences in the tissue analyzed (BM versus CB), CD34$^+$CD38$^-$ purity (moderately purified IB-sorted cells versus highly purified FACS-sorted cells), or post-transduction assay (in vitro culture versus in vivo xenografts). Importantly, our results here suggest that the dual IB CD34$^+$CD38$^-$ purification does not impede LV transduction of long-term HSCs.

We next explored the early myeloid potential of IB-purified CD34$^+$CD38$^-$ cells. Prior work has shown that short-term repopulating activity is enriched in the CD34$^+$CD38$^+$ fraction,[18] suggesting that CD34$^+$CD38$^+$ progenitors may be necessary for early myeloid recovery. However, murine studies have suggested that high doses of purified stem cells can lead to rapid hematopoietic recovery.[19,20] Clinical trials using FACS-sorted CD34$^+$CD90$^+$ cells have demonstrated prompt neutrophil and platelet engraftment in patients transplanted with >0.8 × 10^6 CD34$^+$CD90$^+$ cells/kg.[8-10] However, the purified CD34$^+$CD90$^+$ populations in these studies represented ∼50% of total CD34$^+$ cells, whereas the IB-purified CD34$^+$CD38$^-$ cells evalu-

ated here represent ∼10% of total CD34$^+$ cells. Therefore, it is largely unknown whether high doses of purified CD34$^+$CD38$^-$ cells could provide rapid myeloid reconstitution in a clinical transplant setting, or if co-transplant of CD34$^+$CD38$^+$ cells will be required.

Here, we observed that IB-purified CD34$^+$CD38$^-$ cells were capable of early myeloid reconstitution, but contained less early myeloid potential than an equivalent marrow volume of CD34$^+$ cells. Our xenograft data suggest that approximately two to three times as many IB-purified CD34$^+$CD38$^-$ cells (when transplanted alone) may be required to achieve early myeloid reconstitution comparable with CD34$^+$ cells. In a clinical scenario, it is possible that the total product of CD34$^+$CD38$^-$ cells obtained will be above the threshold required for sufficient myeloid reconstitution. However, we favor the safer approach of adding non-transduced CD38$^+$ cells (containing CD34$^+$CD38$^+$ progenitors) to the graft, because transplant of bulk CD34$^+$ cells in gene therapy clinical trials has historically provided prompt myeloid reconstitution.

Furthermore, add-back of non-transduced CD38$^+$ cells may also play a critical role in achieving optimal long-term engraftment of gene-modified HSCs. In long-term NSG transplant assays, we observed decreased engraftment of both total and gene-marked cells in recipients receiving CD34$^+$CD38$^-$ cells alone as compared with recipients receiving CD34$^+$ cells. However, when non-transduced CD38$^+$ cells were added to transduced CD34$^+$CD38$^-$ cells, levels of gene-modified engraftment were equivalent to those achieved by standard CD34$^+$ transduction/transplant. These data suggest that the CD34$^+$CD38$^-$ dual IB purification method efficiently recovers HSCs but requires co-transplantation of CD34$^+$CD38$^+$ cells for optimal long-term engraftment. In agreement with our findings, prior work has demonstrated that cycling CD34$^+$CD38$^+$ cells facilitate HSC engraftment[21-23] through enhancement of stromal cell-dervived factor 1 (SDF-1)-mediated homing and secretion of metalloproteinase (MMP)-9.[23]

An important advantage of using CD38 as an enrichment marker is that it can cleanly separate HSC-containing and HSC-devoid fractions; virtually no repopulating activity is contained within the CD38$^+$ fraction, and almost all repopulating activity is contained within the CD34$^+$CD38$^{0\%-6\%}$ fraction. Although additional HSC markers have been identified[24,25] (e.g., CD90, CD45RA, and CD49f), in vivo xenograft analysis of human HSC populations suggests that these markers *enrich* for HSCs but do not exclusively *define* HSCs. For example, CD34$^+$CD38$^-$CD45RA$^-$CD90$^+$ cells contain more HSCs per cell than CD34$^+$CD38$^-$CD45RA$^-$90$^-$ cells; however, CD34$^+$CD38$^-$CD45RA$^-$90$^-$ cells *do* contain long-term HSCs capable of multi-lineage reconstitution of NSG mice.[24] Thus, discarding the CD34$^+$CD38$^-$CD45RA$^-$90$^-$ population prior to gene modification or transplant would likely result in a lower total HSC dose and could be disadvantageous in a clinical scenario.

In our CD38 add-back transplant studies, we used a conservative CD38 depletion strategy (6.2- to 7.8-fold reduction in cell

number/LV) in order to maximize the number of HSCs retained in the CD38⁻ fraction. It is possible that further reductions in total cell number and LV dose could be achieved using a more stringent CD38 depletion or using additional cell surface markers (e.g., CD90, CD49f). These strategies may be advantageous if highly purified HSCs can be modified and expanded with compounds such as StemRegenin-1 (SR-1),[26,27] prostaglandin E2 (PGE2),[28,29] or UM171.[30]

In summary, we demonstrate a method to improve the efficiency of gene therapy for genetic blood cell diseases through improved HSC enrichment and reduced LV dose.

MATERIALS AND METHODS

MNC Isolation

Healthy adult BM and mPB were obtained from commercial sources (All Cells and Hemacare). Umbilical CB was obtained after vaginal and cesarean deliveries at UCLA Medical Center. All specimens obtained have been deemed as anonymous medical waste exempt from institutional review board review. MNCs were isolated using Ficoll-Paque PLUS (GE Healthcare) density centrifugation within 48 hr of collection. The total number of MNCs used for IB purification varied with each cell product and ranged from 4×10^6 to 4×10^7 (absolute cell numbers are summarized in Figure S2B).

IB Purification of CD34⁺ and CD34⁺CD38⁻ Cells

All microbeads and magnetic columns used for cell separation were purchased from Miltenyi Biotec. All incubation steps were performed in magnetic-activated cell sorting (MACS) buffer (PBS/0.5% BSA/2 mM EDTA) at 4°C with 10^7 cells/100 μL total volume. Total reagent/buffer volumes were scaled accordingly based on MNC number in order to keep cell density and reagent concentration constant for each processed sample. Concentrations described for each reagent represent the reagent volume:total volume of reagent and MACS buffer.

MNCs were first stained with CD38-PE (1:15, Clone IB6; Miltenyi Biotec), CD34-fluorescein isothiocyanate (FITC) (1:10, Clone 581; BD Biosciences), and CD45-allophycocyanin (APC) (1:10, Clone HI30; BD Biosciences) for 30 min. Stained MNCs were washed once with MACS buffer and divided into equal fractions for further IB processing. Each experiment comparing CD34⁺ and CD34⁺ CD38⁻ IB purification (cell counts and xenograft studies) utilized the total purified cell product isolated from an equal starting volume of MNCs (defined in the text as marrow equivalent).

To purify CD34⁺ cells, we incubated MNCs with anti-CD34 microbeads (1:5) for 30 min, washed them, and added them to an LS column. The column was washed with 3×3 mL of MACS buffer. CD34⁺ CD38⁻ cells were purified by first incubating MNCs with anti-PE microbeads (1:5–1:25 for bead titration studies, 1:10 for mPB purification, 1:40 for BM purification and xenograft studies) and anti-CD15 microbeads (1:5) for 15 min. Cells were washed and applied to an LD column. The column was washed with 2×1 mL fractions

of MACS buffer. After washing, the CD38⁺/CD15⁺ fraction was flushed from the column. The CD38⁻/CD15⁻ flow-through fraction was collected, washed, and subsequently selected with anti-CD34 microbeads as described above. To obtain absolute CD34⁺CD38⁻ cell counts in each fraction, we added 3×100 μL aliquots to 300 μL of MACS buffer and 50 μL of counting beads (eBioscience) and DAPI (1:1,000; Life Technologies), and analyzed them on an LSRII or LSR Fortessa flow cytometer (BD Biosciences) (Figure S2). In xenograft experiments where CD38⁺ cells were added back to the graft, CD3-depleted MNCs were used as a starting material to deplete mature human T cells and avoid xenogeneic GVHD. MNCs were incubated with anti-CD3 microbeads (1:5) at 4°C for 15 min, washed, and separated on an LD column. CD3⁻ cells were immediately processed by further CD34⁺ or CD34⁺CD38⁻ IB purification.

Cell Sorting

BM MNCs were enriched for CD34⁺ cells as described and were stained with CD38-PE (1:15, Clone IB6; Miltenyi) and CD34-APC (1:10, Clone 581; BD Biosciences) in MACS buffer for 30 min at 4°C, followed by washing to remove unbound antibody. DAPI (1:1,000; Life Technologies) was added just before analysis. Cells were gated on viable, single CD34⁺ cells (Figure S1A) prior to defining CD38 intervals. Cells were sorted according to defined intervals of CD38 expression using a FACSAria II (BD Biosciences).

LV Transduction

Construction, packaging, and titering of CCL-UBC-mCitrine-PRE-FB-2XUSE, CCL-UBC-mStrawberry-PRE-FB-2XUSE, and CCL-UBC-mCerulean-PRE-FB-2XUSE have been described.[17] Cells were plated on retronectin (Takara Shuzo)-coated plates (20 μg/mL) at a density of $0.5–1 \times 10^6$ cells/mL in X-VIVO15 medium (Lonza) containing 1× glutamine/penicillin/streptomycin (Gemini BioProducts), 50 ng/mL SCF, 50 ng/mL fms-related tyrosine kinase 3 ligand (Flt3-L), 50 ng/mL thrombopoietin (TPO), and 20 ng/mL IL-3 (PeproTech). LV was added to a final concentration of 2×10^7 TU/mL and incubated with cells for 24 hr prior to transplant. All LV concentrations (transducing units [TU]/mL), cell concentrations (cells/mL), and cell plating densities (cells/cm²) were kept constant during transduction of CD34⁺ and CD34⁺CD38⁻ cells by adjusting the total number of wells for plating/transduction proportional to cell counts (CD34⁺ cells required ~5–10 times more cell culture wells than CD34⁺CD38⁻ cells).

Xenografts

All work with mice was done under protocols approved by the UCLA Animal Care Committee. 6- to 10-week-old male and female NOD.Cg-Prkdsci-dIl2rgtm1Wjil/SzJ (NSG) and NOD.Cg-PrkdcscidIl2rgtm1WjlTg(CMV-IL-3, CSF2, KITLG)1Eav/MloySzJ (NSG-SGM3) mice (Jackson Laboratory) were used as transplant recipients. Mice were irradiated 4–6 hr prior to transplantation using a ¹³⁷Cesium source at a total dose of 250 rad (~101 rad/min). Cells were harvested from retronectin-coated dishes by gentle pipetting and PBS washes. Collection of all cells from each well was verified by visual inspection under the microscope. Collected cells were

washed, resuspended in PBS, and administered via intravenous injection into the retro-orbital sinus. CD34$^-$ cells were irradiated (10 Gy) and added to grafts as filler cells (total cell doses per mouse are listed in Table S1).

Engraftment Analysis

Engraftment of human cells in PB, BM, and spleen of xenograft recipient mice was evaluated by flow cytometry using anti-human CD45-APC (HI30), anti-murine CD45-PE (Clone 30-FII), anti-human CD33-V450 (Clone P67-6), anti-human CD66b-V450 (Clone G10F5), anti-human CD15-V450 (Clone HI98), anti-human CD3-PerCP-Cy5.5 (Clone SK7), anti-human CD19-APC-Cy7 (SJ25CI), and anti-human CD34-PE-Cy7 (Clone 581) (all antibodies are from BD Biosciences).

Determination of Vector Copies per Human Cell

The average vector copies (VCs) per human cell was measured in engrafted NSG BM samples as previously described.[17] In brief, LV DNA content was quantified using a digital droplet PCR probe specific to the HIV-1 Psi region and normalized to the autosomal human gene SDC4.

Statistics

Pairwise comparison was performed by unpaired t test within the framework of one-way ANOVA. Two group comparisons by Wilcoxon rank-sum test were performed when the assumption of normality was not met. Hypothesis testing was two-sided, and a significance threshold of $p = 0.05$ was used. Limiting dilution analysis was performed using online software provided by Walter and Eliza Hall Institute (WEHI) bioinformatics.[31]

SUPPLEMENTAL INFORMATION

Supplemental Information includes four figures and one table and can be found with this article online at http://dx.doi.org/10.1016/j.ymthe.2017.05.023.

AUTHOR CONTRIBUTIONS

K.E.M. designed, performed, and analyzed experiments and wrote the manuscript. D.B. and J.L. performed portions of the research studies. R.P.H. provided study materials and advised experiments. F.U. advised experiments. D.B.K. participated in conception and design of the studies, provided financial support through grant funding, and co-wrote the manuscript.

CONFLICTS OF INTEREST

The authors declare no conflict of interest.

ACKNOWLEDGMENTS

REFERENCES

1. Boztug, K., Schmidt, M., Schwarzer, A., Banerjee, P.P., Díez, I.A., Dewey, R.A., Böhm, M., Nowrouzi, A., Ball, C.R., Glimm, H., et al. (2010). Stem-cell gene therapy for the Wiskott-Aldrich syndrome. N. Engl. J. Med. 363, 1918–1927.

2. Aiuti, A., Cattaneo, F., Galimberti, S., Benninghoff, U., Cassani, B., Callegaro, L., Scaramuzza, S., Andolfi, G., Mirolo, M., Brigida, I., et al. (2009). Gene therapy for immunodeficiency due to adenosine deaminase deficiency. N. Engl. J. Med. 360, 447–458.

3. Aiuti, A., Biasco, L., Scaramuzza, S., Ferrua, F., Cicalese, M.P., Baricordi, C., Dionisio, F., Calabria, A., Giannelli, S., Castiello, M.C., et al. (2013). Lentiviral hematopoietic stem cell gene therapy in patients with Wiskott-Aldrich syndrome. Science 341, 1233151.

4. Candotti, F., Shaw, K.L., Muul, L., Carbonaro, D., Sokolic, R., Choi, C., Schurman, S.H., Garabedian, E., Kesserwan, C., Jagadeesh, G.J., et al. (2012). Gene therapy for adenosine deaminase-deficient severe combined immune deficiency: clinical comparison of retroviral vectors and treatment plans. Blood 120, 3635–3646.

5. Hacein-Bey-Abina, S., Hauer, J., Lim, A., Picard, C., Wang, G.P., Berry, C.C., Martinache, C., Rieux-Laucat, F., Latour, S., Belohradsky, B.H., et al. (2010). Efficacy of gene therapy for X-linked severe combined immunodeficiency. N. Engl. J. Med. 363, 355–364.

6. Kang, E.M., Choi, U., Theobald, N., Linton, G., Long Priel, D.A., Kuhns, D., and Malech, H.L. (2010). Retrovirus gene therapy for X-linked chronic granulomatous disease can achieve stable long-term correction of oxidase activity in peripheral blood neutrophils. Blood 115, 783–791.

7. Modell, B., and Darlison, M. (2008). Global epidemiology of haemoglobin disorders and derived service indicators. Bull. World Health Organ. 86, 480–487.

8. Tricot, G., Gazitt, Y., Leemhuis, T., Jagannath, S., Desikan, K.R., Siegel, D., Fassas, A., Tindle, S., Nelson, J., Juttner, C., et al. (1998). Collection, tumor contamination, and engraftment kinetics of highly purified hematopoietic progenitor cells to support high dose therapy in multiple myeloma. Blood 91, 4489–4495.

9. Negrin, R.S., Atkinson, K., Leemhuis, T., Hanania, E., Juttner, C., Tierney, K., Hu, W.W., Johnston, L.J., Shizurn, J.A., Stockerl-Goldstein, K.E., et al. (2000). Transplantation of highly purified CD34+Thy1+ hematopoietic stem cells in patients with metastatic breast cancer. Biol. Blood Marrow Transplant. 6, 262–271.

10. Michallet, M., Philip, T., Philip, I., Godinot, H., Sebban, C., Salles, G., Thiebaut, A., Biron, P., Lopez, F., Mazars, P., et al. (2000). Transplantation with selected autologous peripheral blood CD34+Thy1+ hematopoietic stem cells (HSCs) in multiple myeloma: impact of HSC dose on engraftment, safety, and immune reconstitution. Exp. Hematol. 28, 858–870.

11. Miller, P.H., Cheung, A.M.S., Beer, P.A., Knapp, D.J.H.F., Dhillon, K., Rabu, G., Rostamirad, S., Humphries, R.K., and Eaves, C.J. (2013). Enhanced normal short-term human myelopoiesis in mice engineered to express human-specific myeloid growth factors. Blood 121, e1–e4.

12. Larochelle, A., Vormoor, J., Hanenberg, H., Wang, J.C., Bhatia, M., Lapidot, T., Moritz, T., Murdoch, B., Xiao, X.L., Kato, I., et al. (1996). Identification of primitive human hematopoietic cells capable of repopulating NOD/SCID mouse bone marrow: implications for gene therapy. Nat. Med. 2, 1329–1337.

13. Bhatia, M., Wang, J.C., Kapp, U., Bonnet, D., and Dick, J.E. (1997). Purification of primitive human hematopoietic cells capable of repopulating immune-deficient mice. Proc. Natl. Acad. Sci. USA 94, 5320–5325.

14. Hogan, C.J., Shpall, E.J., and Keller, G. (2002). Differential long-term and multilineage engraftment potential from subfractions of human CD34+ cord blood cells transplanted into NOD/SCID mice. Proc. Natl. Acad. Sci. USA 99, 413–418.

15. Ishikawa, F., Livingston, A.G., Minamiguchi, H., Wingard, J.R., and Ogawa, M. (2003). Human cord blood long-term engrafting cells are CD34+ CD38-. Leukemia 17, 960–964.

16. McKenzie, J.L., Gan, O.I., Doedens, M., and Dick, J.E. (2007). Reversible cell surface expression of CD38 on CD34-positive human hematopoietic repopulating cells. Exp. Hematol. 35, 1429–1436.

17. Baldwin, K., Urbinati, F., Romero, Z., Campo-Fernandez, B., Kaufman, M.L., Cooper, A.R., Masiuk, K., Hollis, R.P., and Kohn, D.B. (2015). Enrichment of human hematopoietic stem/progenitor cells facilitates transduction for stem cell gene therapy. Stem Cells 33, 1532–1542.

18. Glimm, H., Eisterer, W., Lee, K., Cashman, J., Holyoake, T.L., Nicolini, F., Shultz, L.D., von Kalle, C., and Eaves, C.J. (2001). Previously undetected human hematopoietic cell populations with short-term repopulating activity selectively engraft NOD/SCID-beta2 microglobulin-null mice. J. Clin. Invest. *107*, 199–206.

19. Uchida, N., Aguila, H.L., Fleming, W.H., Jerabek, L., and Weissman, I.L. (1994). Rapid and sustained hematopoietic recovery in lethally irradiated mice transplanted with purified Thy-1.1lo Lin-Sca-1+ hematopoietic stem cells. Blood *83*, 3758–3779.

20. Uchida, N., Tsukamoto, A., He, D., Friera, A.M., Scollay, R., and Weissman, I.L. (1998). High doses of purified stem cells cause early hematopoietic recovery in syngeneic and allogeneic hosts. J. Clin. Invest. *101*, 961–966.

21. Verstegen, M.M.A., van Hennik, P.B., Terpstra, W., van den Bos, C., Wielenga, J.J., van Rooijen, N., Ploemacher, R.E., Wagemaker, G., and Wognum, A.W. (1998). Transplantation of human umbilical cord blood cells in macrophage-depleted SCID mice: evidence for accessory cell involvement in expansion of immature CD34+CD38- cells. Blood *91*, 1966–1976.

22. Bonnet, D., Bhatia, M., Wang, J.C., Kapp, U., and Dick, J.E. (1999). Cytokine treatment or accessory cells are required to initiate engraftment of purified primitive human hematopoietic cells transplanted at limiting doses into NOD/SCID mice. Bone Marrow Transplant. *23*, 203–209.

23. Byk, T., Kahn, J., Kollet, O., Petit, I., Samira, S., Shivtiel, S., Ben-Hur, H., Peled, A., Piacibello, W., and Lapidot, T. (2005). Cycling G1 CD34+/CD38+ cells potentiate the motility and engraftment of quiescent G0 CD34+/CD38-/low severe combined immunodeficiency repopulating cells. Stem Cells *23*, 561–574.

24. Majeti, R., Park, C.Y., and Weissman, I.L. (2007). Identification of a hierarchy of multipotent hematopoietic progenitors in human cord blood. Cell Stem Cell *1*, 635–645.

25. Notta, F., Doulatov, S., Laurenti, E., Poeppl, A., Jurisica, I., and Dick, J.E. (2011). Isolation of single human hematopoietic stem cells capable of long-term multilineage engraftment. Science *333*, 218–221.

26. Boitano, A.E., Wang, J., Romeo, R., Bouchez, L.C., Parker, A.E., Sutton, S.E., Walker, J.R., Flaveny, C.A., Perdew, G.H., Denison, M.S., et al. (2010). Aryl hydrocarbon receptor antagonists promote the expansion of human hematopoietic stem cells. Science *329*, 1345–1348.

27. Wagner, J.E., Jr., Brunstein, C.G., Boitano, A.E., DeFor, T.E., McKenna, D., Sumstad, D., Blazar, B.R., Tolar, J., Le, C., Jones, J., et al. (2016). Phase I/II trial of StemRegenin-1 expanded umbilical cord blood hematopoietic stem cells supports testing as a stand-alone graft. Cell Stem Cell *18*, 144–155.

28. North, T.E., Goessling, W., Walkley, C.R., Lengerke, C., Kopani, K.R., Lord, A.M., Weber, G.J., Bowman, T.V., Jang, I.H., Grosser, T., et al. (2007). Prostaglandin E2 regulates vertebrate haematopoietic stem cell homeostasis. Nature *447*, 1007–1011.

29. Cutler, C., Multani, P., Robbins, D., Kim, H.T., Le, T., Hoggatt, J., Pelus, L.M., Desponts, C., Chen, Y.B., Rezner, B., et al. (2013). Prostaglandin-modulated umbilical cord blood hematopoietic stem cell transplantation. Blood *122*, 3074–3081.

30. Fares, I., Chagraoui, J., Gareau, Y., Gingras, S., Ruel, R., Mayotte, N., Csaszar, E., Knapp, D.J., Miller, P., Ngom, M., et al. (2014). Cord blood expansion. Pyrimidoindole derivatives are agonists of human hematopoietic stem cell self-renewal. Science *345*, 1509–1512.

31. Hu, Y., and Smyth, G.K. (2009). ELDA: extreme limiting dilution analysis for comparing depleted and enriched populations in stem cell and other assays. J. Immunol. Methods *347*, 70–78.

Supplemental Information

Improving Gene Therapy Efficiency

through the Enrichment of Human

Hematopoietic Stem Cells

Katelyn E. Masiuk, Devin Brown, Jennifer Laborada, Roger P. Hollis, Fabrizia Urbinati, and Donald B. Kohn
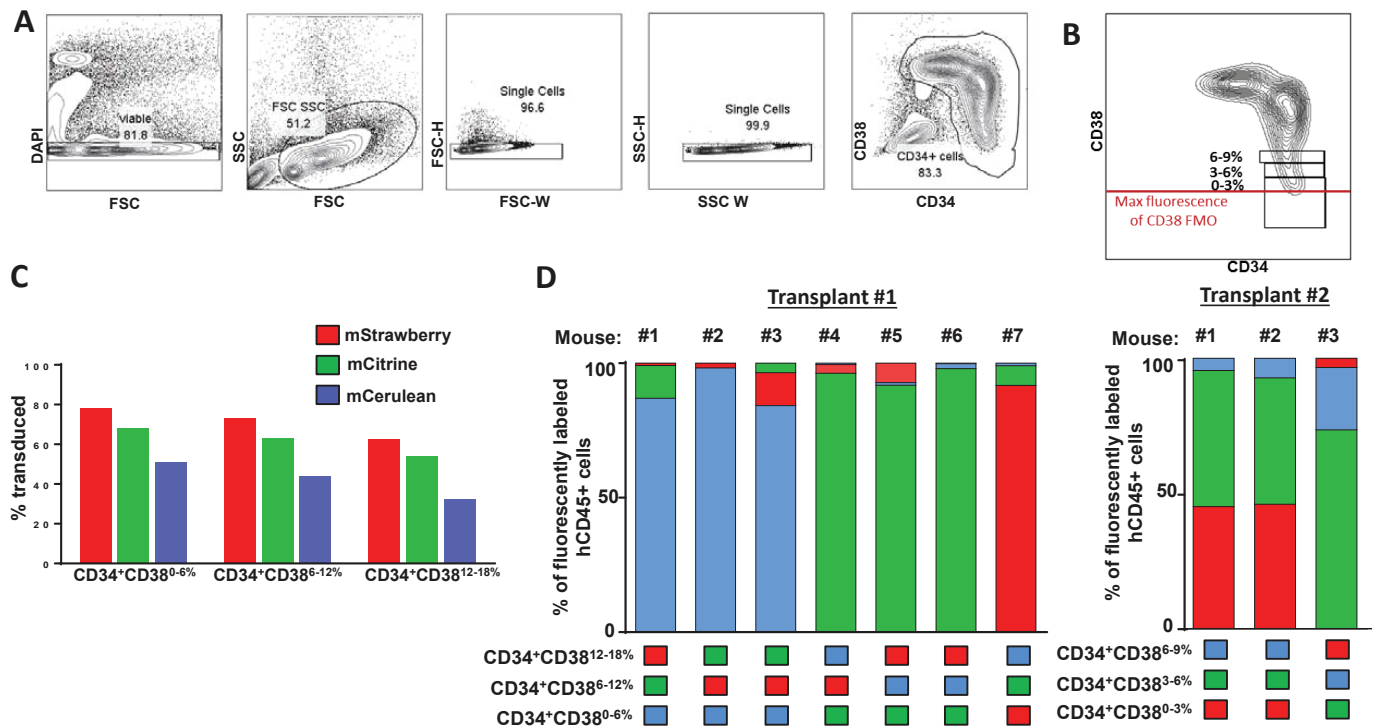
Figure S1

(A) Flow cytometry gating for BM CD34$^+$ cells prior to defining CD38 intervals. Far right panel shows CD34$^+$ cells used to determine intervals of CD38 expression (e.g. CD34$^+$CD38$^{0-3\%}$) **(B)** FACS plot shows sorted CD38 intervals relative to the max fluorescence of the CD38 FMO control (red line). **(C)** Bar graphs show transduction efficiency for each vector (mStrawberry, mCitrine, or mCerulean). Transduced cells were cultured for 14 days and transduction efficiency was measured by flow cytometry. **(D)** Graphs show long-term (16-18 week) fluorescent marking of hCD45+ cells in BM by individual mouse. Each bar represents a single mouse and colors within each bar represent the relative contribution of each labeled fraction. Color coding represents the LV used for each fraction

(green=mCitrine, blue=mCerulean, red=mStrawberry). Lower chart shows the color assigned to each sorted fraction transplanted. Colors were rotated among fractions and mice to account for differences in transduction efficiency among the vectors. Data show that repopulating activity does not appear to be influenced by color choice

A
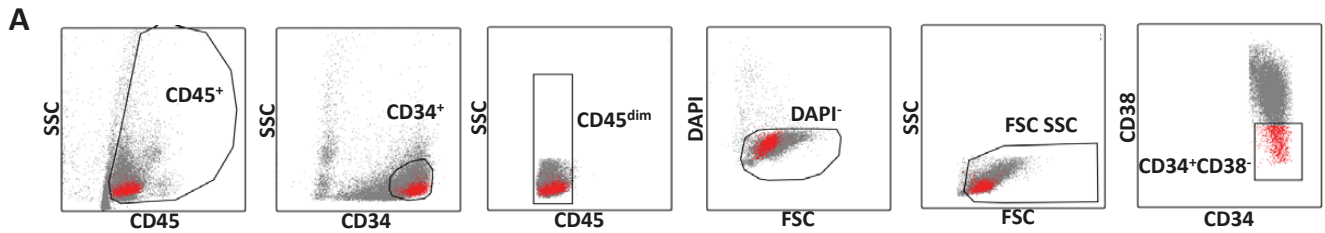
B

Sample	MNCs	CD34+	CD34+CD38-	CD38+
BM #1	4.0×10^7 (69,046)	1.2×10^6 (64,581)	6.6×10^4 (45,298)	2.2×10^7 (10,111)
BM #2	3.5×10^7 (102,668)	1.83×10^6 (84,718)	2.4×10^5 (62,910)	2.0×10^7 (22,241)
BM #3	7.9×10^6 (27,730)	5.5×10^5 (26,458)	4.6×10^4 (18,665)	5.9×10^6 (4,789)
BM#4	3.8×10^6 (37,842)	6.1×10^5 (36,194)	7.1×10^4 (23,649)	6.9×10^6 (2,448)
BM #5	1.5×10^7 (36,755)	4.3×10^5 (28,148)	7.0×10^4 (21,145)	1.1×10^7 (6,220)
mPB#1	2.8×10^7 (38,411)	5.6×10^5 (32,145)	6.2×10^4 (28,849)	2.1×10^7 (4,557)
mPB#2	1.9×10^7 (30,746)	4.8×10^5 (27,023)	3.2×10^4 (17,979)	1.9×10^7 (18,861)
mPB#3	1.2×10^7 (10,421)	5.4×10^5 (9,510)	4.3×10^4 (9,692)	5.7×10^6 (400)

Figure S2

a. Gating for enumeration of CD34+CD38- in MACS purified fractions. CD34+CD38- backgating is shown in red

b. Table shows total cell counts by IB purified fraction. Numbers show total cells isolated in each fraction, with CD34+CD38- cell counts listed in parentheses.

a.

Engraftment (%hCD45+) for CD34+, CD34+CD38-, and Non-transplanted controls at Cell dose #1, #2, #3. Dashed line at 0.015%.

b.

Engrafted mouse (0.017% hCD45+) and Non-transplanted control FACS plots (mCD45 vs hCD45), showing mCD45+ and hCD45+ gates.

Mice transplanted with CD34+ cells:

Cell dose	Number of cells	Engrafted mice
#1	60,000	5/5
#2	30,000	5/7
#3	10,000	0/6

Mice transplanted with CD34+CD38- cells:

Cell dose	Number of cells	Engrafted mice
#1	4,865	5/6
#2	2,432	5/7
#3	810	2/7

Figure S3: Limiting Dilution Analysis of CD34+ and CD34+CD38- IB purified cells.
(A) Engraftment (%hCD45+) for each mouse at 3 different cell doses. Each cell dose represents 34+ or 34+38- cells purified from an equivalent volume of marrow. Dashed line depicts the engraftment cut-off of 0.015% hCD45+, which was arbitrarily chosen as ~20 times the mean engraftment measured in 5 non-transplanted controls. Tables show cell numbers for each transplanted group and the number of mice with engraftment >0.015% at each cell dose.

(B) FACS plots show detection of hCD45+ cells at levels near cut-off for engraftment (0.015% hCD45+). A non-transplanted control is shown for comparison.

Figure S4

a. Determination of human myeloid engraftment in peripheral blood by flow cytometry. Human myeloid engraftment is expressed as the percent of hCD45+CD33/CD66b/CD15+ cells out of total CD45+ (human and murine) cells

b. Values for myeloid engraftment (Figure 5c). Table shows %hCD45+hCD33+ cells in peripheral blood for each mouse analyzed at 3 weeks post-transplant

c. CD38 addback into NSG mice. Gray bars represent mean ± SEM of total human myeloid engraftment in peripheral blood (%hCD45+CD33/CD66b/CD15+ out of total CD45+). Overlay of black bars represent mCitrine+ human myeloid cells

(%mCitrine+hCD45+CD33/CD66b/CD15+ out of total CD45+). Data represents 2 experiments using bone marrow from

independent donors with n=9-10 mice/arm. To account for engraftment variability between donors, data from each experiment was normalized to mean CD34+ values for each experiment.

B.

Transplant Group	Transplant #1 (Highly purified CD34+CD38-)					n	Mean	SEM
CD34+	1.89	1.99	2.02	4.93	0.93	5	2.35	0.68
CD34+CD38-	0.15	0.81	0.11	0.17	0.23	5	0.29	0.13
CD34+CD38- + CD38+	1.00	11.16	0.49	0.80	1.45	5	2.98	2.05
CD38+	0.45	3.45	0.55	0.18		4	1.16	0.77
Transplant Group	Transplant #2 (Moderately purified CD34+CD38-)					n	Mean	SEM
CD34+	12.45	8.09	3.72	4.47	1.50	5	6.05	1.92
CD34+CD38-	7.59	3.01	1.37	3.25	1.04	5	3.25	1.17
CD34+CD38- + CD38+	6.73	8.66	5.94	7.88	0.94	5	6.03	1.35
CD38+	3.98	2.94	3.88	2.20	0.68	5	2.73	0.61

Chapter 3:

PGE2 and Poloxamer Synperonic F108 Enhance Transduction of Human HSPC with a β-Globin Lentiviral Vector

(Mol Ther. Methods Clin. Dev. 2019. In press)

PGE2 and Poloxamer Synperonic F108 Enhance Transduction of Human HSPC with a β-Globin Lentiviral Vector

Katelyn E. Masiuk[1], Ruixue Zhang[1], Kyle Osborne[1], Roger P. Hollis[1], Beatriz Campo-Fernandez[1], Donald B. Kohn[1,2,3]

[1]Department of Microbiology, Immunology & Molecular Genetics, University of California, Los Angeles, California USA, 90095

[2]Department of Pediatrics, David Geffen School of Medicine, University of California, Los Angeles, California USA, 90095

[3]Department of Molecular & Medical Pharmacology, David Geffen School of Medicine, University of California, Los Angeles, California USA, 90095

ABSTRACT

Lentiviral vector (LV)-based hematopoietic stem and progenitor cell (HSPC) gene therapy is becoming a promising alternative to allogeneic stem cell transplantation for curing genetic diseases. Clinical trials are currently underway to treat sickle cell disease using LVs expressing designed anti-sickling globin genes. However, due to the large size and complexity of the human β-globin gene, LV products often have low titers and transduction efficiency, requiring large amounts to treat a single patient. Furthermore, transduction of patient HSPCs often fails to achieve sufficiently high vector copy number (VCN) and transgene expression for clinical benefit. We therefore investigated the combination of two compounds (PGE2 and poloxamer synperonic F108) to enhance transduction of HSPC with a clinical-scale preparation of Lenti/G-AS3-FB. Here, we found that transduction enhancers increased the *in vitro* VCN of bulk myeloid cultures ~10-fold while using a 10-fold lower LV dose. This was accompanied by an increased percentage of transduced colony forming units. Importantly, analysis of immune-deficient NSG xenografts revealed that the combination of PGE2/synperonic F108 increased LV gene transfer in a primitive HSC population with no effects on lineage distribution or engraftment. The use of transduction enhancers may greatly improve efficacy for LV-based HSPC gene therapy.

INTRODUCTION

Sickle cell disease (SCD) is the most prevalent monogenic blood disorder affecting 100,000 people in the US and millions worldwide[1,2]. SCD is caused by a point mutation in the β-globin gene which leads to hemoglobin polymerization and sickling of red blood cells under conditions of low oxygen tension. Sickled red blood cells lead to a number of vascular complications such as pain crises, stroke, and organ damage, which ultimately result in significant morbidity and early mortality[3].

While currently available medical treatments for SCD are aimed at managing disease burden, the only curative option is allogeneic hematopoietic stem cell (HSC) transplantation. However, allogeneic HSC transplantation is unavailable to most patients due to lack of an immunologically matched donor. In recent years, autologous HSC transplant with gene therapy has emerged as a promising alternative which allows patients to serve as their own HSC donor. In this approach, HSPC are collected from a patient, modified *ex vivo* using LVs to express an anti-sickling globin transgene, and transplanted back into the patient to engraft the bone marrow and provide a durable source of healthy, non-sickled red blood cells.

Many successful gene therapies for other genetic blood disorders have used relatively simple LVs with small genomes to drive high levels of a transgene product from a constitutively active, strong promoter[4]. In contrast, current LV candidates for SCD are more complex and utilize large elements of the endogenous β-globin locus control region (LCR) to drive erythroid-specific expression of anti-sickling globin transgenes in mature erythrocytes[5,6]. The large size and complex nature of these LVs has led to a number of hurdles to clinical translation. Globin LVs exhibit poor titers and require large production volumes of GMP-grade LV to treat a single patient, which is both expensive and technically challenging to produce. Additionally, gene transfer of globin LVs to primitive HSCs has been poor, often failing to achieve sufficiently high vector copy numbers and transgene expression to correct the disease[7]. Thus, new methods to improve transduction efficiency of HSC are critical to the future success of gene therapy for SCD using these vectors.

Recently, Heffner *et al.* performed a small molecule screen to identify compounds which enhance LV transduction of HSPC and identified prostaglandin E2 (PGE2) as a leading candidate[8]. They further showed that PGE2 can increase VCN of short term CD34+ hematopoietic progenitor cells by ~2-fold with a simple GFP LV; however, the VCN increase achieved in long-term HSC (LT-HSC) from NSG xenografts was more modest (1.5-fold).

Additionally, Hauber *et al.* reported that a combination of poloxamer synperonic F108 and polybrene (commercially available as LentiBoost), enhanced transduction of short term CD34+ hematopoietic progenitor cells by ~2.5-fold with a simple GFP LV[9]. Transduction enhancement of LT-HSC with LentiBoost in NSG xenografts was not explored.

Here, we found that the combination of PGE2 and poloxamer synperonic F108 markedly enhances gene transfer (~10 fold) in CD34+ HSPC using a clinical preparation of a globin LV (Lenti/G-AS3-FB). These effects were reproducible among CD34+ HSPC from multiple donors mobilized by either granulocyte colony stimulating factor (G-CSF) or Plerixafor. Importantly, transduction enhancement (~6-fold) was evident in NSG xenografts *in vivo*, indicating that these compounds effectively target primitive CD34+ cells capable of 15-week engraftment. Collectively, these results suggested that the addition of transduction enhancers to current gene therapy trials for SCD may overcome the limiting obstacles and achieve sufficiently high VCN for clinical benefit.

RESULTS

PGE2 and poloxamer synperonic F108 increase gene transfer of a globin LV in CD34+ HSPC

We first explored the use of PGE2 and poloxamer synperonic F108 to enhance transduction of G-CSF mobilized peripheral blood (mPB) CD34+ HSPC with a clinical preparation of Lenti/G-AS3-FB (Figure 1A). Similar to previously reported work using simple GFP LVs[8,9], we found that both PGE2 and poloxamer synperonic F108 used alone enhanced transduction with a complex globin LV. Strikingly, the combination of the two compounds showed synergistic effects, enhancing LV transduction ~10-fold (Figure 1B). We further explored the combination with commonly used transduction enhancers protamine sulfate and polybrene. The addition of protamine sulfate did not further enhance transduction (Figure 1C) while the addition of polybrene showed a dose dependent increase in VCN (Figure 1D). However, the addition of polybrene also exhibited a dose dependent toxicity (Figure S1). We additionally compared the transduction enhancing effects of PGE2 to the more stable PGE2 analog 16,16-dimethyl-PGE2 (dmPGE2) which has been used clinically[10] and is available in GMP formulations. Here, we found the two compounds to be interchangeable in their effects on transduction (Figure 1E). Based on current clinical protocols for expanding cord blood units which utilize a 2-hour pulse exposure of PGE2 to promote HSC engraftment[10], we evaluated the transduction enhancement effects of 2-hour PGE2 pulse exposure prior to addition of LV. Here we observed that a 2-hour PGE2 pulse exposure could modestly enhance transduction, but greater transduction enhancement was achieved with 24-hour PGE2 exposure (Figure 1F).
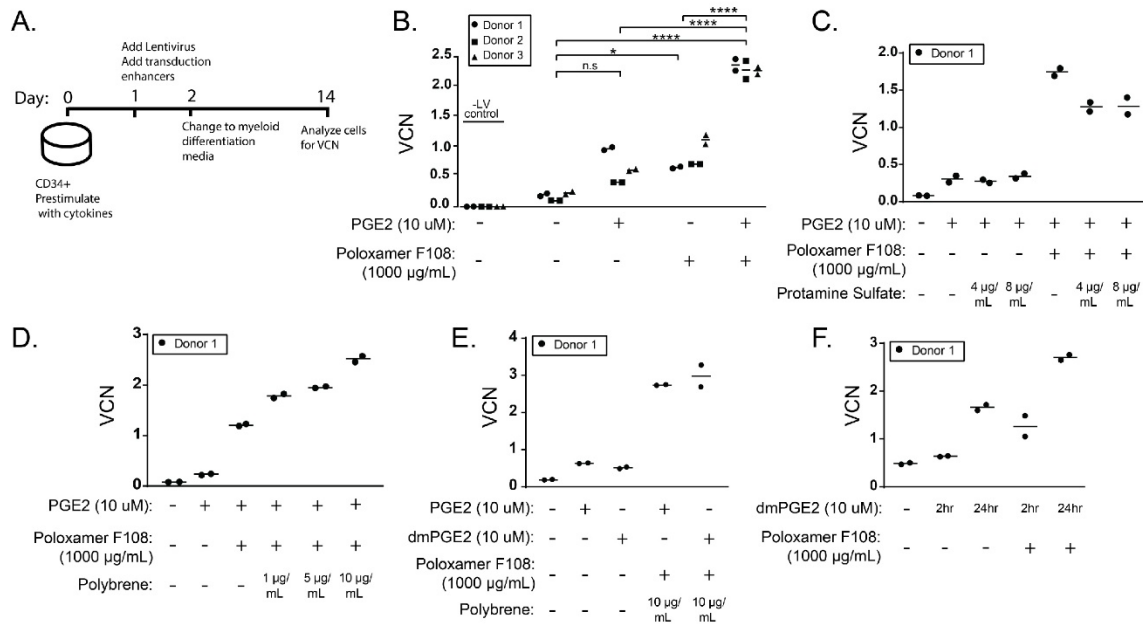
Figure 3-1: Optimization of transduction enhancers for increased gene transfer to G-CSF mPB CD34+ cells

A. Experimental set-up for determination of VCN: G-CSF mPB CD34+ cells were pre-stimulated with cytokines for 24 hours. Lenti/G-AS3-FB was added with or without transduction enhancers for an additional 24 hours. The following day, cells were washed and transferred to *in vitro* myeloid differentiation culture. VCN was analyzed after 12 days of culture.
B. G-CSF mPB CD34+ HSPC were transduced in the presence of different drug combinations with Lenti/G-AS3-FB at $2x10^7$ TU/mL. Data represent mean of 2 replicate culture wells for 3 independent mPB CD34+ donors. (n = 3/arm; one-way ANOVA with Bonferroni's multiple comparison, n.s. not significant, *p≤0.05, ****p ≤ 0.0001).
C-E. G-CSF mPB CD34+ HSPC were transduced in the presence of different drug combinations with Lenti/G-AS3-FB at $2x10^7$ TU/mL (bars represent mean, n=2 replicate wells/condition)
F. G-CSF mPB CD34+ HSPC were pre-treated with a pulse of dmPGE2 for 2 hours, washed, and transduced with LV, or treated with PGE2 for 24 hours (at the same as the addition of LV). (bars represent mean, n=2 replicate wells/condition)

PGE2 and poloxamer synperonic F108 mediate increased transduction in multiple HSPC donors mobilized with G-CSF and Plerixafor

We next evaluated the combination of 10 µM dmPGE2 and 1 mg/mL poloxamer synperonic F108 in G-CSF mobilized PB CD34+ cells from three different healthy donor cell lots. Cells were transduced with a clinical preparation of Lenti/G-AS3-FB at a range of concentrations ($2x10^6$ TU/mL- $2x10^7$ TU/mL) in the presence of dmPGE2/poloxamer synperonic F108 or vehicle control. We first assessed any potential toxicity of these compounds. Here, we found that the addition of dmPGE2/poloxamer synperonic F108

did not alter viable CD34+ cell counts or the percentage of viable cells (Figure 2A,B). Methylcellulose cultures plated after transduction revealed no differences in clonogenic potential nor lineage differentiation (Figure 2C,D).
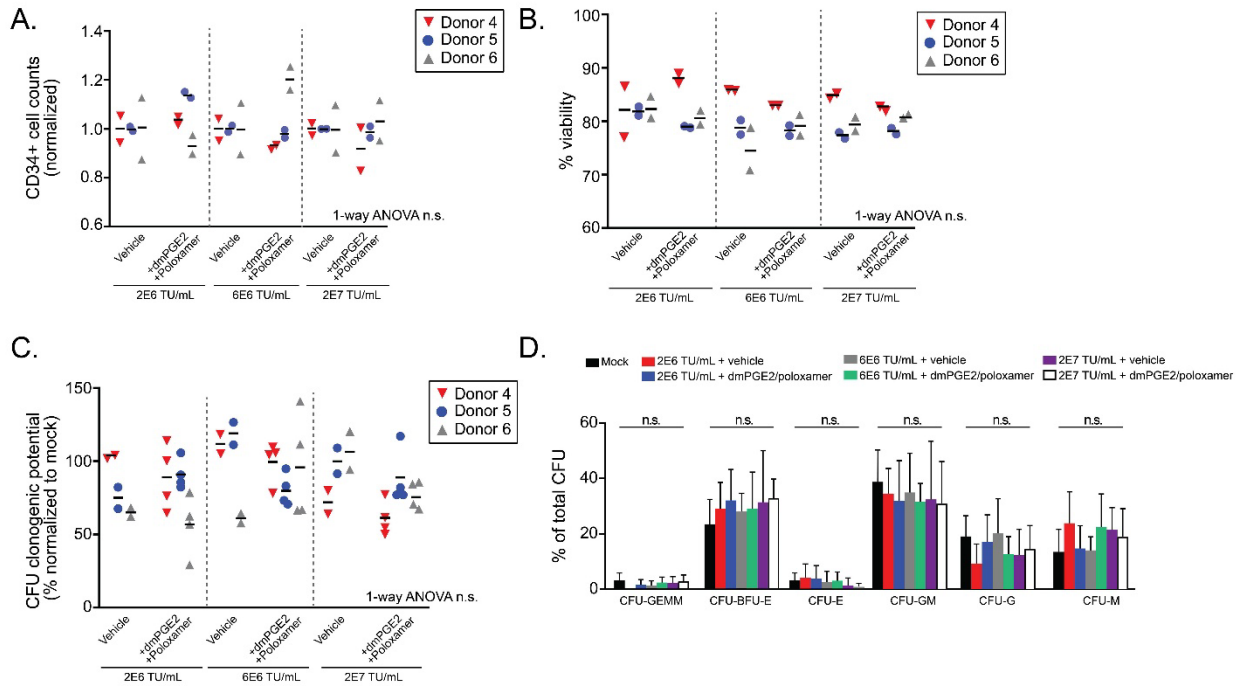

Figure 3-2: Transduction enhancers do not affect the viability or clonogenic potential of G-CSF mPB CD34+ cells.
A. CD34+ cell counts at 24 hours following transduction with and without transduction enhancers at 3 different LV doses. Data represent measurements from 2 replicate culture wells for 3 independent mPB CD34+ donors (each marked with a distinct color/symbol). For each combination of donor/LV dose, the cell count was normalized to vehicle control (bars represent mean for each donor; n=3/arm; one-way ANOVA; n.s. not significant).
B. Percentage of viable cells at 24 hours following transduction determined by flow cytometry viability staining analysis. Data represent measurements from 2 replicate culture wells for 3 independent mPB CD34+ donors. (bars represent mean for each donor; n=3/arm; one-way ANOVA; n.s. not significant).
C. Clonogenic potential (percentage of colonies formed of total cells plated) of transduced CD34+ cells. Data represent measurements from 2-4 replicate CFU cultures for 3 independent mPB CD34+ donors. Data for each donor are normalized to the mean clonogenic potential of 4 replicate non-transduced "mock" control wells for that donor. (bars represent mean for each donor; n=3/arm, one-way ANOVA, n.s. not significant).
D. CFU lineage distribution for transduced CD34+ cells. CFUs were scored in the following categories: CFU-GEMM (CFU-granulocyte/erythroid/macrophage/megakaryocyte), BFU-E (burst-forming unit-erythroid), CFU-E (CFU-erythroid), CFU-GM (CFU-granulocyte/macrophage), CFU-G (CFU-granulocyte), CFU-GM (CFU-macrophage). Data show the frequency of each individual colony type as a percentage of total colonies. Data represent measurements from 2-4 replicate CFU cultures for 3 independent mPB CD34+ donors (bars represent mean ± SD; one-way ANOVA, n.s. not significant).

VCN analysis of bulk myeloid cultures 12 days after transduction revealed a consistent ~10 fold increase in VCN, even at a LV dose of 2×10^6 TU/mL (10-fold lower than the current clinical protocol dose) (Figure 3A). In order to determine if the increased gene transfer in bulk cultures reflected increased integrations to a small number of cells or an increase in the percentage of transduced cells, VCN was determined for individual colony forming units (CFUs) from methylcellulose cultures. Both myeloid and erythroid colonies transduced in the presence of transduction enhancers showed both a dramatic increase in the percentage of transduced cells (Figure 3B) and the average VCN in transduced cells (Figure 3C, D).
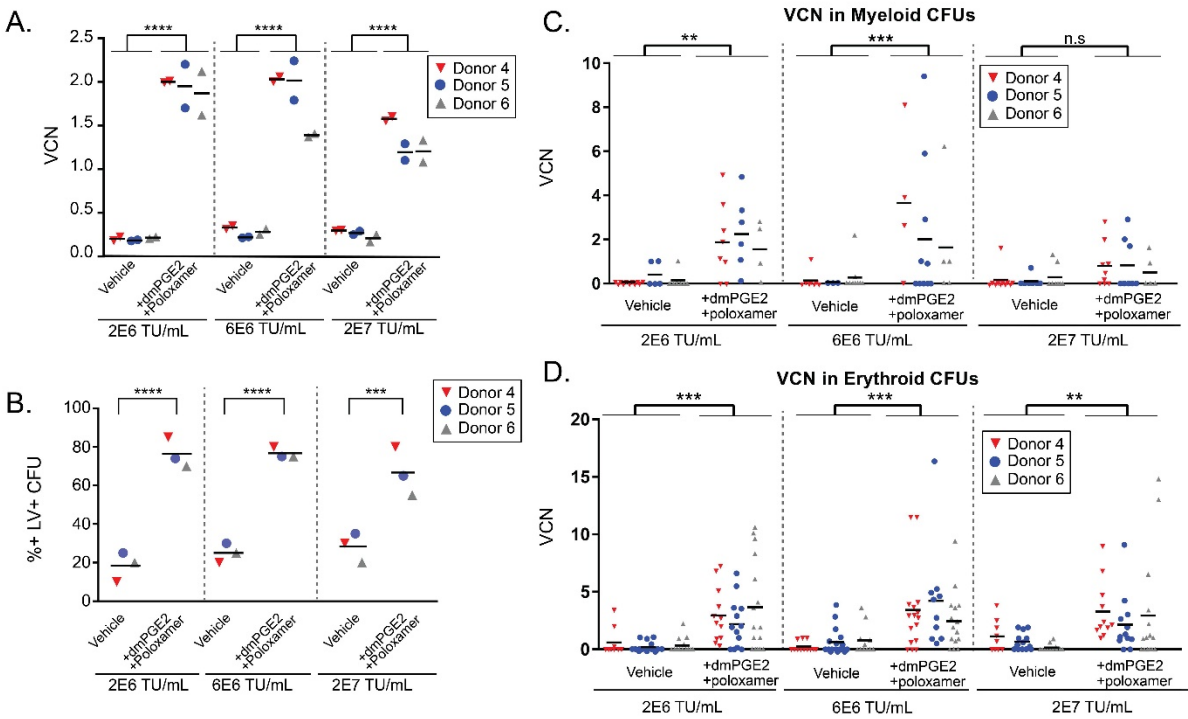

Figure 3-3: Transduction enhancers Improve Gene Transfer in G-CSF mPB CD34+ cells
A. VCN in 12 day myeloid differentiated cultures is shown for G-CSF mPB CD34+ cells transduced with and without transduction enhancers at 3 different LV doses. Data represent measurements from 2 replicate culture wells for 3 independent mPB CD34+ donors. (bars represent mean for each donor; n = 3; one-way ANOVA with Bonferroni's multiple comparison; **** p ≤ 0.0001).
B. Percentage of individual colonies containing integrated viral copies is shown for G-CSF mPB CD34+ cells transduced with and without transduction enhancers at 3 different LV doses. A positive colony was defined as VCN>0.5. Data represent a single percentage (calculated from 20 analyzed colonies) for each LV dose/transduction condition for 3 independent mPB CD34+ donors. (bars represent mean; n = 3; one-way ANOVA with Bonferroni's multiple comparison, ***p ≤ 0.001, **** p ≤ 0.0001).
C. VCN in individual myeloid CFU colonies. Data represent VCN measured in 3-11 colonies per donor/transduction condition/LV dose (bar represents mean VCN for each donor/condition; n = 3; one-way ANOVA with Bonferroni's multiple comparison; **p ≤ 0.01, ***p ≤ 0.001, n.s. not significant).
D. VCN in individual erythroid CFU colonies. Data represent VCN measured in 9-17 colonies per donor/transduction condition/LV dose (bar represents mean for each donor/condition; (n = 3; one-way ANOVA with Bonferroni's multiple comparison; **p ≤ 0.01, ***p ≤ 0.001).

While G-CSF mobilization represents the standard collection regimen for isolating HSC from healthy adult donors, the use of G-CSF is contraindicated in patients with SCD due to its potential to induce sickle crisis[11]. Recently, it has been demonstrated that Plerixafor can achieve safe and successful mobilization of patients with SCD and produces higher CD34+ cell doses than those which can historically be achieved using traditional bone marrow aspiration[12]. As Plerixafor-mobilized CD34+ will likely be the preferred source of HSPC for SCD gene therapy, we confirmed that transduction enhancers show similar efficacy in this cell type. Transduction of three different cell lots of Plerixafor-mobilized CD34+ cells with Lenti/G-AS3-FB in the presence of dmPGE2 and poloxamer synperonic F108 achieved a high VCN and percentage of PCR+ colonies (Figure S2). Furthermore, erythroid differentiation of transduced cells showed enhanced expression of the LV transgene RNA (βAS3 globin) (Figure S3), confirming that transduction enhancers facilitate increased net transgene expression in the population of modified cells.

Transduction enhancers facilitate improved gene transfer in HSC capable of long-term engraftment in NSG mice

We next evaluated the effect of PGE2/poloxamer synperonic F108 treatment on *in vivo* hematopoiesis utilizing NSG xenografts. G-CSF mobilized CD34+ HSPC from three independent donor cell lots were transduced with Lenti/G-AS3-FB at 2×10^6 TU/mL in the presence of no culture additives, vehicle controls (0.1% DMSO and 1% H_2O), or PGE2/poloxamer synperonic F108 and injected into sublethally irradiated NSG mice. At 6 weeks post-transplant, peripheral blood (PB) engraftment analyses revealed no differences among arms suggesting that transduction enhancers do not impair early hematopoiesis from engrafting progenitor cells (Figure 4A). Similarly, no differences among groups were observed for longer term (15 week) bone marrow (BM) engraftment (Figure 4B) and lineage distribution of engrafted cells (Figure 4C), suggesting no adverse effects of transduction enhancers on HSPC function. *In vitro* copy number analysis of transplanted cells (analyzed by short term myeloid culture) revealed a typical ~10-fold increase in VCN in cells treated with PGE2/poloxamer synperonic F108 (Figure 4D). *In vivo*, engrafted hCD45+ transduced in the presence of transduction enhancers

showed a ~6-fold increase in VCN, confirming that PGE2/poloxamer synperonic F108 enhances transduction of a primitive HSC population capable of longer-term NSG engraftment (Figure 4E).
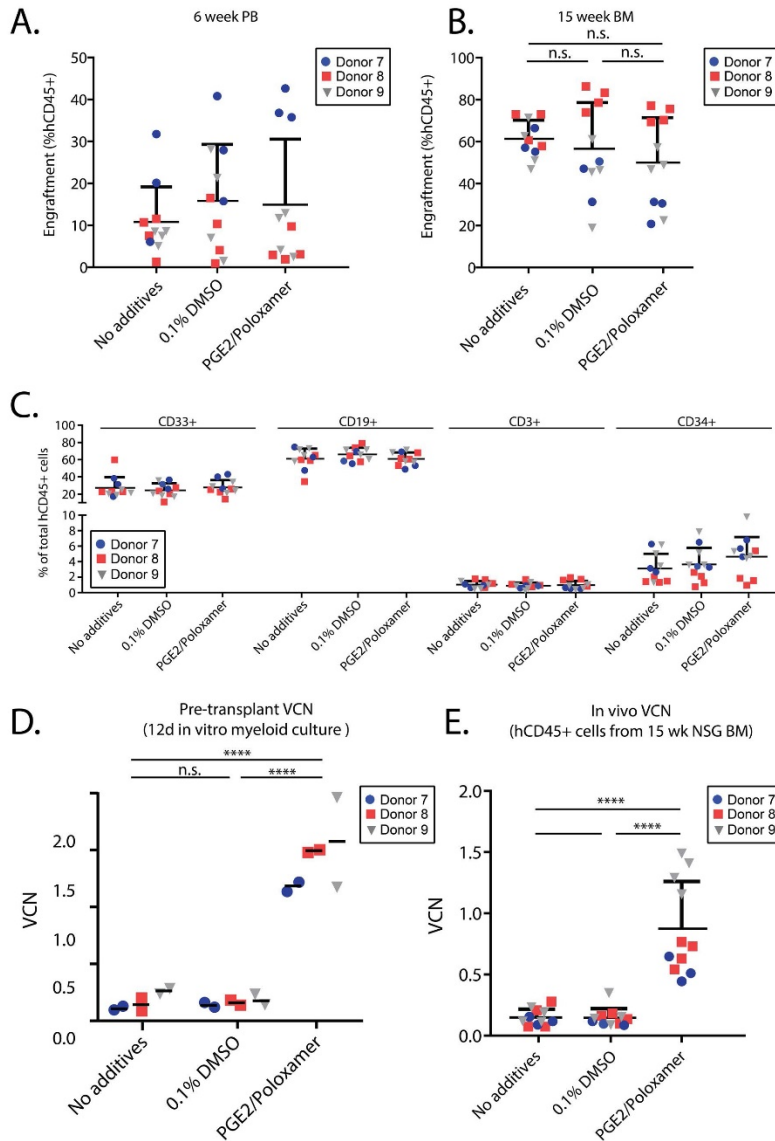
Figure 3-4: Transduction enhancers achieve high copy number in NSG xenografts
A. PB engraftment levels at 6 weeks post-transplant. Engraftment was defined as the percentage of human CD45+ cells of total CD45+ cells (mCD45 + hCD45). G-CSF mPB CD34+ cells from 3 independent CD34+ donors (each marked with a distinct color/symbol) were transplanted into 11 different NSG mice per condition (mean ± SD; n=11; one-way ANOVA; n.s. not significant).
B. Engraftment levels in the BM at 15 weeks post-transplant (mean ± SD; n=11; one-way ANOVA with Tukey's multiple comparisons; n.s. not significant).
C. Lineage distribution of engrafted hCD45+ cells. Lineages are represented as a percentage of total hCD45+ cells (mean ± SD; one-way ANOVA; n.s. for all lineages).
D. Pre-transplant VCN measured for each donor in 12 day myeloid culture assay (bars represent mean of 2 replicate wells for each donor/condition; n=3; one-way ANOVA with Tukey's multiple comparison; ****p ≤ 0.0001, n.s. not significant).
E. In vivo VCN measured in hCD45+ cells engrafted in NSG BM (mean ± SD; one-way ANOVA; with Tukey's multiple comparisons; ****p ≤ 0.0001, n.s. not significant).

41

DISCUSSION

While gene therapy for SCD has made remarkable progress, poor gene transfer of globin LV remains an important hurdle to successful clinical translation. A number of transduction enhancers have previously been reported to improve LV transduction of HSPC, including Vectofusin-1[13], rapamycin[14], cyclosporine A[15], UM171[16], staurosporine[17], and cyclosporine H[18]. In our hands, many transduction enhancing compounds which show promising results using simple GFP LVs have had minimal results in transduction enhancement of globin LVs. This may highlight the relative difficulty of using globin LVs compared to simple GFP LVs; transduction of HSPC with globin LVs often saturates at low VCNs and does not increase at higher LV doses. Limits in the transduction efficiency of globin LV may be due to their large size[19] or complex design. Notably, our studies here have shown that the combination of PGE2 and poloxamer synperonic F108 markedly enhances HSPC transduction with globin LVs to levels which we anticipate to be clinically efficacious.

While the magnitude of transduction enhancement that we observed with each PGE2 and poloxamer synperonic F108 alone was consistent with prior reports[8,9], we observed an additive and potentially synergistic transduction enhancement of these compounds when used in combination. It is possible that each compound may enhance viral transduction at different steps of the viral life cycle. Poloxamers are amphiphilic polymers which have been shown to fluidize membranes[20], increase lipid exchange, and enhance transmembrane transport[21,22]. Thus, a possible mechanism of action may involve enhancing the interaction between viral particles and the host cell membrane.

When transducing HSPC with PGE2, Zonari *et al.* detected a marked increase in late RT copies within 6 hrs after transduction suggesting that PGE2 mediates transduction enhancement prior to nuclear entry and integration. Additional experiments from Zonari et al. suggest that PGE2 does not work through cyclophilinA-mediated uncoating but it does effect endocytosis as no improvement in VCN is seen with non-endocytosis-dependent envelopes[23]. Additionally, Heffner et al. found no effect of PGE2 on viral fusion using a VPR-Beta-lactamase assay[8], which implies that the enhancement occurs post-fusion but during the endocytosis phase of viral transduction. Future work to

elucidate the mechanisms of these compounds may further aid in improving LV transduction methods.

Unexpectedly, CD34+ cells transduced with PGE2/poloxamer synperonic F108 showed a dose-dependent decrease in VCN when increasing LV dose. This is in contrast to the modest dose dependent increase in VCN observed in the absence of transduction enhancers. One possibility that could explain this finding is that high LV doses of 2E7 TU/mL in the presence of PGE2/poloxamer synperonic F108 increases transduction to a toxic level, with highly transduced cells being selectively eliminated. While we cannot rule out this possibility, we note that high VCN colonies were still detectable at the lower (2E6 TU/mL) LV dose, and that there was no clear relationship observed between cell counts, viability, nor clonogenic potential and LV dose. An additional speculative possibility is that there is an optimal ratio for poloxamer molecules and LV particles where high levels of LV particles may become detrimental to transduction. While this mechanism remains to be explored, investigators using this combination of compounds may need to titrate individual LV dose. Importantly, using a lower LV dose to achieve higher VCN may be highly advantageous for clinical gene therapy due to the vast expense and time required to produce and validate each lot of GMP grade LV.

Interestingly, while we observed marked enhancement of HSPC transduction *in vitro*, this effect was somewhat diminished in NSG xenografts. This is consistent with results observed by Heffner et al. using PGE2 alone[8], and suggests that PGE2/poloxamer synperonic F108 may preferentially enhance transduction of short-term progenitor cells with more modest effects in the LT-HSC compartment. Nonetheless, we predict that if a 6-fold increase in gene transfer to primitive HSC could be achieved in a clinical setting, this would be sufficient to achieve a therapeutic transgene expression level.

An important consideration surrounding this work is defining a benchmark for a drug product (DP) VCN in vitro which may be clinically efficacious after transplant. The first promising case of SCD gene therapy was reported in the HGB-205 trial with the LentiGlobin BB305[24]. A 12-year-old patient, who had been on prophylactic red-cell transfusions for four years prior to treatment, received a CD34+ cell product with an average VCN of 1.1. After 15 months of follow-up, the patient showed stable gene

marking in the PB (VCN ~2) and expressed therapeutic anti-sickling globin in 48% of all globin tetramers. Clinical outcomes and analysis of SCD-related biologic parameters indicated stable correction of the disease, suggesting that SCD gene therapy can be successful when high VCN and transgene expression are achieved.

In contrast, subsequent SCD patients treated in the HGB-206 study showed less efficacious results; PB levels of the LentiGlobin BB305 vector were low (median = 0.08, range 0.05-0.13) in all treated subjects, with no evidence of clinical benefit[7]. Similarly, a cohort of patients with beta thalassemia treated with LentiGlobin BB305 in the HGB-204 study showed low PB VCN (median = 0.3, range, 0.1 to 0.9)[25]. In both of these studies, the in vitro drug product VCN measured prior to transplant was much higher (HGB-205: median = 0.6, range 0.3-1.3; HGB-204: median = 0.7, range 0.3-1.5), representing a 2-8-fold drop off after transplant.

The observed drop between measured drug product VCN in vitro and post-engraftment PB VCN in vivo is likely multifactorial. One reason for this observed effect is the limitation of in vitro assays, which predominantly measure gene transfer to short-term erythroid or myeloid progenitor cells. As progenitor cells are more easily transduced than long-term HSC (LT-HSC), these assays often overestimate the true in vivo VCN determined by the level of gene transfer into engrafting LT-HSC. This effect is well understood in the field, and can be observed here in our NSG xenograft studies. Therefore, while an ideal target for in vivo VCN may be around 2 copies/cell, using in vitro assays to predict a target DP VCN for an individual patient may be challenging in practice.

An additional factor that may affect the observed drop between in vitro and in vivo VCN (in a clinical transplant setting) is the competition between non-modified endogenous HSCs and modified transplanted HSCs. Thus, the number of gene modified cells retained in vivo can be highly dependent on the quality of the graft and the effectiveness of the conditioning regimen. The problem of low quality HSC may be of particular importance in SCD due to sub-optimal CD34+ cell number obtained from BM collection and reduced quality of HSC obtained from an inflammatory BM environment[26]. Transfusion lead-in and Plerixafor mobilization protocols have been explored to improve

the quality and quantity of CD34+ HSPC collected[12,27] and monitoring of plasma busulfan concentrations with dose adjustments has been explored to optimize myeloablation[28].

While improvements in HSC quality and engraftment may mitigate the observed decline in VCN post-transplant, clinical data suggests that improvements of pre-transplant in vitro VCN are also required. In support of this, early clinical results from HGB206 describing a new protocol with a proprietary method of lentiviral transduction have reported both enhanced DP VCN (median = 4.0, range 2.8 – 5.6) and early in vivo PB VCN (range 1.4-2.9)[29].

While we can only cautiously compare the reported in vitro DP VCN from HGB-206 to our own studies (due to differences in LV construct, GMP manufacturing process, and protocols for measuring in vitro VCN), our transduction protocol using PGE2/poloxamer synperonic F108 in plerixafor mobilized CD34+ donors yielded an in vitro DP VCN of 2.5-6.8. Therefore, we anticipate that a historic 2-fold decrease in VCN post-transplant would still maintain in vivo VCN in a therapeutically efficacious range. As more patients are treated, we anticipate that we can better characterize the correlation between in vitro and in vivo VCN, and may be able to further refine targets for in vitro VCN prior to transplant.

In summary, the use of PGE2/poloxamer synperonic F108 as transduction enhancers provides a promising strategy to overcome current limitations in gene therapy for SCD, and may further support the clinical translation of novel LV-based HSPC gene therapies for genetic blood cell disorders of different origin.

MATERIALS AND METHODS

Transduction Enhancers

Poloxamer synperonic F108 (Kolliphor P338, BASF, Ludwigshafen, Germany) was prepared in a stock solution of 100 mg/mL by dissolving in sterile water overnight and filtering through a 0.22 uM filter. Poloxamer synperonic F108 stock solution was stored at 4°C. PGE2 or dmPGE2 (Cayman Chemicals, Ann Arbor, MI, USA) were dissolved in DMSO to make 10 mM stock solutions and stored as single-use aliquots at -80°C.

Lentiviral Transduction

CD34+ cells from healthy donors mobilized with G-CSF or Plerixafor were purchased from Hemacare (Van Nuys, CA, USA) or StemExpress (Folsom, CA, USA). Cells were plated at a density of 5×10^5-1×10^6 cells/mL in X-Vivo-15 (Lonza, Basel, Switzerland) with 1× L-glutamine, penicillin, and streptomycin (L-Glut/Pen/Strep, Gemini BioProducts, West Sacramento, CA, USA), 50 ng/mL SCF, 50 ng/mL TPO, and 50 ng/mL Flt3L (PeproTech, Rocky Hill, NJ, USA) and cultured at 5% CO_2, 37°C and humidified atmosphere throughout. 24 hours after cytokine pre-stimulation, cells were transduced by adding Lenti/G-AS3-FB (Lentigen, Gaithersburg, MD, USA) and transduction enhancers/vehicle control directly to the cells. 24 hours after transduction, cells were collected, washed, and used for downstream applications described below.

In vitro myeloid differentiation cultures

Transduced CD34+ cells were cultured in Basal BM Medium (BBMM) [Iscove's Modified Dulbecco's Medium (IMDM, Life Technologies, Grand Island, NY), 1x LGlut/Pen/Strep, 20% FBS, 0.52% BSA] with cytokines (5 ng/ml IL-3, 10 ng/ml IL-6, 25 ng/ml hSCF, [PeproTech]) at 37°C, 5% CO_2. Cells were split every 2-3 days and supplemented with fresh BBMM plus cytokines. After 12 days of culture, cells were collected and genomic DNA was extracted using the Purelink Genomic DNA Mini Kit (Invitrogen, Carlsbad, CA, USA).

In vitro erythroid differentiation

Transduced CD34+ cells were transferred into erythroid culture. The in vitro erythroid differentiation technique used is based on a 3-phase protocol adapted from Giarratana et al[30]. The basic erythroid medium was IMDM (Life Technologies), 1x LGlut/Pen/Strep, 10% BSA, 40 µg/ml inositol, 10 µg/ml folic acid, 1.6 µM monothioglycerol, 120 µg/ml transferrin, and 10 µg/ml insulin (all from Sigma-Aldrich, St. Louis, MO, USA). During the first phase (6 days), the cells were cultured in the presence of 1×10^{-6} M hydrocortisone (Sigma-Aldrich), 100 ng/ml hSCF, 5 ng/ml hIL-3 (Peprotech), and 3 IU/ml erythropoietin (Epo) (Janssen Pharmaceuticals). In the second phase (3 days), the cells were transferred onto a stromal cell layer (MS-5, murine stromal cell line [31] (provided by Gay Crooks, UCLA) with the addition of only Epo (3 IU/ml) to basic erythroid medium. At day 11, all the cytokines were removed from the medium and the cells were co-cultured on the MS-5 stromal layer until day 14, when they were collected to extract genomic DNA and RNA.

Colony Forming Unit (CFU) assay

CFU assays were performed using Methocult H4435 Enriched methylcellulose (StemCell Technologies, Vancouver, Canada. Cat. # 04445) according to manufacturer's instructions with minor modifications. Briefly, 25, 50 and 100 transduced CD34+ cells were plated in duplicates into 35 mm gridded cell culture dishes. After 14 days of culture at 5% CO_2, 37°C and humidified atmosphere, the different types of hematopoietic colonies were identified and counted. CFU were then plucked for genomic DNA isolation (NucleoSpin Tissue XS, Clontech Laboratories Inc., Mountain View, CA, USA).

Vector Copy Number (VCN) determination

For VCN determination, the Psi region of the lentiviral vector genome assay was duplexed with the SDC4 endogenous reference gene. The Psi assay sequences were as follows: 5′- ACCTGAAAGCGAAAGGGAAAC -3′ (forward primer), 5′-CGCACCCATCTCTCTCCTTCT -3′ (reverse primer) and 5′-FAM-AGCTCTCTCGACGCAGGACTCGGC -31ABFQ-3′ (probe) (Integrated DNA Technologies, San Diego, CA, USA). The SDC4 assay sequences were as follows: 5′-

CAGGGTCTGGGAGCCAAGT -3′ (forward primer), 5′-GCACAGTGCTGGACATTGACA-3′ (reverse primer) and 5′-HEX-CCCACCGAACCCAAGAAACTAGAGGAGAAT -31ABFQ-3′ (probe) (Integrated DNA Technologies).

Reaction mixtures of 22-µL volume, comprising 1 × Droplet Digital (dd)PCR Master Mix (Bio-Rad, Hercules, CA, USA), 400 nmol/L primers and 100 nmol/L probe for each set, 40 U DraI (New England Biolabs, Ipswich, MA, USA) and 30–100 µg of the gDNA to study, were prepared and incubated at 37°C for 1 hour. Droplet generation was performed as described in Hindson *et al.*[32] with 20 µL of each reaction mixture. The droplet emulsion was then transferred with a multichannel pipet to a 96-well propylene plate (Eppendorf), heat sealed with foil, and amplified in a conventional thermal cycler (T100 Thermal Cycler, Bio-Rad). Thermal cycling conditions consisted of 95°C 10 min, (94°C 30 s and 60°C 1 min) (55 cycles), 98°C 10 min (1 cycle) and 12°C hold. After PCR, the 96-well plate was transferred to a droplet reader (Bio-Rad). Acquisition and analysis of the ddPCR data was performed with the QuantaSoft software (Bio-Rad), provided with the droplet reader.

Determination of %βAS3-globin mRNA by ddPCR

RT-PCR to detect %βAS3-globin mRNA/total beta-globin transcript (%AS3) was performed as described in Urbinati *et al.*[33]. Isolation of RNA was done using the RNeasy Plus Mini Kit (QIAGEN, Hilden, Germany), followed by reverse transcription as described on the Invitrogen protocol (final concentration: 10 U/µL M-MLV, 500 µmol/L dNTPs, 150 ng/µL random primers, 2 U/µL RNase OUT, 10 mmol/L DTT, 1 × First strand buffer). Two TaqMan hydrolysis probes were used to obtain the ratio of (1) target (HBBAS3) over (2) reference (HBBTotal: all variants of endogenous β-globin–like mRNA transcripts) for the quantification of gene expression by ddPCR. Reaction mixtures and thermal cycling conditions were as described earlier. The assay sequences were as follows: GGA GAA GTC TGC CGT TAC TG (HBBAS3/Total F2), CAC TAA AGG CAC CGA GCA CT (HBBAS3/Total R2), 5′FAM-ACA AGG TGA-ZEN-ACG TGG ATG CCG TTG-3′ Iowa Black FQ (HBBAS3 probe), 5′HEX-AAC CTC TGG-

ZEN-GTC CAA GGG TAG ACC AGC AG-3′ Iowa Black FQ (HBBTotal probe) (Integrated DNA Technologies).

NSG transplants

6-12 week old NSG mice were sub-lethally irradiated using a Cs-137 source at 250 Rad with a dose rate of approximately 100 Rad/min. 24 hours after irradiation, $1x10^6$ mPB CD34+ cells (transduced in the presence of dmPGE2/Poloxamer synperonic F108 or vehicle control) were transplanted via retro-orbital injection. NSG xenograft experiments used all female mice to avoid sex-based variations in engraftment.

Analysis of NSG xenografts for engraftment and VCN

PB was collected from transplanted mice via retro-orbital puncture at 6 weeks. After euthanasia at 15 weeks, BM was isolated by crushing femurs and tibias using a mortar and pestle. PB and BM engraftment (expressed as the percentage of hCD45+ cells of total CD45+ [hCD45+mCD45+]) were determined by staining for: mCD45-PE (30-F11), hCD45-APC (HI30), and DAPI. For VCN and lineage distribution analysis, hCD45+ cells were enriched from bone marrow using a bead based selection kit (Miltenyi Biotec, Inc., Bergisch Gladbach, Germany). Human CD45 enriched cells were stained with Ghost 780 (viability dye, Tonbo Biosciences, San Diego, CA, USA) and the following antibodies: hCD45-FITC (HI30), mCD45-PE (30F11), hCD3-PerCp-Cy5.5 (UCHT1), hCD33-BV421 (WM53), hCD34-APC (581), hCD19-PE-Cy7 (SJ25C1). All antibodies were purchased from BD Biosciences (San Jose, CA, USA). Genomic DNA was extracted from hCD45-enriched cells using the Purelink Genomic DNA Mini Kit (Invitrogen, Carlsbad, CA, USA) and analyzed for VCN as described above.

Statistical Analysis

Values are represented as means ± SD, unless stated otherwise. GraphPad Prism 6.0 (GraphPad Software, San Diego, CA) was utilized for all statistical analyses. Statistical details of each experiment can be found in the figure legends, including the mean and error bars, numbers of replicates, statistical tests, and p values from comparative analyses that were performed. P value was calculated with a confidence interval of 95%

to indicate the statistical significance between groups. A P value < 0.05 was considered statistically significant.

ACKNOWLEDGEMENTS

DECLARATIONS OF INTEREST

The authors declare no competing interests.

AUTHOR CONTRIBUTIONS

Conceptualization, D.B.K, R.P.H., B.C-F; Formal Analysis, K.E.M., B.C-F.; Investigation, K.E.M., K.O., R.X., B.C-F; Writing – Original Draft Preparation, K.E.M.; Writing – Review & Editing Preparation, K.E.M., R.P.H, D.B.K.; Visualization, K.E.M.; Supervision, D.B.K., B.C-F., R.P.H.; Funding Acquisition, D.B.K

REFERENCES

1.	Brousseau DC, Panepinto JA, Nimmer M, Hoffmann RG. The number of people with sickle-cell disease in the United States: National and state estimates. *Am J Hematol.* 2010;85(1):77-78.

2.	Modell B, Darlison M. Global epidemiology of haemoglobin disorders and derived service indicators. *Bull World Health Organ.* 2008;86(6):480-487.

3.	Madigan C, Malik P. Pathophysiology and therapy for haemoglobinopathies; Part I: sickle cell disease. *Expert Rev Mol Med.* 2006;8(09):1-23.

4.	Morgan RA, Gray D, Lomova A, Kohn DB. Hematopoietic Stem Cell Gene Therapy: Progress and Lessons Learned. *Cell Stem Cell.* 2017;21(5):574-590.

5.	Romero Z, Urbinati F, Geiger S, et al. β-globin gene transfer to human bone marrow for sickle cell disease. *J Clin Invest.* 2013;123(8):3317-3330.

6.	Negre O, Bartholomae C, Beuzard Y, et al. Preclinical evaluation of efficacy and safety of an improved lentiviral vector for the treatment of β-thalassemia and sickle cell disease. *Curr Gene Ther.* 2015;15(1):64-81.

7.	Kanter J, Walters MC, Hsieh MM, et al. Interim Results from a Phase 1/2 Clinical Study of Lentiglobin Gene Therapy for Severe Sickle Cell Disease. *Blood.* 2016;128(22):1176 LP-1176.

8.	Heffner GC, Bonner M, Christiansen L, et al. Prostaglandin E2 Increases Lentiviral Vector Transduction Efficiency of Adult Human Hematopoietic Stem and Progenitor Cells. *Mol Ther.* 2018;26(1):320-328.

9.	Hauber I, Beschorner N, Schrödel S, et al. Improving Lentiviral Transduction of CD34 [+] Hematopoietic Stem and Progenitor Cells. *Hum Gene Ther Methods.* 2018;29(2):104-113.

10.	Cutler C, Multani P, Robbins D, et al. Prostaglandin-modulated umbilical cord blood hematopoietic stem cell transplantation. *Blood.* 2013;122(17).

11. Fitzhugh CD, Hsieh MM, Bolan CD, Saenz C, Tisdale JF. Granulocyte colony-stimulating factor (G-CSF) administration in individuals with sickle cell disease: time for a moratorium? *Cytotherapy*. 2009;11(4):464-471.

12. Lagresle-Peyrou C, Lefrère F, Magrin E, et al. Plerixafor enables safe, rapid, efficient mobilization of hematopoietic stem cells in sickle cell disease patients after exchange transfusion. *Haematologica*. 2018;103(5):778-786.

13. Fenard D, Ingrao D, Seye A, et al. Vectofusin-1, a new viral entry enhancer, strongly promotes lentiviral transduction of human hematopoietic stem cells. *Mol Ther - Nucleic Acids*. 2013;2:e90.

14. Wang CX, Sather BD, Wang X, et al. Rapamycin relieves lentiviral vector transduction resistance in human and mouse hematopoietic stem cells. *Blood*. 2014;124(6):913-923.

15. Petrillo C, Cesana D, Piras F, et al. Cyclosporin A and rapamycin relieve distinct lentiviral restriction blocks in hematopoietic stem and progenitor cells. *Mol Ther*. 2015;23(2):352-362.

16. Ngom M, Imren S, Maetzig T, et al. UM171 Enhances Lentiviral Gene Transfer and Recovery of Primitive Human Hematopoietic Cells. *Mol Ther - Methods Clin Dev*. 2018;10:156-164.

17. Lewis G, Christiansen L, McKenzie J, et al. Staurosporine Increases Lentiviral Vector Transduction Efficiency of Human Hematopoietic Stem and Progenitor Cells. *Mol Ther - Methods Clin Dev*. 2018;9:313-322.

18. Petrillo C, Thorne LG, Unali G, et al. Cyclosporine H Overcomes Innate Immune Restrictions to Improve Lentiviral Transduction and Gene Editing In Human Hematopoietic Stem Cells. *Cell Stem Cell*. 2018;23:820-832.

19. Canté-Barrett K, Mendes RD, Smits WK, van Helsdingen-van Wijk YM, Pieters R, Meijerink JPP. Lentiviral gene transfer into human and murine hematopoietic stem cells: size matters. *BMC Res Notes*. 2016;9(1):312.

20. Höfig I, Atkinson MJ, Mall S, et al. Poloxamer synperonic F108 improves cellular transduction with lentiviral vectors. 2012.

21. Batrakova E V, Li S, Vinogradov S V, Alakhov VY, Miller DW, Kabanov A V. Mechanism of pluronic effect on P-glycoprotein efflux system in blood-brain barrier: contributions of energy depletion and membrane fluidization. *J Pharmacol Exp Ther*. 2001;299(2):483-493.

22. Krylova OO, Melik-Nubarov NS, Badun GA, Ksenofontov AL, Menger FM, Yaroslavov AA. Pluronic L61 Accelerates Flip–Flop and Transbilayer Doxorubicin Permeation. *Chem - A Eur J*. 2003;9(16):3930-3936.

23. Zonari E, Desantis G, Petrillo C, et al. Efficient Ex Vivo Engineering and Expansion of Highly Purified Human Hematopoietic Stem and Progenitor Cell Populations for Gene Therapy. *Stem Cell Reports*. 2017;8(4):977-990.

24. Ribeil J-A, Hacein-Bey-Abina S, Payen E, et al. Gene Therapy in a Patient with Sickle Cell Disease. *N Engl J Med*. 2017;376(9):848-855.

25. Soni S, Hacein-Bey-Abina S, Vichinsky E, et al. Gene Therapy in Patients with Transfusion-Dependent β-Thalassemia. *N Engl J Med*. 2018;378(16):1479-1493.

26. Zhang D, Xu C, Manwani D, Frenette PS. Neutrophils, platelets, and inflammatory pathways at the nexus of sickle cell disease pathophysiology. *Blood*. 2016;127(7):801-809.

27. Tisdale J, Kanter J, Mapara M, Kwiatkowski J. Current Results of Lentiglobin Gene Therapy in Patients with Severe Sickle Cell Disease Treated Under a Refined Protocol in the Phase 1 Hgb-206 Study. *Blood*. 2018;132(Suppl 1):1026-1026.

28. Thompson AA, Walters MC, Kwiatkowski J, et al. Gene Therapy in Patients with Transfusion-Dependent β-Thalassemia. *N Engl J Med*. 2018;378(16):1479-1493.

29. Tisdale J, Kanter J, Mapara M, Kwiatkowski J. Current Results of Lentiglobin Gene Therapy in Patients with Severe Sickle Cell Disease Treated Under a

Refined Protocol in the Phase 1 Hgb-206 Study. *Blood*. 2018;132(Suppl 1):1026-1026.

30. Giarratana M-C, Kobari L, Lapillonne H, et al. Ex vivo generation of fully mature human red blood cells from hematopoietic stem cells. *Nat Biotechnol*. 2005;23(1):69-74.

31. Suzuki J, Fujita J, Taniguchi S, Sugimoto K, Mori KJ. Characterization of murine hemopoietic-supportive (MS-1 and MS-5) and non-supportive (MS-K) cell lines. *Leukemia*. 1992;6(5):452-458.

32. Hindson BJ, Ness KD, Masquelier DA, et al. High-throughput droplet digital PCR system for absolute quantitation of DNA copy number. *Anal Chem*. 2011;83(22):8604-8610.

33. Urbinati F, Wherley J, Geiger S, et al. Preclinical studies for a phase 1 clinical trial of autologous hematopoietic stem cell gene therapy for sickle cell disease. *Cytotherapy*. 2017;19(9):1096-1112.
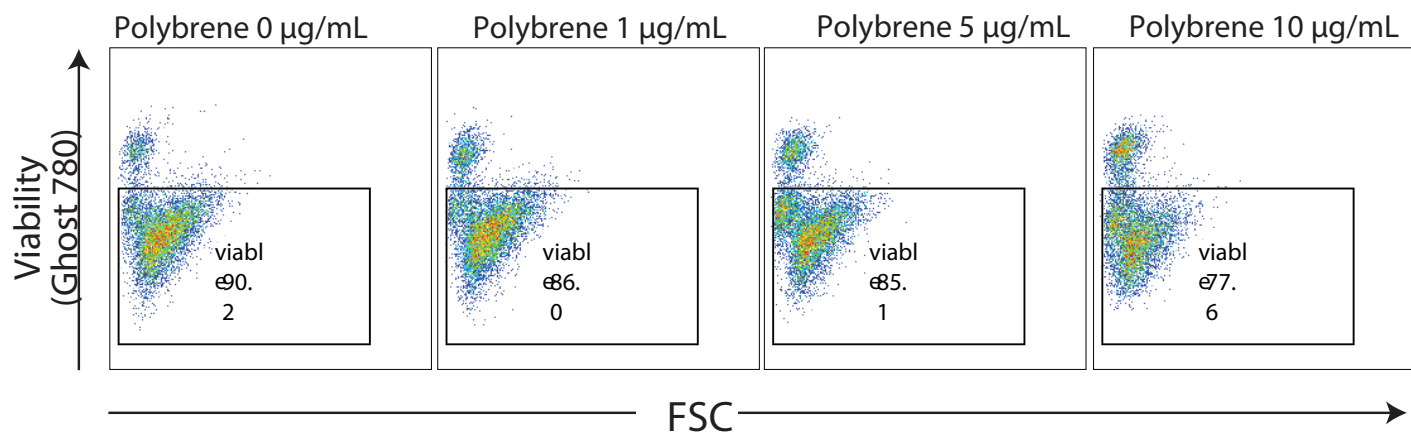
Figure S3-1: Dose-dependent toxicity of polybrene in LV transduction cultures
G-CSF mPB CD34+ cells were transduced with Globe1-AS3 in the presence of PGE2/ poloxamer F-108 and increasing doses of polybrene. FACS plots show viability of cells measured 24 hours post-transduction
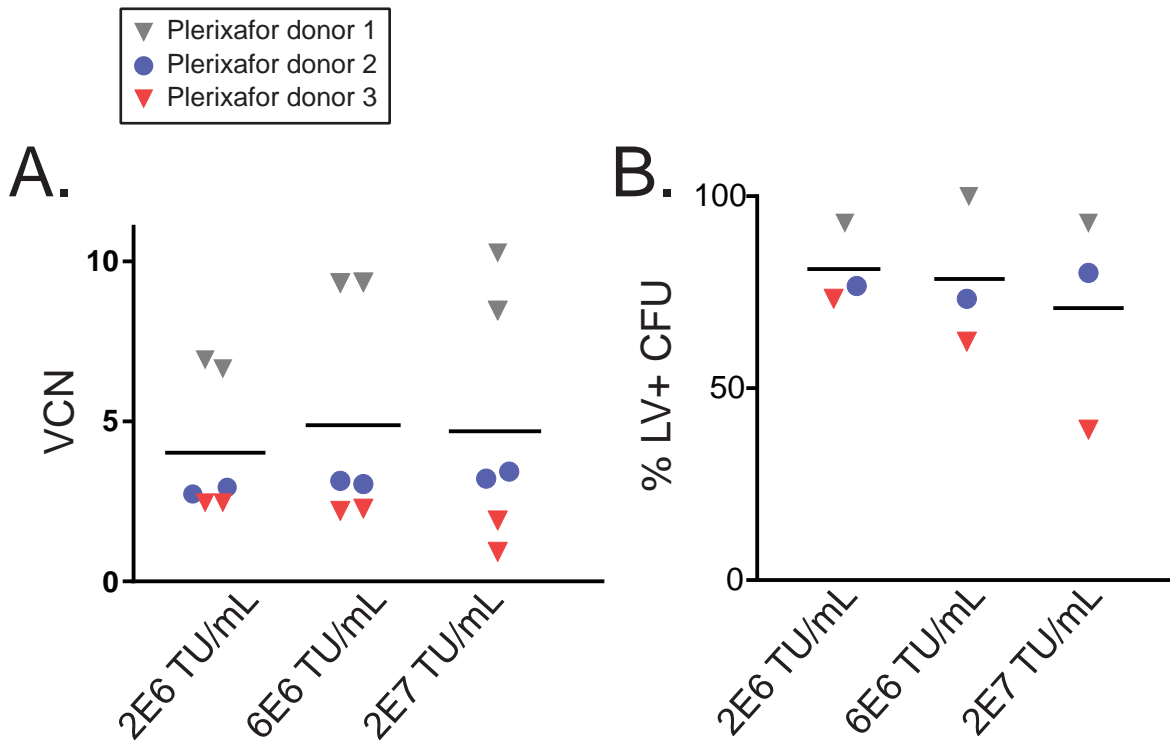
Figure S3-2: Transduction of Plerixafor-mobilized CD34+ cells with LV Globe1-AS3

A. VCN in 12 day myeloid differentiated cultures for Plerixafor mPB CD34+ cells transduced with trans-duction enhancers at 3 different LV doses. Data represent measurements from 2 replicate culture wells for 3 independent mPB CD34+ donors (each marked with a distinct color/symbol).
B. Percentage of individual colonies containing integrated viral copies for Plerixafor mPB CD34+ cells transduced with transduction enhancers at 3 different LV doses. A positive colony was defined as VCN>0.5. Data represent a single percentage (calculated from 30 analyzed colonies) for each LV dose in each of 3 independent CD34+ donors.
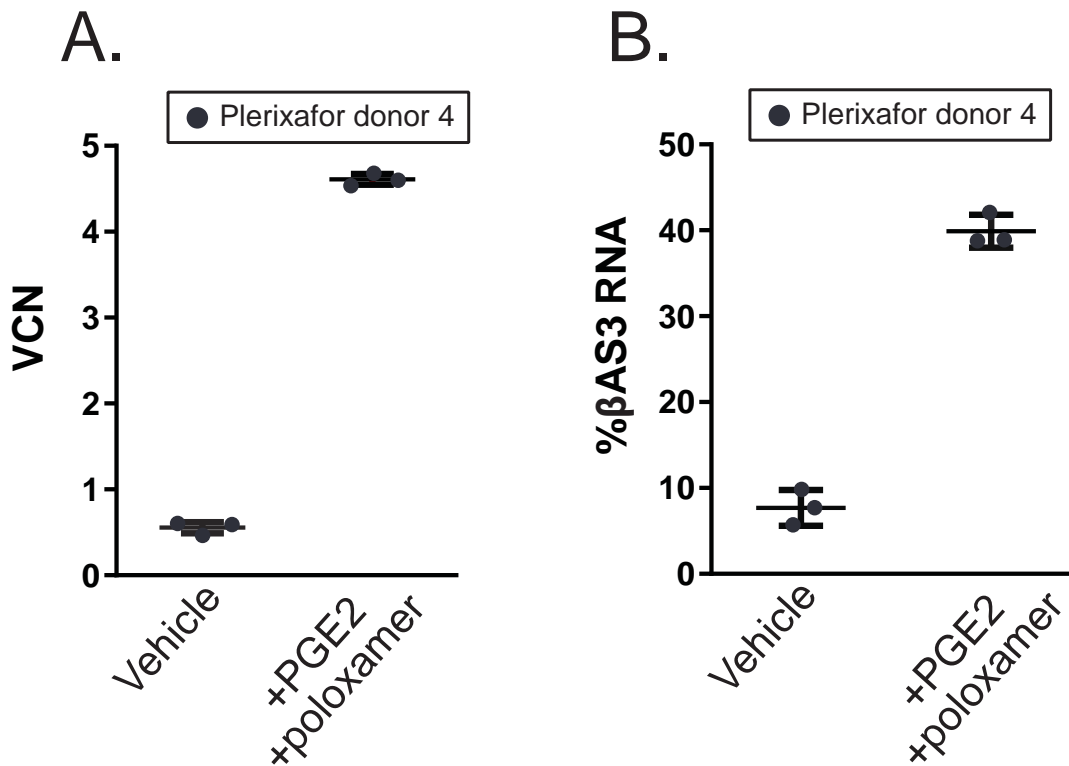
Figure S3-3: Correlation between enhanced VCN and enhanced βAS3 transgene expression

A. VCN in 12 day erythroid differentiated cultures for Plerixafor mPB CD34+ cells transduced with vehicle control or transduction enhancers at 2×10^6 TU/mL. Data represent mean ± SD of 3 replicate culture wells from one CD34+ donor.

B. Corresponding percentage of viral βAS3 RNA (as a percentage of total β-globin RNA) measured in erythroid differentiated cells. Data represent mean ± SD of 3 replicate culture wells from one CD34+ donor.
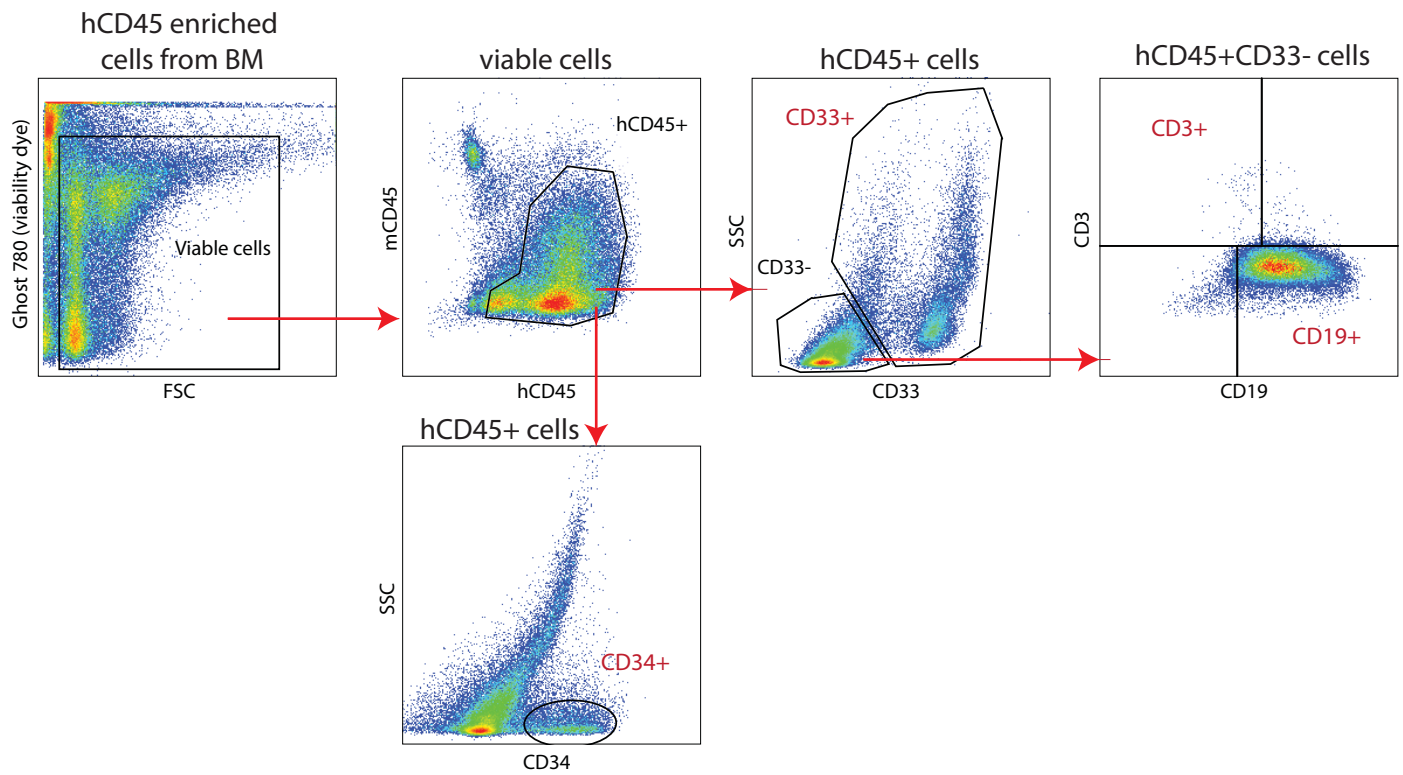
Figure S3-4: Determination of lineage distribution in NSG xenografts

Human CD45+ cells were magnetically enriched from the BM of engrafted NSG mice. Plots show flow cytometry gating strategy used to determine the relative contribution of each lineage to total engrafted hCD45+ cells. Lineages analyzed are marked in red and include: CD34+, CD33+, CD3+, and CD19+.

Chapter 4:

Lentiviral Gene Therapy in HSCs Restores Lineage Specific Foxp3 Expression and Suppresses Autoimmunity in a Mouse Model of IPEX Syndrome

Cell Stem Cell

Lentiviral Gene Therapy in HSCs Restores Lineage-Specific Foxp3 Expression and Suppresses Autoimmunity in a Mouse Model of IPEX Syndrome

Graphical Abstract

Authors

Katelyn E. Masiuk, Jennifer Laborada, Maria Grazia Roncarolo, Roger P. Hollis, Donald B. Kohn

Correspondence

dkohn1@mednet.ucla.edu

In Brief

Masiuk et al. use a lentiviral vector designed from endogenous *FOXP3* regulatory elements in HSCs to achieve lineage-specific FoxP3 expression. This strategy restores functional Treg cell development from FoxP3^{mut} HSCs and reverses autoimmunity *in vivo*. These findings suggest preclinical efficacy for lentiviral gene therapy for the treatment of IPEX syndrome.

Highlights

- An endogenously regulated FoxP3 lentiviral vector shows Treg cell-selective expression

- Modification of FoxP3^{mut} HSCs with the FoxP3 LV generates functional Treg cells

- Treg cells derived from FoxP3^{mut} HSCs function *in vivo* to prevent autoimmunity

CellPress

Short Article
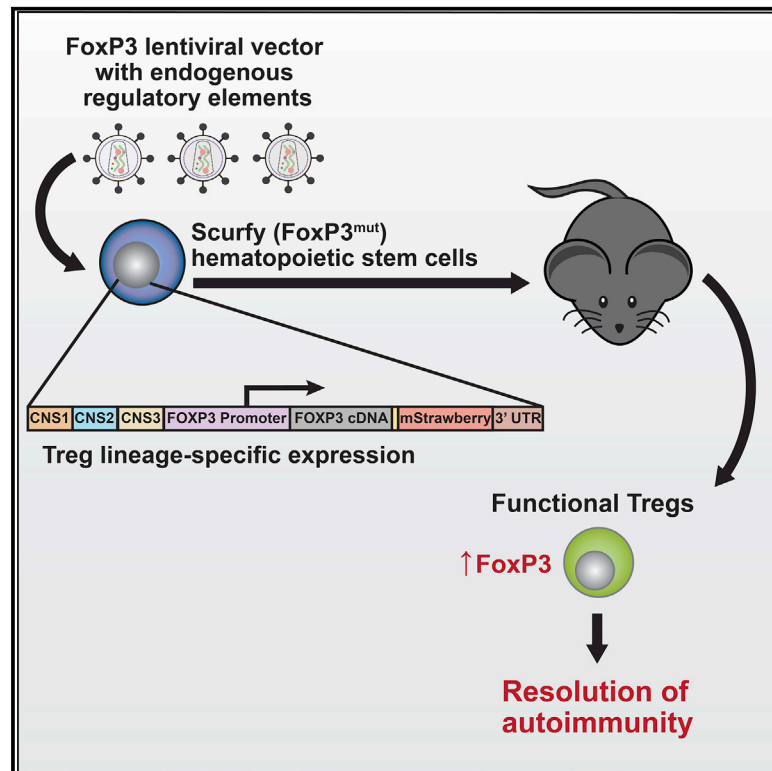
Lentiviral Gene Therapy in HSCs Restores Lineage-Specific Foxp3 Expression and Suppresses Autoimmunity in a Mouse Model of IPEX Syndrome

Katelyn E. Masiuk,[1] Jennifer Laborada,[1] Maria Grazia Roncarolo,[2] Roger P. Hollis,[1] and Donald B. Kohn[1,3,*]

[1]Department of Microbiology, Immunology and Molecular Genetics, University of California, Los Angeles, Los Angeles, CA, USA
[2]Division of Stem Cell Transplantation and Regenerative Medicine, Department of Pediatrics, Stanford University, Stanford, CA, USA
[3]Lead Contact

SUMMARY

Immune dysregulation, polyendocrinopathy, enteropathy, X-linked (IPEX) syndrome is a devastating autoimmune disease caused by mutations in FoxP3, a transcription factor required for the development and function of regulatory T cells (Treg cells). Allogeneic hematopoietic stem cell transplant (HSCT) can be curative, but suitable donors are often unavailable. Here, we demonstrate a strategy for autologous HSCT and gene therapy utilizing a lentiviral vector (LV) to restore FoxP3 expression under the control of endogenous human *FOXP3* regulatory elements. Both murine transplant models and humanized mice engrafted with LV-modified HSCs show high levels of LV expression selective for CD4+CD25+FoxP3+ Treg cells. LV transduction of scurfy (FoxP3^{mut}) HSCs restores development of functional FoxP3+ Treg cells that suppress T cell proliferation *in vitro* and rescue the scurfy autoimmune phenotype *in vivo*. These findings demonstrate preclinical efficacy for the treatment of IPEX patients by autologous HSC transplant and may provide valuable insights into new cell therapies for autoimmunity.

INTRODUCTION

Lentiviral vector (LV)-based hematopoietic stem and progenitor cell (HSPC) gene therapy has recently demonstrated remarkable success, with a number of phase I and II trials reporting safe and efficacious correction of genetic blood cell disorders (Morgan et al., 2017). One excellent candidate disease for HSPC gene therapy is immune dysregulation polyendocrinopathy enteropathy X-linked (IPEX) syndrome. IPEX is a devastating autoimmune disease caused by mutations in the gene encoding FoxP3 (Bennett et al., 2001; Wildin et al., 2001), a transcription factor required for the proper development and function of regulatory T (Treg) cells (Fontenot et al., 2003). Treg cells are critical for providing dominant suppression of autoreactive conventional T (Tconv) cells; thus, their absence causes severe and often fatal multi-organ autoimmunity. Allogeneic HSPC transplantation can

be curative for IPEX patients but is limited due to a lack of suitable donors and immunologic transplant complications (Barzaghi et al., 2018).

Previous work has explored gene therapy for IPEX through *ex vivo* correction and adoptive transfer of autologous T cells. Passerini et al. (2013) demonstrated that a LV that confers constitutive FoxP3 expression (under the EF1a promoter) can convert IPEX Tconv cells to Treg-like cells with suppressive function. Although adoptive T cell transfer may offer a promising clinical strategy, generating sufficient Treg cell numbers that maintain long-term *in vivo* persistence after adoptive transfer may prove difficult (Riley et al., 2009). As an alternative strategy, we have explored LV modification of HSCs to restore physiologic FoxP3 expression, which could ideally provide IPEX patients with a life-long source of Treg cells that develop under physiologic conditions in the thymus and periphery.

Here, we describe the development of a LV regulated by human *FOXP3* genetic elements that recapitulates physiologic FoxP3 expression. In contrast to an ectopic expression strategy, this lineage-specific vector shows an expression pattern highly selective for the Treg cell lineage and shows no impairment of HSPC function. LV modification of scurfy (a FoxP3^{mut} mouse model of IPEX) HSPC generates FoxP3+ Treg cells with *in vivo* suppressive capacity capable of curing the autoimmune scurfy phenotype. Additionally, humanized mouse models engrafted with LV-modified human HSPC from healthy donors show high levels of Treg-cell-selective LV expression, suggesting that this approach may be similarly efficacious in human IPEX patients.

RESULTS

Development of an Endogenously Regulated FoxP3 LV

Many successful LV-based gene therapies to date have utilized constitutively active promoters to drive high levels of expression of a therapeutic protein (Morgan et al., 2017). To determine whether ubiquitous, high levels of FoxP3 expression throughout the hematopoietic system could be a suitable strategy for IPEX HSPC gene therapy, we evaluated the effects of a LV expressing FoxP3 cDNA under the control of the MNDU3 promoter. Although ubiquitous FoxP3 expression did not adversely affect HSPC viability (Figures S1A and S1E) or early engraftment (Figures S1B and S1C), we noted a profound defect in mature blood cell production in both murine (Figures S1C and S1D) and NSG (NOD-scid IL2rγ^{null}) xenograft models (Figure S1F), suggesting
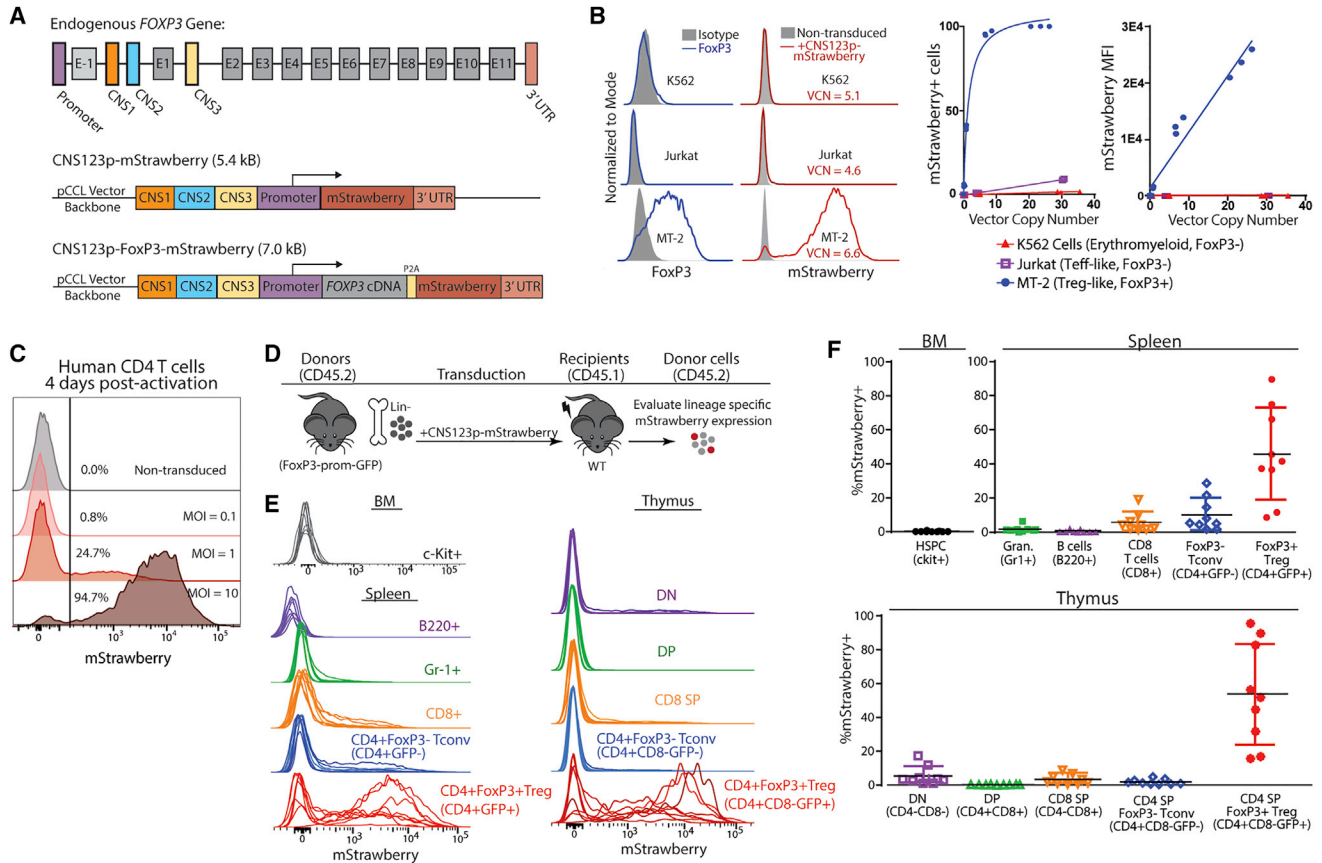
Figure 1. The FoxP3 Reporter LV Shows Expression Selective for the Treg Cell Lineage

(A) Endogenous human *FOXP3* gene shows location of regulatory regions (promoter, CNS1, CNS2, CNS3, and 3′ UTR) included in vector. Vector maps show design of CNS123p-mStrawberry and CNS123p-FoxP3-mStrawberry constructs within the pCCL vector backbone.

(B) Analysis of human hematopoietic cell lines transduced with CNS123p-mStrawberry. Histograms show endogenous FoxP3 status of each cell line (left) and mStrawberry expression (right) in each cell line transduced with CNS123p-mStrawberry. Plots show mStrawberry expression in human hematopoietic cell lines over a range of vector copy numbers (n = 12 per cell line).

(C) Activated human CD4 cells transduced with different doses of CNS123p-mStrawberry. Histograms show mStrawberry expression in viable CD4+ cells analyzed 4 days after activation. (see also Figure S2B).

(D) Experimental design to evaluate *in vivo* lineage-specific expression of CNS123p-mStrawberry. Lin− HSPCs were isolated from CD45.2 FoxP3-prom-GFP mice and transduced with CNS123p-mStrawberry. Transduced lin− HSPCs were transplanted into lethally irradiated congenic CD45.1 recipients. CD45.2 donor cells within each hematopoietic lineage were analyzed at 20 weeks post-transplant for mStrawberry reporter LV expression (see also Figure S2A).

(E) Histograms depict mStrawberry reporter expression in each hematopoietic lineage in bone marrow, thymus, and spleen of engrafted mice. Each individual histogram line represents mStrawberry expression for an individual mouse (n = 9 mice; see also Figure S2C).

(F) y axis represents the percentage of mStrawberry+ cells within each hematopoietic lineage in the BM, spleen, and thymus (n = 9 mice).

Data in (E) represent mean ± SD.

that ubiquitous FoxP3 expression is detrimental to HSPC proliferation and differentiation. We therefore sought to design a LV based on the endogenous *FOXP3* gene to confer targeted and developmentally appropriate FoxP3 expression. Here, we utilized three previously characterized conserved regulatory regions within the *FOXP3* gene: conserved noncoding sequence (CNS) 1; CNS2; and CNS3 (Figure 1A). The three CNS elements were added upstream of the *FOXP3* promoter, and the *FOXP3* 3′ UTR was added after the expression cassette. Two LVs were designed using this construct to drive the expression of the fluorescent reporter mStrawberry only (hereby referred to as "CNS123p-mStrawberry") or the *FOXP3* cDNA and mStrawberry through a 2A linkage element ("CNS123p-FoxP3-mStrawberry").

The Endogenously Regulated LV CNS123p-mStrawberry Shows High Specificity for the Treg Cell Lineage

We first evaluated the specificity of the CNS123p-mStrawberry reporter LV in three human cell lines representing different hematopoietic lineages (Figure 1B). Analysis of transduced cells by flow cytometry revealed mStrawberry expression restricted to the FoxP3+ MT-2 cells (Treg-like cells) with low inherent "leakiness" of expression in FoxP3− cell types (K562 [erythromyeloid] and Jurkat [Tconv-like cells]), even at very high vector copy numbers (up to ∼25 copies/cell). Transduction of activated human CD4 T cells (which induce FoxP3 upon activation) also showed a LV dose-dependent increase in mStrawberry expression (Figure 1C). These results suggest that the CNS123p elements confer highly specific gene

expression in FoxP3+ cells and lack basal expression in inappropriate cell types.

In order to evaluate *in vivo* lineage specificity of the CNS123p-mStrawberry reporter LV, we transduced CD45.2 lineage-marker-negative (lin−) HSPC from the bone marrow of FoxP3-prom-GFP reporter mice (which co-express FoxP3 and GFP) with CNS123p-mStrawberry and transplanted the modified cells into congenic CD45.1 recipients (Figure 1D). 20 weeks post-transplant, mStrawberry expression was evaluated in hematopoietic lineages of donor CD45.2 cells. Here, we observed that mStrawberry expression from CNS123p-mStrawberry closely matched GFP expression from the endogenous *FOXP3* gene. mStrawberry expression was selective for the Treg cell lineage (CD4+GFP+), with minimal mStrawberry expression in all other lineages (Figures 1E and 1F). Variability of mStrawberry expression among mice could partly be explained by variations in the VCN of engrafted HSCs; mice engrafted with high vector copy number (VCN) showed the brightest mStrawberry expression in the CD4+GFP+ Treg cell lineage and highest degree of background expression in CD4+GFP− Tconv cell (Figure S2C). These results suggest that expression of CNS123p-mStrawberry is highly concordant with endogenous FoxP3 expression throughout hematopoietic development.

LV Correction of FoxP3 Mutant HSCs from the Scurfy Mouse Generates Functional Treg Cells with Suppressive Function

We next determined whether CNS123p-FoxP3-mStrawberry (encoding FoxP3 cDNA) could restore functional Treg cell development from scurfy (FoxP3^{mut}) HSCs. In the absence of treatment, scurfy mice succumb to a fatal lymphoproliferative disorder starting ∼21 days after birth. Therefore, we rescued neonatal scurfy mice (CD45.2) at birth by injection of wild-type (WT) splenocytes (CD45.1) to allow for survival to adulthood and provide a source of scurfy HSPC. To assess restoration of functional Treg cell development, we transplanted WT CD45.1 recipients with one of three different sources of CD45.2 HSPC: (1) Scurfy lin− cells transduced with CNS123p-mStrawberry; (2) scurfy lin− cells transduced with CNS123p-FoxP3-mStrawberry; and (3) WT FoxP3-GFP lin− cells transduced with CNS123p-mStrawberry (Figure 2A).

Analysis of reconstituted donor thymocytes from each of the three sources revealed no changes in lineage distribution, suggesting that the lineage-specific CNS123p-FoxP3-mStrawberry LV did not alter thymocyte differentiation (Figure 2B). Transplant recipients reconstituted with WT FoxP3-GFP HSCs showed 3.7% ± 0.6% (mean ± SD) GFP+ cells within the CD4 single-positive (CD4 SP) population, and recipients reconstituted with LV-corrected scurfy HSCs showed 2.1% ± 0.4% mStrawberry+ cells, confirming that corrected scurfy HSPC produced CD4 SP thymocytes, which express FoxP3 (Figure 2C). Donor thymocytes were further evaluated for the expression of Treg cell surface markers. Although uncorrected (FoxP3^{mut}) Sf-Treg cells in the thymus showed low expression of the Treg cell surface markers CD25 and GITR, mStrawberry^{high} cSf-Treg cells showed CD25 and GITR expression comparable to WT-Treg cells (Figure 2C). In contrast, mStrawberry^{low} cSf-Treg cells showed low Treg cell surface marker expression (Figure S2D), suggesting that phenotypic Treg cell restoration only occurs in cells expressing high levels of mStrawberry/FoxP3.

We next characterized the suppressive function of splenic cSf-Treg cells. Three groups of putative Treg cells (Sf-Treg cells, cSf-Treg cells, and WT-Treg cells) were fluorescence-activated cell sorting (FACS) sorted from the spleens of transplant recipients (Figure 2D) and evaluated for their capacity to suppress WT CD4 T cell proliferation at a 1:1 suppressor-to-effector ratio (Figure 2E). Although uncorrected (FoxP3^{mut}) Sf-Treg cells showed no suppression of T cell proliferation relative to control (no Treg cells), mStrawberry^{high} cSf-Treg cells dramatically inhibited effector T cell proliferation, confirming that CNS123p-FoxP3-mStrawberry restores functional suppressive activity to Treg cells.

To determine whether corrected scurfy CD4 Tconv cells were capable of generating inducible Treg cells (iTreg cells), cSf Tconv (CD4+mStrawberry−) cells or WT Tconv (CD4+GFP−) cells were FACS sorted and activated using CD3 and CD28 beads in the presence of transforming growth factor β (TGF-β). Four days after activation with TGF-β, cSf Tconv cell showed robust induction of mStrawberry (Figure 2F), demonstrating that corrected Sf-Tconv cells are capable of *de novo* FoxP3 induction. Collectively, our data suggest that LV correction of scurfy HSCs promotes physiologic restoration of a functional Treg cell compartment.

The Lineage-Specific FoxP3 LV (CNS123p-FoxP3-mStrawberry) Generates Treg Cells Capable of Rescuing Scurfy Mice

The most stringent test of Treg cell function is the ability to reverse clinical disease signs in neonatal scurfy mice through *in vivo* suppression of autoimmunity. To this end, we first attempted to transplant neonatal scurfy mice with WT or LV-corrected scurfy HSPC. Long-term survival was poor in all arms despite detectable engraftment of donor cells, suggesting low efficacy of purified HSPC transplant (even from WT donors) in the scurfy model (Figures S3A and S3B).

We speculated that poor survival in scurfy mice transplanted with WT HSPC may be due to the rapid onset of irreversible multi-organ autoimmune damage, which occurs long before HSPC can generate mature Treg cells to control the autoimmune response in this model system. We therefore pursued an alternative approach, in which mature, corrected scurfy Treg cells (generated through transplant of WT recipients) were adoptively transferred to scurfy neonates. Lin− HSPC from CD45.2 scurfy mice (rescued with CD45.1 splenocytes at birth) or WT mice (FoxP3-prom-GFP) were transduced with CNS123p-mStrawberry or CNS123p-FoxP3-mstrawberry LV and transplanted into congenic CD45.1 WT recipients (Figure 3A). 8 weeks after transplant, donor CD45.2+CD4+ cells were purified from spleens of transplant recipient to obtain three groups of bulk CD4+ cells containing putative Treg cells: uncorrected scurfy CD4+ (Sf-CD4+); corrected scurfy CD4+ (cSf-CD4+); or wild-type CD4+ (WT-CD4+). FACS analysis of purified CD45.2+CD4+ cells showed no detectable contaminating CD45.1 cells from recipient mice or from the initial rescue of scurfy donors (Figure S3C).

Purified CD4+ cells (Figure S3D) were injected into scurfy neonates, which were analyzed for progression of the autoimmune phenotype at 21 days. Untreated (sham PBS injection) scurfy mice showed typical external signs of disease progression, including scaly, thickened ear skin (Figure 3B) and splenomegaly (Figure 3C). Untreated mice also exhibited an inflammatory
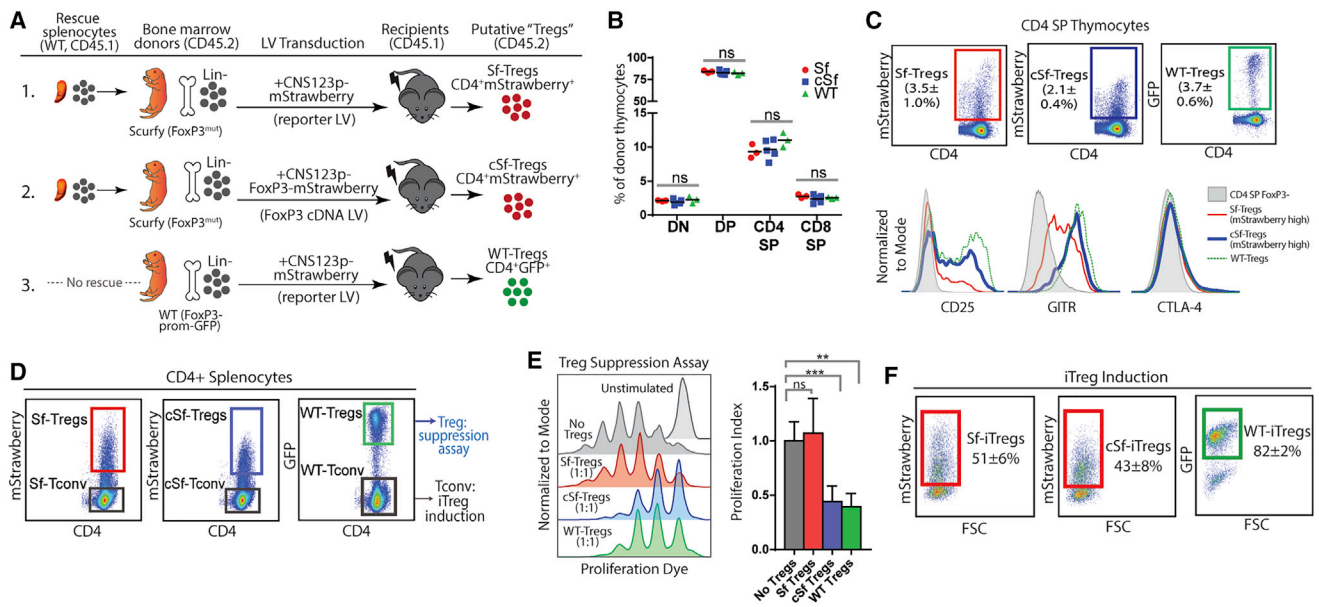
Figure 2. Lineage-Specific FoxP3 Expression Restores Treg Cell Development from Scurfy (FoxP3 Mutant) HSCs

(A) Transplant setup to evaluate Treg cell development. Scurfy (FoxP3^{mut}) mice were rescued with WT CD45.1 splenocytes at birth to allow survival into adulthood to serve as bone marrow donors. Lin− HSPCs were isolated from rescued scurfy (FoxP3^{mut}) or wild-type (FoxP3-prom-GFP) donor mice and transduced with CNS123p-mStrawberry or CNS123p-FoxP3-mStrawberry. Transduced lin− HSPCs were transplanted into lethally irradiated WT CD45.1 congenic recipients. After 12 weeks, donor cells from each transplant cohort were evaluated for thymic and splenic reconstitution of Treg cells. Treg cell populations from each group were identified as CD4+mStrawberry+ cells (uncorrected scurfy Treg cells [Sf-Treg cells]; corrected scurfy Treg cells [cSf-Treg cells]) or CD4+GFP+ cells (wild-type Treg cells [WT-Treg cells]).

(B) Lineage distribution of total donor thymocytes in mice reconstituted with Sf, cSf, or WT BM lin− cells (n = 3–5 mice/arm).

(C) Thymic Treg cell reconstitution. FACS plots show donor CD45.2+CD4SP cells in the thymus of transplant recipients. Gates delineate thymic Sf-Treg cells, cSf-Treg cells, and WT-Treg cells. Bottom panel shows expression of the Treg cell surface markers CD25, GITR, and CTLA4 within each putative Treg cell population (surface marker expression for Sf-Treg cells and cSf-Treg cells is shown for mStrawberry^{high} cells or cells expressing the top 50% of mStrawberry expression). Histograms depict one representative experiment of 3 (see also Figure S2D).

(D) FACS sort for splenic Treg and Tconv cells. Splenic Treg cell populations (mStrawberry^{high} or GFP+ gates) were FACS sorted for a Treg cell suppression assay. Tconv cell populations (mStrawberry− or GFP− gates) were sorted for an iTreg cell induction assay.

(E) *In vitro* Treg cell suppression assay. Sorted Treg cells (shown in D) were co-cultured with responder T cells (Tresp cells) (congenic WT CD4+ cells labeled with a fluorescent proliferation dye) at a 1:1 ratio in the presence of bead-bound CD3 and CD28 antibodies. Histograms depict Tresp cell proliferation in one of three representative experiments. Bar graph shows proliferation index for each Treg cell culture condition (n = 6–9 Tresp cell cultures per arm from 3 different Treg cell sources per arm; data normalized to internal "no Treg cell" control for each experiment).

(F) Sorted splenic Tconv cells (shown in D) were activated with CD3 and CD28 antibodies in the presence of 20 ng/mL interleukin-2 (IL-2) and 20 ng/mL TGF-β for 4 days to induce iTreg cells. FACS plots show mStrawberry or GFP expression from each group (n = 3 mice/group).

Data in (B), (C), (E), and (F) are presented as mean ± SD. Data in (B) were analyzed by Kruskal-Wallis test for each lineage. Data in (E) are analyzed by Kruskal-Wallis test for overall comparison for all groups and Mann-Whitney U test for pairwise comparisons. *p < 0.05; **p < 0.01; ***p < 0.001; NS, not significant.

phenotype, including a high percentage of activated CD62L-CD44+ CD4 T cells (Figure 3D) and elevated levels of inflammatory serum cytokines (Figure 3E) compared to age-matched WT controls. Our initial pilot studies investigating adoptive transfer of cSf CD4 to scurfy neonates showed minimal correction of the activated T cell phenotype (Figures S3D and S3E) and external scurfy signs (data not shown). We speculated this may be due to low levels of gene transfer (CD4 VCN < 2; <3% mStrawberry+ cells); thus, we included the transduction-enhancing agent poloxamer F108 (Hauber et al., 2018) to our protocol, which enhanced gene transfer (CD4 VCN > 3; >5% mStrawberry; Figure S3D). Adoptive transfer of cSf-CD4 under this protocol resulted in complete correction of all measures of the scurfy phenotype such that these mice were phenotypically indistinguishable from age-matched WT controls (Figure 3B). In contrast, scurfy mice receiving uncorrected Sf-CD4 cells showed no signs of disease amelioration (Figures 3B–3E), con-

firming that the bone marrow transplant (BMT) and CD4 purification procedure did not carry over any contaminating CD45.1 WT Treg cells from transplant recipients or the initial rescue of scurfy HSPC donors. Collectively, these results suggest that high levels of gene modification with CNS123p-FoxP3-mStrawberry can generate CD4+ Treg cells capable of suppressing autoimmune responses *in vivo*.

The CNS123p-mStrawberry LV Shows High Levels of Lineage-Specific Expression in a Humanized Mouse Model

We next explored the expression patterns of the CNS123p-mStrawberry reporter LV in a humanized xenograft model. Healthy human CD34+ HSPCs isolated from cord blood were transduced with CNS123p-mStrawberry and transplanted into NSG neonates (Figure 4A). Engrafted hCD45+ cells were analyzed at 12–16 weeks post-transplant by flow cytometry to determine LV expression in each hematopoietic lineage (Figures 4B, 4C, and
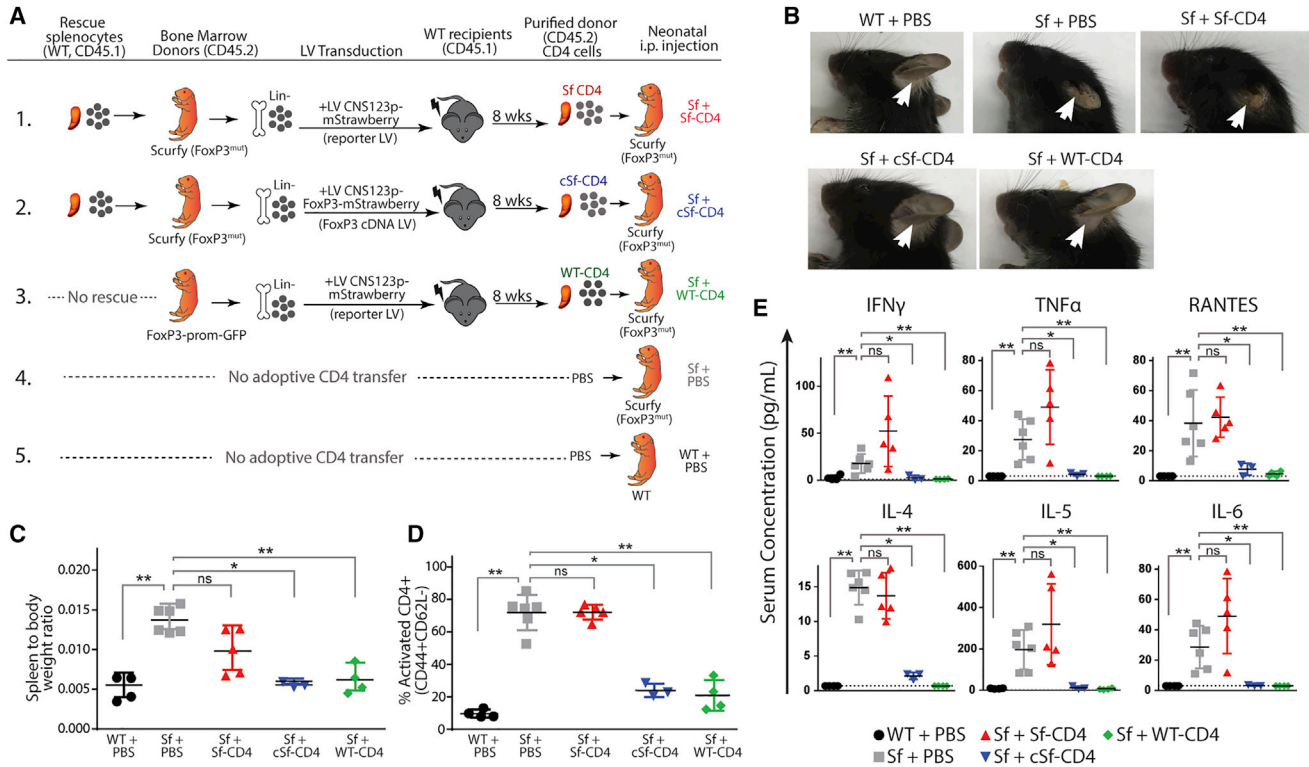
Figure 3. The Lineage-Specific FoxP3 cDNA Vector Generates Functional Treg Cells Capable of Rescuing the Scurfy Mouse

(A) Assay for *in vivo* Treg cell function: three groups of CD4 cells containing putative Treg cells were generated by congenic bone marrow transplants: uncorrected scurfy CD4 (Sf-CD4; no. 1); corrected scurfy CD4 (cSf-CD4; no. 2); and wild-type CD4 (WT-CD4; no. 3). To obtain Sf-CD4 and cSf-CD4, CD45.2 Lin− HSPCs were isolated from scurfy donors (rescued at birth by CD45.1 splenocytes) and transduced with either CNS123p-mStrawberry (Sf-CD4; no. 1) or CNS123p-FoxP3-mStrawberry (cSf-CD4; no. 2). To obtain WT-CD4, CD45.2 Lin− HSPCs were isolated from FoxP3-prom-GFP donors and transduced with CNS123p-mStrawberry (no. 3). Transduced cells were transplanted into lethally irradiated congenic (CD45.1) recipients. 8 weeks post-transplant, donor CD45.2+CD4+ cells were purified with magnetic beads from the spleens of transplant recipients and injected intraperitoneally into scurfy neonates. Scurfy neonates and age-matched WT receiving PBS injection were also analyzed as control conditions no. 4 and no. 5. The autoimmune phenotype of all groups was evaluated at 21 days of life (see also Figure S3).

(B) Photographs of scurfy mice or WT controls at 21 days. White arrows highlight ear skin phenotype in mice from each group. Ear skin inflammation (characterized by small, thickened, scaly ears) is seen in untreated scurfy mice (Sf + PBS) and scurfy mice receiving uncorrected scurfy CD4 cells ("Sf + Sf-CD4"). Normal ear skin without inflammation is seen in WT controls ("WT + PBS") and scurfy mice receiving wild-type or corrected scurfy CD4 cells ("Sf + WT-CD4" and "Sf + cSf-CD4").

(C) Spleen-to-body-weight ratio for rescued scurfy mice or WT littermate controls.

(D) Activated (CD44+CD62L−) CD4 T cells (expressed as a percentage of total CD4 splenocytes) in the spleens of rescued scurfy mice or WT littermate controls.

(E) Serum cytokine levels in rescued scurfy mice or WT littermate controls.

Data in (C)–(E) are presented as mean ± SD. Data on (C)–(E) represent n = 3 independent experiments pooled for analysis with a total of 3–6 mice/arm. Data in (C)–(E) were analyzed by Kruskal-Wallis test for overall comparison for all groups, and Mann-Whitney U test was performed for pairwise comparisons. *p < 0.05; **p < 0.01.

S4A). In bone marrow (BM), no mStrawberry expression was detected in CD33+ myeloid, CD19+ B cells, or CD34+ HSPC lineages, with all expression restricted to CD3+ T cells. In the thymus, mStrawberry expression was selective for CD4+CD25+ Treg cells with minimal expression in the double negative (DN), double positive (DP), CD4SP, or CD8SP stages. In the spleen, mStrawberry expression was brightest in CD4+CD25+ Treg cells with lower levels of expression observed in CD4+CD25− Tconv cells and CD8+ T cells. The intensity of mStrawberry fluorescence positively correlated with the level of gene correction (Figure S4C), and expression intensity was highest in the CD4+CD25+ Treg cell subset for each mouse analyzed (Figures 4B and S4C).

Although CD25 is a useful cell surface marker that identifies FoxP3+ Treg cells, we more stringently determined the Treg

cell lineage specificity of CNS123p-mStrawberry with intracellular FoxP3 staining. Human CD4+ cells isolated from the spleens of humanized NSG-SGM3 mice were FACS sorted into mStrawberry+ and mStrawberry− populations prior to FoxP3 staining (Figure 4D). We observed that 81% of mStrawberry+ cells were also FoxP3+, although only 2.5% of mStrawberry− cells were FoxP3+, suggesting high concordance of CNS123p-mStrawberry expression and endogenous FoxP3 expression in a humanized mouse model.

During thymopoiesis, active demethylation of the CNS2 region is a critical event that induces heritable commitment to the Treg cell lineage (Toker et al., 2013). Demethylated CNS2 maintains stable high levels of FoxP3 expression through its enhancer function on the FoxP3 promoter (Li et al., 2014; Zheng et al.,
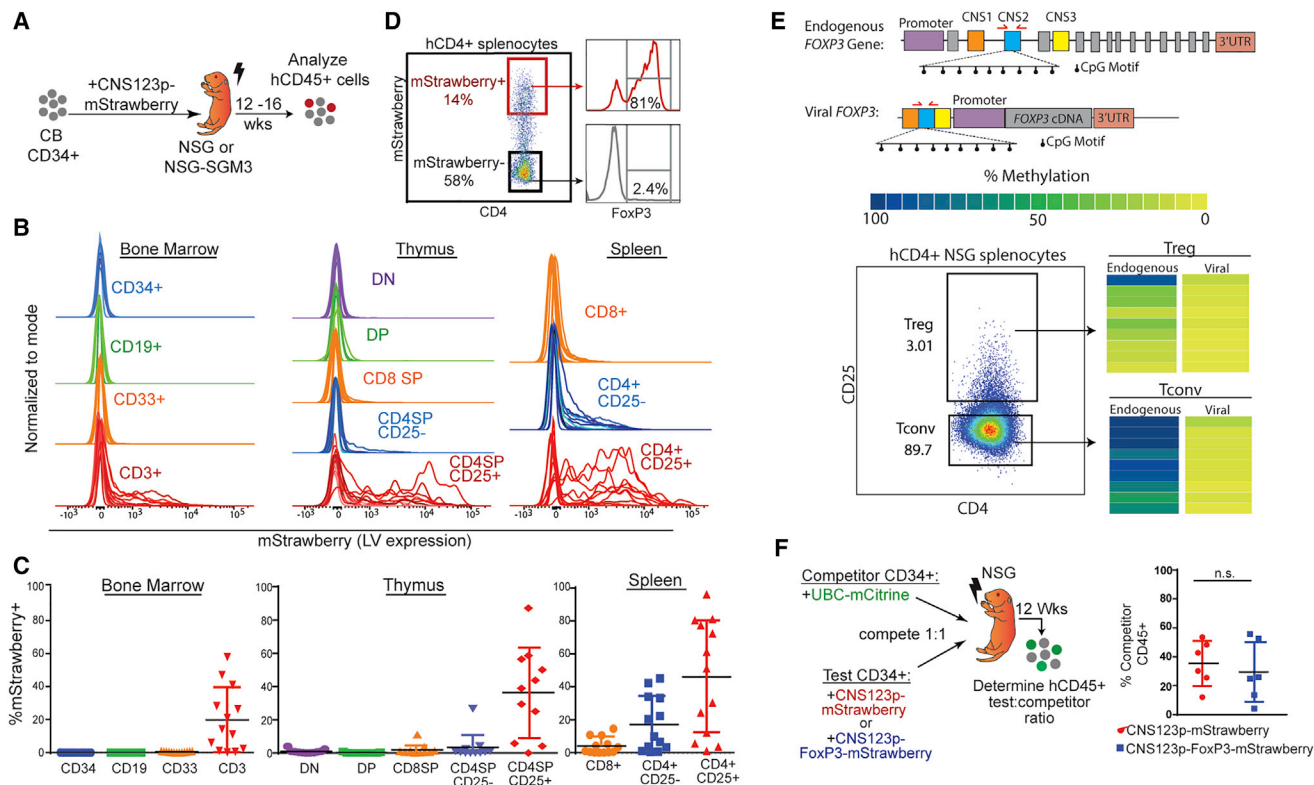
Figure 4. The FoxP3 Reporter Vector CNS123p-mStrawberry Shows Treg Cell Lineage-Selective Expression in a Humanized Mouse Model

(A) Experimental setup for humanized mouse models. Cord blood CD34+ HSPCs were transduced with CNS123p-mStrawberry and transplanted into neonatal NSG mice (B, C, E, and F) or NSG-SGM3 mice (D). 12–16 weeks post-transplant, engrafted hCD45+ cells were analyzed for mStrawberry expression.

(B) mStrawberry reporter expression in each hematopoietic lineage. Each overlaid histogram represents mStrawberry expression in an individual mouse (n = 10–14 mice humanized with 2 different cord blood CD34+ donors; see also Figures S4A–S4C).

(C) Percentage of mStrawberry+ cells in each lineage shown in (B).

(D) Co-expression of FoxP3 and mStrawberry in humanized mice. Splenic human CD4+ cells were FACS sorted into mStrawberry+ and mStrawberry− populations followed by intracellular staining for FoxP3 expression. Left panel shows sorting of human CD4+ cells by mStrawberry expression, and right panel shows FoxP3 expression in sorted populations. Results are representative of 2 independent experiments.

(E) CNS2 methylation analysis of T cell populations from humanized mice. Figure shows the locations of CNS2 within the endogenous *FOXP3* gene and CNS2 within the viral genome. Red arrows indicate differential primer binding sites for amplification of endogenous or viral CNS2. FACS plot shows sorting gates used to define Treg cell (CD4+CD25+) and Tconv cell (CD4+CD25−) populations in CD4-enriched cells isolated from the pooled spleens of 3–5 humanized mice. Heatmap represents the percentage of methylated reads detected at each of the 9 CpG sites within endogenous and viral CNS2. Results are representative of 2 independent experiments using pooled NSG cohorts humanized from 2 different CB CD34+ donors (see also Figures S4D–S4F).

(F) Experimental setup for NSG competitive repopulation assay. "Test" CB CD34+ cells were transduced with either CNS123p-mStrawberry or CNS123p-FoxP3-mStrawberry, and "competitor" CD34+ cells were transduced with a UBC-mCitrine vector. Test and competitor cells were co-transplanted at a 1:1 ratio into NSG neonates, and the percentage of competitor (mCitrine+) CD45+ cells engrafted in the BM at 12 weeks was determined for each group (n = 6 mice per group; humanized from 2 different CB CD34+ donors).

Data in (F) represent mean ± SD. Data in (F) were analyzed by Mann-Whitney U test.

2010); thus, we were interested in evaluating CpG methylation patterns within the viral CNS2 element contained within CNS123p-FoxP3-mStrawberry. Genomic DNA from Tconv cell and Treg cell subsets (generated in humanized mice) was analyzed for methylation of 9 regulated CpG sites present in endogenous and viral CNS2 utilizing pyrosequencing primers specific for each sequence (Figure 4E). As expected, CpG sites within the endogenous *FOXP3* CNS2 were methylated in sorted Tconv cells and demethylated in sorted Treg cells. Interestingly, viral CNS2 remained fully demethylated in both populations, suggesting that viral CNS2 is not regulated in the same manner as endogenous CNS2 during Treg cell differentiation from HSCs.

Lastly, we evaluated the effects of CNS123p-FoxP3-mStrawberry on HSPC function using a competitive transplant model. CD34+ "test cells" were transduced with either CNS123p-mStrawberry or CNS123p-FoxP3-mStrawberry, combined with an equal number of fluorescently labeled (UBC-mCitrine transduced) competitor cells, and transplanted into neonatal NSG mice (Figure 4F). At 12 weeks post-transplant, engrafted hCD45+ cells were evaluated for the relative contribution of fluorescently labeled competitor cells. Here, we observed no difference in the relative proportions of competitor cells between groups. This suggests that, unlike constitutive FoxP3 expression from MNDU3-FoxP3, lineage-specific FoxP3 expression from CNS123p-FoxP3-mStrawberry

shows no detrimental effects on hCD45+ reconstitution in engrafted mice.

DISCUSSION

Our studies and others (Santoni de Sio et al., 2017) revealed that a lineage-specific strategy for restoration of FoxP3 expression is important to avoid impaired hematopoietic differentiation. Thus, we sought to develop a LV-based therapy to treat IPEX, which could restore physiologic FoxP3 expression within the developing hematopoietic system, resulting in the development of functional Treg cells and resolution of autoimmunity. To accomplish this, we included the three FoxP3 CNS enhancer sequences in the LV. These sequences are highly conserved, and their role in FoxP3 regulation has been previously well characterized in mouse models (Zheng et al., 2010). In these studies, we have further shown that these three elements in combination with the FoxP3 promoter are sufficient to drive gene expression in a lineage-selective manner in a human model of Treg cell development.

Although LV CNS123p-mStrawberry showed a high degree of selectivity for the Treg cell lineage, we noted that, at higher VCN, LV expression could be seen in off-target lineages not typically associated with FoxP3 expression, including CD8 T cells and CD4 Tconv cells. This is consistent with prior work describing a FoxP3 transgenic mouse line (FoxP3-Tg) containing ~16 copies of the endogenous FoxP3 gene, in which almost all CD4+ cells (including CD4+CD25− cells) express FoxP3 and show suppressive function (Brunkow et al., 2001; Khattri et al., 2001, 2003; Miao et al., 2009). Thus, the expression pattern from multiple copies of LV CNS123p-mStrawberry closely mimics that seen with multiple endogenous FOXP3 gene copies.

An important question is whether leaky expression at high copy numbers (either from the FoxP3 LV or from the FoxP3-Tg mouse) has negative outcomes. FoxP3-Tg mice were reported to be viable, had normal thymocyte development, and showed a phenotype of general immune suppression. Although our main goal in generating a lineage-specific LV was to avoid HSC impairment, it is not clear that perfectly specific (versus highly selective) expression for the Treg cell lineage is required to treat IPEX. We currently hypothesize that leaky FoxP3 expression in Tconv cells could further induce a state of immune suppression and be advantageous in severe inflammatory diseases, where the benefit of intense immunosuppressive drug regimens outweighs the risks, such as IPEX, autoimmune disease, or prevention of organ rejection.

Furthermore, we noted divergent regulation of endogenous CNS2 and viral CNS2 in humanized mouse models. CNS2 is responsible for maintaining stable FoxP3 expression in committed Treg cells (Li et al., 2014). Recent evidence has suggested that demethylation of CNS2 is an active process initiated by Tet enzymes during thymic Treg cell development, which allows the CNS2 enhancer region to drive high levels of FoxP3 expression in committed Treg cells (Toker et al., 2013; Yue et al., 2016). Interestingly, although we observed the predicted patterns of endogenous CNS2 methylation in Tconv cells and demethylation in Treg cell subsets, the viral CNS2 sequence was fully demethylated in both cell types. This suggests that introduction of a demethylated CNS2 region at the HSC state

(via LV transduction) may allow this region within the LV to remain demethylated throughout development; in contrast, endogenous CNS2 may be methylated earlier in embryogenesis, with specific demethylation occurring during thymopoiesis and Treg cell development. Despite the discordance between endogenous and viral CNS2 methylation, LV expression remains highly selective for the Treg cell lineage, suggesting that demethylated CNS2 alone does not drive FoxP3 expression and that CNS1, CNS3, and the FoxP3 promoter may confer additional specificity. Furthermore, as hypermethylation of CNS2 is associated with reduced FoxP3 expression (Li et al., 2014) and impaired Treg cell function in patients with autoimmune disorders (Guo et al., 2016), it is tempting to speculate that a LV that maintains demethylated CNS2 could be advantageous for improving FoxP3 expression in autoimmune disorders, though this possibility remains to be explored.

An important consideration surrounding clinical translation is the level of HSC correction and engraftment required to resolve autoimmunity in IPEX patients. Reports of allogeneic HSC transplant in IPEX patients demonstrate that successful resolution of autoimmunity can be achieved with partial donor chimerism (Barzaghi et al., 2018). In some of these cases, it has been shown that donor Treg cells exhibit a selective advantage with full donor chimerism in the Treg cell compartment despite low levels of total donor engraftment (Kasow et al., 2011; Seidel et al., 2009).

Our studies suggest that, in its current form, the LV we have designed is less efficient than the endogenous FOXP3 gene in generating FoxP3 protein expression; multiple copies of the FoxP3 LV were required to produce Treg cells that could functionally correct autoimmunity in the scurfy mouse. It is possible that the human FOXP3 regulatory elements and human FoxP3 protein function sub-optimally in the mouse system, that there are additional FOXP3 genomic enhancers that we have not included in the LV design, or that the mutant scurfy FoxP3 protein may have a dominant-negative action on WT FoxP3 protein expressed from the LV. Despite these potential limitations, we have shown that Treg cell function can be restored with the LV when high copy number is achieved in the scurfy model. Further studies will aim to evaluate the corrective VCN required to restore the development of functional Treg cells from human IPEX HSCs.

An additional limitation of our *in vivo* studies was the fact that we were unable to directly transplant scurfy recipients with corrected scurfy HSCs, perhaps due to the rapid onset of disease in this model, which was also not rescued in the control group transplanted with wild-type donor stem cells. This precludes the direct demonstration that corrected scurfy HSCs are capable of developing into functional Treg cells in a FoxP3[mut] recipient. However, clinical evidence has shown that IPEX patients undergoing allogeneic bone marrow transplant generate Treg cells with "recent thymic emigrant" phenotype (CD4+CD45RA+CD31+), suggesting that *de novo* Treg cell generation in the thymus occurs in IPEX patients and that a HSCT with gene therapy strategy would be theoretically efficacious from this perspective.

In summary, we demonstrate the development of an endogenously regulated LV, which successfully restores Treg cell development from FoxP3[mut] HSCs. Corrected Treg cells closely resemble WT Treg cells in phenotype and function and,

importantly, are capable of reversing the autoimmune phenotype of the scurfy mouse. Furthermore, humanized mouse models reveal efficient gene modification of HSCs and high levels of lineage-specific expression, suggesting favorable translation of this therapy for IPEX patients. More broadly, this work demonstrates a strategy to reprogram the immune system at the HSC level to restore immunologic tolerance. Although IPEX is a rare disease, its severity and lack of suitable treatment make it an excellent gateway disease to provide biologic insight into the development of new HSC-based therapies, which modulate immunologic tolerance. These findings pave the way for the treatment of IPEX patients by autologous HSCT and may provide valuable insights into new treatments for patients with autoimmune disorders of different origin.

STAR★METHODS

Detailed methods are provided in the online version of this paper and include the following:

- KEY RESOURCES TABLE
- CONTACT FOR REAGENT AND RESOURCE SHARING
- EXPERIMENTAL MODEL AND SUBJECT DETAILS
  - Mice
  - Cell lines
  - Primary Cells
  - Lentiviral vectors
- METHOD DETAILS
  - Lentiviral transduction
  - Determination of vector copies (VC) per cell
  - Murine Congenic Transplants
  - Murine CD4 isolation
  - Treg Suppression Assay and induction of iTregs
  - Rescue of scurfy neonates with corrected Tregs and analysis
  - Humanized xenografts
  - Human CD4 enrichment from NSG spleens
  - Methylation Analysis/Bisulfite Sequencing
  - Flow cytometry
- QUANTIFICATION AND STATISTICAL ANALYSIS
- DATA AND SOFTWARE AVAILABILITY

SUPPLEMENTAL INFORMATION

Supplemental Information includes four figures and can be found with this article online at https://doi.org/10.1016/j.stem.2018.12.003.

REFERENCES

Baldwin, K., Urbinati, F., Romero, Z., Campo-Fernandez, B., Kaufman, M.L., Cooper, A.R., Masiuk, K., Hollis, R.P., and Kohn, D.B. (2015). Enrichment of human hematopoietic stem/progenitor cells facilitates transduction for stem cell gene therapy. Stem Cells 33, 1532–1542.

Barzaghi, F., Amaya Hernandez, L.C., Neven, B., Ricci, S., Kucuk, Z.Y., Bleesing, J.J., Nademi, Z., Slatter, M.A., Ulloa, E.R., Shcherbina, A., et al.; Primary Immune Deficiency Treatment Consortium (PIDTC) and the Inborn Errors Working Party (IEWP) of the European Society for Blood and Marrow Transplantation (EBMT) (2018). Long-term follow-up of IPEX syndrome patients after different therapeutic strategies: An international multicenter retrospective study. J. Allergy Clin. Immunol. 141, 1036–1049.e5.

Bennett, C.L., Christie, J., Ramsdell, F., Brunkow, M.E., Ferguson, P.J., Whitesell, L., Kelly, T.E., Saulsbury, F.T., Chance, P.F., and Ochs, H.D. (2001). The immune dysregulation, polyendocrinopathy, enteropathy, X-linked syndrome (IPEX) is caused by mutations of FOXP3. Nat. Genet. 27, 20–21.

Brunkow, M.E., Jeffery, E.W., Hjerrild, K.A., Paeper, B., Clark, L.B., Yasayko, S.A., Wilkinson, J.E., Galas, D., Ziegler, S.F., and Ramsdell, F. (2001). Disruption of a new forkhead/winged-helix protein, scurfin, results in the fatal lymphoproliferative disorder of the scurfy mouse. Nat. Genet. 27, 68–73.

Cooper, A.R., Patel, S., Senadheera, S., Plath, K., Kohn, D.B., and Hollis, R.P. (2011). Highly efficient large-scale lentiviral vector concentration by tandem tangential flow filtration. J. Virol. Methods 177, 1–9.

Dull, T., Zufferey, R., Kelly, M., Mandel, R.J., Nguyen, M., Trono, D., and Naldini, L. (1998). A third-generation lentivirus vector with a conditional packaging system. J. Virol. 72, 8463–8471.

Fontenot, J.D., Gavin, M.A., and Rudensky, A.Y. (2003). Foxp3 programs the development and function of CD4+CD25+ regulatory T cells. Nat. Immunol. 4, 330–336.

Guo, H., Zheng, M., Zhang, K., Yang, F., Zhang, X., Han, Q., Chen, Z.-N., and Zhu, P. (2016). Functional defects in CD4+ CD25high FoxP3+ regulatory cells in ankylosing spondylitis. Sci. Rep. 6, 37559.

Hauber, I., Beschorner, N., Schrödel, S., Chemnitz, J., Kröger, N., Hauber, J., and Thirion, C. (2018). Improving lentiviral transduction of CD34+ hematopoietic stem and progenitor cells. Hum. Gene Ther. Methods 29, 104–113.

Kasow, K.A., Morales-Tirado, V.M., Wichlan, D., Shurtleff, S.A., Abraham, A., Persons, D.A., and Riberdy, J.M. (2011). Therapeutic in vivo selection of thymic-derived natural T regulatory cells following non-myeloablative hematopoietic stem cell transplant for IPEX. Clin. Immunol. 141, 169–176.

Khattri, R., Kasprowicz, D., Cox, T., Mortrud, M., Appleby, M.W., Brunkow, M.E., Ziegler, S.F., and Ramsdell, F. (2001). The amount of scurfin protein determines peripheral T cell number and responsiveness. J. Immunol. 167, 6312–6320.

Khattri, R., Cox, T., Yasayko, S.-A., and Ramsdell, F. (2003). An essential role for Scurfin in CD4+CD25+ T regulatory cells. Nat. Immunol. 4, 337–342.

Li, X., Liang, Y., LeBlanc, M., Benner, C., and Zheng, Y. (2014). Function of a Foxp3 cis-element in protecting regulatory T cell identity. Cell 158, 734–748.

Logan, A.C., Nightingale, S.J., Haas, D.L., Cho, G.J., Pepper, K.A., and Kohn, D.B. (2004). Factors influencing the titer and infectivity of lentiviral vectors. Hum. Gene Ther. *15*, 976–988.

Miao, C.H., Harmeling, B.R., Ziegler, S.F., Yen, B.C., Torgerson, T., Chen, L., Yau, R.J., Peng, B., Thompson, A.R., Ochs, H.D., and Rawlings, D.J. (2009). CD4+FOXP3+ regulatory T cells confer long-term regulation of factor VIII-specific immune responses in plasmid-mediated gene therapy-treated hemophilia mice. Blood *114*, 4034–4044.

Morgan, R.A., Gray, D., Lomova, A., and Kohn, D.B. (2017). Hematopoietic stem cell gene therapy: progress and lessons learned. Cell Stem Cell *21*, 574–590.

Passerini, L., Rossi Mel, E., Sartirana, C., Fousteri, G., Bondanza, A., Naldini, L., Roncarolo, M.G., and Bacchetta, R. (2013). CD4$^+$ T cells from IPEX patients convert into functional and stable regulatory T cells by FOXP3 gene transfer. Sci. Transl. Med. *5*, 215ra174.

Riley, J.L., June, C.H., and Blazar, B.R. (2009). Human T regulatory cell therapy: take a billion or so and call me in the morning. Immunity *30*, 656–665.

Santoni de Sio, F.R., Passerini, L., Valente, M.M., Russo, F., Naldini, L., Roncarolo, M.G., and Bacchetta, R. (2017). Ectopic FOXP3 expression preserves primitive features of human hematopoietic stem cells while impairing functional T cell differentiation. Sci. Rep. *7*, 15820.

Seidel, M.G., Fritsch, G., Lion, T., Jürgens, B., Heitger, A., Bacchetta, R., Lawitschka, A., Peters, C., Gadner, H., and Matthes-Martin, S. (2009). Selective engraftment of donor CD4+25high FOXP3-positive T cells in IPEX syndrome after nonmyeloablative hematopoietic stem cell transplantation. Blood *113*, 5689–5691.

Toker, A., Engelbert, D., Garg, G., Polansky, J.K., Floess, S., Miyao, T., Baron, U., Düber, S., Geffers, R., Giehr, P., et al. (2013). Active demethylation of the Foxp3 locus leads to the generation of stable regulatory T cells within the thymus. J. Immunol. *190*, 3180–3188.

Wildin, R.S., Ramsdell, F., Peake, J., Faravelli, F., Casanova, J.-L., Buist, N., Levy-Lahad, E., Mazzella, M., Goulet, O., Perroni, L., et al. (2001). X-linked neonatal diabetes mellitus, enteropathy and endocrinopathy syndrome is the human equivalent of mouse scurfy. Nat. Genet. *27*, 18–20.

Wunderlich, M., Brooks, R.A., Panchal, R., Rhyasen, G.W., Danet-Desnoyers, G., and Mulloy, J.C. (2014). OKT3 prevents xenogeneic GVHD and allows reliable xenograft initiation from unfractionated human hematopoietic tissues. Blood *123*, e134–e144.

Yue, X., Trifari, S., Äijö, T., Tsagaratou, A., Pastor, W.A., Zepeda-Martínez, J.A., Lio, C.W., Li, X., Huang, Y., Vijayanand, P., et al. (2016). Control of Foxp3 stability through modulation of TET activity. J. Exp. Med. *213*, 377–397.

Zheng, Y., Josefowicz, S., Chaudhry, A., Peng, X.P., Forbush, K., and Rudensky, A.Y. (2010). Role of conserved non-coding DNA elements in the Foxp3 gene in regulatory T-cell fate. Nature *463*, 808–812.

STAR★METHODS

KEY RESOURCES TABLE

REAGENT or RESOURCE	SOURCE	IDENTIFIER
Antibodies		
Ghost Dye Red 780	Tonbo Biosciences	Cat#13-0865
Ghost Dye Violet 510	Tonbo Biosciences	Cat#13-0870
CellTrace Violet Cell Proliferation Kit	ThermoFisher	Cat#C34557
DAPI	ThermoFisher	Cat#D1306
Anti-mouse CD45 APC (30-F11)	Tonbo Biosciences	Cat#20-0451; RRID:AB_2621573
Anti-mouse CD45 PE (30-F11)	BD Biosciences	Cat#553081; RRID:AB_394611
Anti-mouse CD45.1 biotin (A20)	Miltenyi Biotec	Cat# 130-101-902
Anti-mouse CD45.1 V450 (A20)	BD Biosciences	Cat#560520; RRID:AB_1727490
Anti-mouse CD45.1 APC (A20)	BD Biosciences	Cat# 558701 RRID:AB_1645214
Anti-mouse CD45.2 V450 (104)	Tonbo Biosciences	Cat#75-0454; RRID:AB_2621950
Anti-mouse CD117 (ckit) APC (2B8)	BD Biosciences	Cat#553356; RRID:AB_398536
Anti-mouse Gr-1 APC (1A8)	BD Biosciences	Cat#560599; RRID:AB_1727560
Anti-mouse B220 PerCP (RA3-6B2)	BD Biosciences	Cat#553093; RRID:AB_394622
Anti-mouse CD3-PerCP (145-2C11)	BD Biosciences	Cat#553067; RRID:AB_394599
Anti-mouse CD8a PE-Cy7 (53-6.7)	BD Biosciences	Cat#552877; RRID:AB_394506
Anti-mouse CD8a APC-Cy7 (53-6.7)	BD Biosciences	Cat#557654; RRID:AB_396769
Anti-mouse CD4 APC (RM4-5)	BD Biosciences	Cat#553051; RRID:AB_398528
Anti-mouse CD4-PE-Cy7 (RM4-5)	BD Biosciences	Cat#552775; RRID:AB_394461
Anti-mouse GITR-APC (DTA-1)	Tonbo Biosciences	Cat#20-5874; RRID:AB_2621605
Anti-mouse CTLA4(CD152)-APC (UC10-4F10-11)	Tonbo Biosciences	Cat#20-1522; RRID:AB_2621592
Anti-mouse CD25-APC (PC61.5)	Tonbo Biosciences	Cat#20-0251; RRID:AB_2621567
Anti-mouse CD25-PerCp-Cy5.5 (PC61)	BD Biosciences	Cat#551071; RRID:AB_394031
Anti-mouse CD44 PerCp-Cy5.5 (IM7)	BD Biosciences	Cat#560570; RRID:AB_1727486
Anti-mouse CD62L PECy7 (MEL-14)	Biolegend	Cat#104418; RRID:AB_313103
Anti-human CD45 APC (H130)	BD Biosciences	Cat#561864; RRID:AB_11153499
Anti-human CD45 V450 (H130)	BD Biosciences	Cat#560367; RRID:AB_1645573
Anti-human CD45 PECy7 (H130)	BD Biosciences	Cat#557748; RRID:AB_396854
Anti-human CD45 FITC (H130)	BD Biosciences	Cat#555482; RRID: AB_395874
Anti-human CD4 FITC (RPA-T4)	BD Biosciences	Cat#555346; RRID:AB_395751
Anti-human CD4 APC (RPA-T4)	BD Biosciences	Cat#555349; RRID:AB_398593
Anti-human CD8 APC (SK1)	Tonbo Biosciences	Cat#20-0087; RRID:AB_2621552
Anti-human CD25 V450 (M-A251)	BD Biosciences	Cat#560355; RRID:AB_1645565
Anti-human CD25 PerCp-Cy5.5 (M-A251)	BD Biosciences	Cat#560503; RRID:AB_1727453
Anti-human CD3 PerCP-Cy5.5 (UCHT1)	BD Biosciences	Cat#560835; RRID:AB_2033956
Anti-human CD34 APC (581)	BD Biosciences	Cat#555824; RRID:AB_398614
Anti-human CD34 PE-Cy7 (581)	BD Biosciences	Cat#560710; RRID:AB_1727470
Anti-human CD19 PE-Cy7 (SJ25C1)	BD Biosciences	Cat#557835; RRID:AB_396893
Anti-human CD33 BV421 (WM53)	BD Biosciences	Cat#562854
Anti-human FoxP3 PE (236A/E7)	BD Biosciences	Cat#560852; RRID:AB_10563418
PE Mouse IgG1 kappa Isotype Control (MOPC-21)	BD Biosciences	Cat#554680; RRID:AB_395506
Anti-human FoxP3 APC (236A/E7)	ThermoFisher	Cat#17-4777-42; RRID:AB_10804651
APC Mouse IgG1 kappa Isotype Control (P3.6.2.8.1)	ThermoFisher	Cat#17-4714-81; RRID:AB_763650
In Vivo Ready Anti-Human CD3 (OKT3)	Tonbo Biosciences	Cat#:40-0037; RRID:AB_2621438

(Continued on next page)

Continued

REAGENT or RESOURCE	SOURCE	IDENTIFIER
In Vivo Ready Anti-Mouse CD3e (145-2C11)	Tonbo Biosciences	Cat#:40-0031; RRID:AB_2621436
In Vivo Ready Anti-Mouse CD28 (37.51)	Tonbo Biosciences	Cat#:40-0281; RRID:AB_2621445
Bacterial and Virus Strains		
NEB Stable Competent *E. coli* (High Efficiency)	New England Biolabs	C3040I
LV MNDU3-GFP	Logan et al., 2004	Addgene Plasmid #81071
LV MNDU3-FoxP3-IRES-GFP	Dr. Gay Crooks, UCLA	N/A
LV UBC-mCitrine	Baldwin et al., 2015	N/A
LV CNS123p-mStrawberry	This paper	GenBank: MK012431
LV CNS123p-FoxP3-mStrawberry	This paper	GenBank: MK012431
Biological Samples		
Human Cord Blood	UCLA Hospital	N/A
Human T cells	UCLA Virology Core	N/A
Chemicals, Peptides, and Recombinant Proteins		
Recombinant Human Flt3 ligand	PeproTech	Cat#300-19
Recombinant Human TPO	PeproTech	Cat#300-18
Recombinant Human SCF	PeproTech	Cat#300-07
Recombinant Murine TPO	PeproTech	Cat#315-14
Recombinant Murine SCF	PeproTech	Cat#250-03
Recombinant Human TGF-β1	PeproTech	Cat#100-21
Recombinant Human IL-2	PeproTech	Cat#200-02
Ficoll Paque Plus	GE Healthcare	Cat#17144003
X-vivo-15	Lonza	Cat#04-744Q
RPMI	Lonza	Cat#12-115Q
Stem Span SFEM	Stem Cell Technologies	Cat#09650
Polybrene (Hexadimethrine bromide)	Sigma Aldrich	Cas# 28728-55-4
RetroNectin Recombinant Human Fibronectin Fragment	Takara	Cat#T100A
Poloxamer F108 (Kolliphor P 338)	BASF	Cas# 9003-11-6
Purelink Genomic DNA Mini Kit	ThermoFisher	Cat#K182002
Critical Commercial Assays		
Murine Lineage Cell Depletion kit	Miltenyi Biotec	Cat#130-090-858
CD4 T Cell Isolation kit, mouse	Miltenyi Biotec	Cat#130-104-454
CD4 T Cell Isolation kit, human	Miltenyi Biotec	Cat#130-096-533
CD34 isolation kit, human	Miltenyi Biotec	Cat#130-046-702
Human CD3/CD28 beads	ThermoFisher	Cat#11131D
Murine CD3/CD28 beads	ThermoFisher	Cat#11456D
MILLIPLEX MAP Mouse Cytokine/Chemokine Magnetic Bead Panel	Millipore Sigma	Cat#MCYTMAG-70K-PX32
eBioscience Foxp3 / Transcription Factor Staining Buffer Set	ThermoFisher	Cat#00-5523-00
ddPCR Supermix for Probes	BioRad	Cat#186-3026
CpG methylation analysis of human FoxP3 CNS2	EpigenDx	Assay ADS783FS2
NEBuilder HiFi DNA Assembly Cloning Kit	New England Biolabs	Cat#E5520S
Deposited Data		
CNS123p-mStrawberry LV sequence	This paper	GenBank: MK012431
CNS123p-FoxP3-mStrawberry LV sequence	This paper	GenBank: MK012431
Experimental Models: Cell Lines		
K562	ATCC	CCL-243
MT-2	NIH Aids Reagent Program	Catalog#237
Jurkat	ATCC	TIB-152

(*Continued on next page*)

REAGENT or RESOURCE	SOURCE	IDENTIFIER
293T	ATCC	CRL-3216
HT-29	ATCC	HTB-38
Experimental Models: Organisms/Strains		
Mouse: CD45.2: C57/BL6	Jackson Laboratories	JAX: 000664
Mouse: CD45.1: B6.SJL	Jackson Laboratories	JAX: 002014
Mouse: FoxP3-prom-GFP: B6.Cg-Foxp3^{tm2Tch}/J	Jackson Laboratories	JAX: 006772
Mouse: Scurfy: B6.Cg-Foxp3sf/J	Jackson Laboratories	JAX: 004088
Mouse: NSG: NOD.Cg-Prkdc^{scid}Il2rg^{tm1Wjl}/SzJ	Jackson Laboratories	JAX:005557
Mouse: NSG-SGM3: NOD.Cg-Prkdc^{scid}Il2rg^{tm1Wjl} Tg(CMV-IL3,CSF2,KITLG)1Eav/MloySzJ	Jackson Laboratories	JAX:013062
Oligonucleotides		
Psi U5 Forward Primer: 5′ AAG TAG TGT GTG CCC GTC TG 3′	IDT Technologies	N/A
Psi U5 Reverse Primer: 5′ CCT CTG GTT TCC CTT TCG CT 3′	IDT Technologies	N/A
Psi Probe: 5′ FAM-CCC TCA GAC-ZEN*-CCT TTT AGT CAG TGT GGA AAA TCT CTA G-IBFQ** 3′; *ZEN = internal modification from IDT-Integrated DNA Technologies, **IBFQ = Iowa Black FQ	IDT Technologies	N/A
uc378 Forward Primer: 5′ CGC CCC CTC CTC ACC ATT AT 3′	IDT Technologies	N/A
uc378 Reverse Primer: 5′ CAT CAC AAC CAT CGC TGC CT 3′	IDT Technologies	N/A
uc378 Probe: 5′ HEX-TTA CCT TGC-ZEN*-TTG TCG GAC CAA GGC A-IBFQ** 3′; *ZEN = internal modification from IDT-Integrated DNA Technologies, **IBFQ = Iowa Black FQ	IDT Technologies	N/A
SDC4 Forward Primer: 5′ CAG GGT CTG GGA GCC AAG T 3′	IDT Technologies	N/A
SDC4 Reverse Primer: 5′ GCA CAG TGC TGG ACA TTG ACA 3′	IDT Technologies	N/A
SDC4 Probe: 5′ HEX-CCC ACC GAA-ZEN*-CCC AAG AAA CTA GAG GAG AAT-IBFQ** 3′; *ZEN = internal modification from IDT-Integrated DNA Technologies, **IBFQ = Iowa Black FQ	IDT Technologies	N/A
FoxP3 CNS2 Viral F: TGGAGTTAGATTGTTTGGGA	EpigenDx	Custom assay
FoxP3 CNS2 Viral R: CACCTATAAATCCAAATACCCCAC	EpigenDx	Custom assay
Recombinant DNA		
pMDL-gp-rre	Addgene	81071
CCL vector backbone	Addgene	12251
pRSV-rev	Addgene	12253
pMD2.G	Addgene	12259
dsDNA gBlock fragments	IDT	N/A

CONTACT FOR REAGENT AND RESOURCE SHARING

Further information and requests for resources and reagents should be directed to, and will be fulfilled by, the Lead Contact, Donald B. Kohn M.D. (dkohn1@mednet.ucla.edu)

EXPERIMENTAL MODEL AND SUBJECT DETAILS

Mice

All animals involved in experiments were cared for and handled in accordance with protocols approved by the UCLA Animal Research Committee under the Division of Laboratory Medicine.

B6 (CD45.2), B6.SJL (CD45.1), B6-FoxP3^{GFP} (CD45.2), B6-scurfy, NSG and NSG-SGM3 mice were purchased from Jackson labs and colonies were maintained at UCLA. NSG and NSG-SGM3 mice were housed in a specialized barrier facility designed for the care of immunocompromised mice, while all other mice were maintained under standard SPF conditions. At 21 days of age, mice were separated by sex and housed 4-5 mice per cage. No experimental procedures, drugs, or tests were performed on mice prior to the studies described. Experimental groups were assigned to mice randomly and distributed evenly among cages.

The following breeding strategy was used for scurfy mice. Heterozygous female scurfy mice (CD45.2, X/X^{Sf}, phenotypically normal) were mated with wild-type B6 (CD45.2) or B6.SJL (CD45.1) males to produce sub-colonies of CD45.2, CD45.1, and CD45.1/CD45.2 scurfy mice. Neonatal (d0-d1) scurfy males (X^{sf}/Y) were rescued by intraperitoneal injection of 60×10^6 WT splenocytes and re-mated to heterozygous scurfy females (X/X^{Sf}) to obtain scurfy females (X^{sf}/ X^{sf}). Rescued scurfy male (X^{sf}/Y) and scurfy female (X^{sf}/ X^{sf}) mice were mated to generate litters in which all pups were FoxP3 deficient. Prior to establishment of hemizygous male and homozygous female FoxP3^{null} breeders, FoxP3 genotyping was performed by Transnetyx using verified protocols. We observed no difference in disease progression between male and female scurfy mice, thus they were used interchangeably.

Cell lines
MT2 cells were obtained through the NIH AIDS Reagent Program. Jurkat and K562 cells were obtained from ATCC. Cells were maintained in R10 (RPMI [GIBCO]/10% FBS [GIBCO]/1x Penicillin/Streptomycin/Glutamine [PSG, Gemini Bio Products]) at 37°C.

Primary Cells
Cord blood CD34+ cells
Umbilical cord blood was obtained after vaginal and cesarean deliveries at UCLA Medical Center. All specimens obtained have been deemed as anonymous medical waste exempt from IRB review. Mononuclear cells were isolated using Ficoll-Paque PLUS (GE Healthcare) density centrifugation within 48 hours of collection followed by CD34 enrichment according to manufacturer's instruction (Miltenyi Biotec). CD34+ cells from single cords were frozen in cryovials in 90% FBS (GIBCO)/10% DMSO (Sigma Aldrich) and stored for later use.
Human CD4 cells
Peripheral blood was obtained from healthy adult donors (made available as de-identified human material through the UCLA Virology Core, IRB #11-000443). Mononuclear cells were isolated using Ficoll-Paque PLUS (GE Healthcare) density centrifugation within 48 hours of collection. Human CD4 cells were isolated by negative selection according to manufacturer's instruction (Miltenyi Biotec).
Murine Lin- cells
Bone marrow cells were obtained by crushing aseptically isolated femurs, tibias, pelvises, spines, and humeri in a mortar and pestle. Lin- cells were obtained using a lineage depletion kit (Miltenyi Biotec) according to manufacturer's instructions.

Lentiviral vectors
Construction of MNDU3-GFP (Logan et al., 2004) and UBC-mCitrine (Baldwin et al., 2015) has been described. MNDU3-FoxP3-IRES-GFP was a kind gift from Dr. Gay Crooks at UCLA. The CNS123p-mStrawberry and CNS123p-FoxP3-mStrawberry lentiviral vectors were cloned into an empty CCL backbone (Dull et al., 1998). Fragments were synthesized as gBlocks (R) (Integrated DNA Technologies) with compatible ends to be cloned using NEBuilder(R) HiFi DNA Assembly Kit (New England Biolabs) Lentiviral vectors were packaged with a VSV-G pseudotype using 293T cells, concentrated and titered on HT29 cells as described (Cooper et al., 2011).

METHOD DETAILS

Lentiviral transduction
Method 1: Cell lines
MT2, K562, and Jurkat cells were plated at 1E6 cells/mL and transduced with CNS123p-mStrawberry at a range of concentrations (1E5 TU/mL −1E8 TU/mL, MOI 0.1-100) followed by a change to fresh R10 the following day. After 10 days of culture, cells were analyzed by flow cytometry for mStrawberry expression and genomic DNA was isolated for vector copy number analysis.
Method 2: Human T cells
Human CD4 T cells were plated at 50,000 cells/well in a 96 well plate in serum free X-vivo-15 (Lonza) and 10 ng/mL hIL2 (Peprotech). Cells were activated with CD3/CD28 Dynabeads at a 1:1 bead:cell ratio. 24 hours after activation, LV was added to the well. 24 hours after the addition of LV, media was removed and changed to fresh culture media.
Method 3: Murine lin- cells
Freshly isolated lin- cells were resuspended in murine transduction media (Stem Span SFEM [Stem Cell Technologies], 1x PSG [Gemini Bio Products], 100 ng/mL mTPO, 10 ng/ml mSCF [Peprotech], 5 mg/mL polybrene [Sigma Aldrich]) at 2×10^6 lin$^-$ cells/mL, plated on retronectin (Takara) coated wells (20 ng/mL for 2 hours at RT) and incubated with LV overnight. In some transplants used to generate corrected Tregs for adoptive transfer (Figures 3 and S3D), 1 mg/mL poloxamer KP338 (BASF) was added during transduction to improve gene transfer efficiency.
Method 4: Human CD34+ cells
Upon thawing, CD34+ cells were washed twice with RPMI/20%FBS and resuspended in human transduction medium (X-vivo-15 [Lonza], 1x PSG [Gemini Bio Products], 50 ng/mL SCF, 50 ng/mL TPO, 50 ng/mL Flt3L [Peprotech]) at 1E6 cells/mL. Cells were cultured in transduction medium for 24 hours, followed by incubation with LV for another 24 hours.

Determination of vector copies (VC) per cell

Genomic DNA was extracted from samples using the PureLink genomic DNA kit (Invitrogen). The average VC/cell was measured using ddPCR. Reaction mixtures were prepared consisting of 22 μl volumes containing 1 × ddPCR Master Mix (Bio-Rad), primers, and probe specific to the HIV-1 Psi region (400 nM and 100 nM for primers and probe, respectively), DraI (40 U; New England Biolabs), and 1.1 μl of the genomic DNA sample. Droplet generation was performed using the QX100 Droplet Generator (Bio-Rad). Thermal cycling conditions consisted of 95°C 10 minutes, 94°C 30 s and 60°C 1 minute (55 cycles), 98°C 10 minutes (1 cycle), and 12°C hold. The concentration of specific amplified portions was quantified using the QX200 Droplet Reader/Quantasoft V1.7 (Bio-Rad) and normalized using primers to the autosomal human gene SDC4 gene, or uc378 gene for murine samples. Primer/probe sequences are listed in the Key Resources Table.

Murine Congenic Transplants

Transduced lin- cells were collected, washed, and resuspended in PBS. 6-10 week old B6.SJL (CD45.1) or B6 (CD45.2) recipients were irradiated with 1200 Rad (Dose rate ~100 Rad/min) using a split dose of 600 + 600 Rad with 3-4 hours between doses. Cells were injected via retro-orbital injection 1-4 hours after the last radiation dose. Transplanted cell doses ranged from 5E5-1E6 lin- cells per mouse.

Murine CD4 isolation
Method 1 (Figure 2)

Murine splenocytes were obtained by aseptic removal and gentle crushing of spleens through a 70 μM mesh filter. Splenocytes were enriched for CD4+ cells using a CD4 isolation kit (Miltenyi Biotec). Briefly, splenocytes were labeled with a cocktail of biotinylated antibodies labeling CD4- cells, followed by labeling with anti-biotin magnetic beads. CD4- cells were separated on an LS column (Miltenyi Biotec) while CD4+ cells were collected in the flow through.
Method 2: Purification of corrected scurfy CD4 (Figure 3)

In experiments utilizing adoptive transfer of CD45.2+CD4+ cells to scurfy neonates, an additional step was performed to ensure the removal of WT CD45.1 cells (from transplant recipients or from the initial rescue of scurfy HSC donors) from the purified cell product. Splenocytes were labeled with a cocktail of biotinylated antibodies labeling CD4- cells, and a biotinylated antibody to CD45.1 (Miltenyi Biotec) followed by labeling with anti-biotin magnetic beads. CD45.1+CD4- cells were separated on an LS column (Miltenyi Biotec) while CD45.2+CD4+ cells were collected in the flow through.

Treg Suppression Assay and induction of iTregs

CD4-enriched splenocytes were labeled with CD4-APC, and Ghost 780 viability dye (Tonbo Biosciences) prior to FACS sorting. Viable CD4+GFP+ (WT Tregs) or CD4+mStrawberry^{high} (Uncorrected and corrected scurfy Tregs) were sorted for evaluation of suppressive function, while CD4+GFP- and CD4+mStrawberry- cells were sorted for induction of iTregs. *Treg suppression assay:* Tresp cells (CD4+ enriched, wild-type B6 splenoctyes) were labeled with 5 μM Cell Trace violet proliferation dye (Thermo Fisher) for 20 min at 37°C, washed twice in PBS, and co-cultured with sorted Tregs at a 1:1 ratio in R10 without cytokines in a 96 well U bottom plate. Experiments ranged from 2.5E4-5E4 Tresp cells/well (depending on the number of cells collected during the FACS sort). Mouse CD3/CD28 T Activator Dynabeads (ThermoFisher) were added to cultures at a ratio of 1 bead:1 Tresp cell. Cells were cultured for 3 days followed by FACS analysis for dilution of proliferation dye. Proliferation index was calculated using FlowJo V7.6.5 (TreeStar).
iTreg induction

Sorted GFP- and mStrawberry- cells were plated in R10 with 20ng/mL hTGFβ, 20 ng/mL mIL2, and 1 μg/mL CD28 (clone 37.51). Cells were plated on 6 well culture dishes with plate-bound CD3e (clone 145-2C11, coated for 2 hours at 37°C). Cells were analyzed for mStrawberry expression 4 days post-activation.

Rescue of scurfy neonates with corrected Tregs and analysis

Scurfy rescues were performed in small cohorts when a litter of scurfy pups was born and available transplant recipients (harboring putative Tregs for transfer) were approximately 8 weeks post-transplant. For each distinct experiment number (#1-5), donor CD45.2+CD4+ cells (containing putative Tregs) were purified in bulk from pooled spleens of transplant recipients from each arm. A small aliquot of each purified cell product was analyzed by flow cytometry to determine the percentage of %GFP+ or %mStrawberry+ cells and to confirm effective CD45.1 depletion. All transferred cell products contained < 0.1% CD45.1 cells. A small aliquot of each purified cell product was also used for VCN analysis. Absolute numbers of CD4 cells and the relative Treg content of each population are listed in Figure S3. For each experiment, cells from each arm were injected into 1-3 scurfy neonates depending on the number of pups available and total cell number collected in order to achieve a target dose of ~1E6 putative Tregs/mouse.

Scurfy neonates were injected with intraperitoneally with purified CD45.2+CD4+ cells resuspended in 50 uL of PBS using a 29 gauge insulin syringe. Mice were analyzed at 21d of age. Blood was collected by submandibular puncture into serum separator tubes (RAM Scientific) and centrifuged at 500xg for 10 min to obtain plasma for cytokine analysis. Cytokines were analyzed by the UCLA

Immune Assessment Core using the Luminex platform. Mice and dissected spleens were weighted to determine spleen to body weight ratio.

Humanized xenografts

Transduced CD34+ cells were collected, washed in PBS, and incubated with OKT3 (Tonbo Biosciences, 1µg/100 µL) for 30 min on ice to prevent GVHD from contaminating T cells present in the CD34+ graft (Wunderlich et al., 2014). Immediately prior to transplant, 1-3 day old neonatal NSG mice were irradiated at a dose of 125 Rad with a ^{137}Cs source and dose rate of 100 Rads/min. Each mouse received $1\text{-}3 \times 10^5$ CD34$^+$ cells.

Human CD4 enrichment from NSG spleens

Human CD4 cells were enriched from the spleens of engrafted NSG and NSG-SGM3 mice. Mice were labeled with the direct lineage depletion beads (to deplete murine cells) and human CD4 T cell isolation kit (to deplete CD4- human cells) (Miltenyi Biotec). Cells were labeled according to manufacturers' instructions. Labeled cell types were depleted on an LS column, while unlabeled human CD4+ cells were collected in the flow-through.

Methylation Analysis/Bisulfite Sequencing

Genomic DNA was extracted from sorted Treg (CD4+CD25+) and Tconv (CD4+CD25-) subsets using the Purelink Genomic DNA mini kit (Invitrogen). CpG dinucleotide methylation analysis of CNS2 of the human FoxP3 gene was performed by EpigenDx and determined by bisulfite treatment of RNase-treated genomic DNA, followed by PCR amplification and pyrosequencing (EpigenDx assay ADS783-FS2). A custom assay was performed by EpigenDx for methylation analysis of FoxP3 CNS2 from integrated LV DNA using the following primers which uniquely recognize viral CNS2: FoxP3 CNS2 Viral F: TGGAGTTAGATTGTTTGGGA; FoxP3 CNS2 Viral R: CACCTATAAATCCAAATACCCCAC.

Flow cytometry

Single cell suspensions from BM were obtained by crushing femurs as described above. Thymus and spleen were prepared by crushing tissue through a 70 uM strainer. Samples were prepared for flow cytometry using the following method: Cells were resuspended in 50 uL of FACS buffer (phosphate buffered saline [PBS,Corning]/0.5% Bovine Serum Albumin [BSA, Sigma]) and incubated with 1 µL of each antibody and 0.5 µL of Ghost 780 or Ghost 510 viability dye (Tonbo Biosciences) for 20-30 min at 4°C. Cells were washed once in FACS buffer prior to analysis. In panels where DAPI was used as a viability dye, a 1 mg/mL stock of DAPI was added to washed cells at a 1:5000 dilution 5 minutes prior to analysis (final concentration 0.2 ug/mL).

For intracellular FoxP3 staining, cells were first stained with cell surface markers and fixable viability dye as described above. After washing, cells were fixed and permeabilized using the FoxP3 staining buffer set (eBioscience) according to manufacturers' directions. Human FoxP3-PE or human FoxP3-APC (ebioscience, clone 236A/E7) was added for 30-60 min at RT. FoxP3+ gates were set using an isotype control. Samples were acquired on a LSRII or LSR-Fortessa flow cytometer (BD Biosciences). Data were analyzed using FlowJo V10 (TreeStar).

Antibody manufacturers and clones are listed in the Key Resources Table. The following antibody/fluorophore panels were used for each experiment:

Figure 1B: *mStrawberry expression in cell lines*: DAPI, mStrawberry; *FoxP3 stain of cell lines*: Ghost 780 viability dye, FoxP3-APC; Figure 1C: *hCD4 cells*: DAPI, mStrawberry; Figures 1E and 1F: *Bone Marrow*: mStrawberry, GFP (from FoxP3-GFP-prom mice), CD45.2-V450, cKit-APC, Ghost780; *Thymus*: mStrawberry, GFP (from FoxP3-GFP-prom mice), CD45.2-V450, CD4-APC, CD8-PE-Cy7, Ghost780; *Spleen Panel 1*: mStrawberry, GFP (from FoxP3-GFP-prom mice), CD45.2-V450, Gr-1-APC, B220-PerCP, Ghost780; *Spleen Panel 2*: mStrawberry, GFP (from FoxP3-GFP-prom mice), CD45.2-V450, CD4-APC, CD3-PerCP, CD8-PE-Cy7, Ghost780; Figure 2B: *Thymus lineage distribution*: mStrawberry, GFP (from FoxP3-GFP-prom mice), CD45.2-V450, CD4-PE-Cy7, CD8-APC-Cy7, Ghost 510;

Figure 2C/Figure S2D: *Treg surface markers*: mStrawberry, GFP (from FoxP3-GFP-prom mice), CD45.2-V450, CD4-PE-Cy7, CD8-APC-Cy7, Ghost 510, Treg surface marker (CD25-APC, GITR-APC, or CTLA4-APC, 1 tube for each marker); Figure 2D: *FACS sort for Treg suppression assay and iTreg induction*: mStrawberry (from LV), GFP (from FoxP3-GFP-prom mice), CD4-APC, Ghost 780; Figure 2E: *Treg suppression assay*: CellTrace violet, CD4-APC, Ghost 780; Figure 2F: *iTreg induction*: mStrawberry, GFP (from FoxP3-GFP-prom mice), Ghost 780; Figure 3D: *Activated T cells in rescued scurfy spleens*: CD4-APC, CD44-PerCPCy5.5, CD62L-PE-Cy7, Ghost780/or DAPI; Figures 4B and 4C: *Bone marrow*: mStrawberry, hCD45-APC, CD33-BV421, CD19-PECy7, CD34-FITC, CD3-PerCPCy5.5, Ghost 780; *Spleen*: mStrawberry, hCD45 PE-Cy7, CD3-PerCPCy5.5, CD4-FITC, CD8-APC, CD25-V450, Ghost 780; *Thymus*: mStrawberry, hCD45 PE-Cy7, CD4-FITC, CD8-APC, CD25-V450, Ghost 780; Figure 4D: *FACS sort of CD4 enriched splenocytes*: mStrawberry, hCD4-FITC; *FoxP3 stain*: hCD4-FITC, FoxP3-APC; Figure 4E: *Treg sort for methylation analysis*: hCD4-APC, hCD45-FITC, CD25-PerCPCy5.5, Ghost 780; Figure 4F: *Competitive transplant assay*: hCD45-APC, mCitrine, Ghost780; Figure S1A: DAPI, GFP; Figure S1B: mCD45-APC, mCD45.1-V450, GFP; Figure S1E: GFP, CD34-APC, Ghost 780; Figure S1F: GFP, mCD45-PE, hCD45-V450; Figure S3C: GFP, mStrawberry, CD4-PECy7, CD45.1-APC, CD45.2-V450, Ghost 780; Figure S3F: mStrawberry, CD4-PECy7, CD45.2-V450, Ghost-780; Figure S3G: *mStrawberry analysis*: CD4-APC, DAPI, mStrawberry; *FoxP3 stain*: mCD4-APC, hFoxP3-PE, Ghost-780;

QUANTIFICATION AND STATISTICAL ANALYSIS

Values are represented as means ± SD, unless stated otherwise. GraphPad Prism 6.0 was utilized for all statistical analyses. Statistical details of each experiment can be found in the Figure Legends, including the mean and error bars, numbers of replicates, statistical tests, and p values from comparative analyses that were performed. P value was calculated with a confidence interval of 95% to indicate the statistical significance between groups. A P value < 0.05 was considered statistically significant. Statistically significant differences between groups are noted in figures with asterisks ($*p < 0.05$, $**p < 0.01$, $***p < 0.001$).
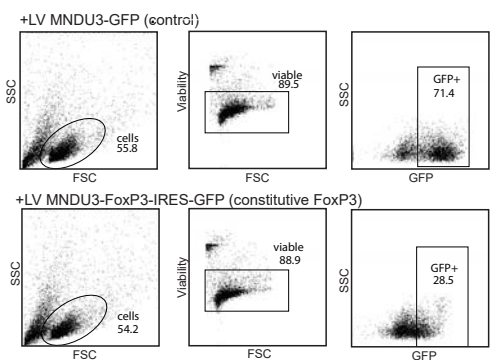
DATA AND SOFTWARE AVAILABILITY

The accession number for the FoxP3 LV sequence reported in this paper is GenBank: MK012431.
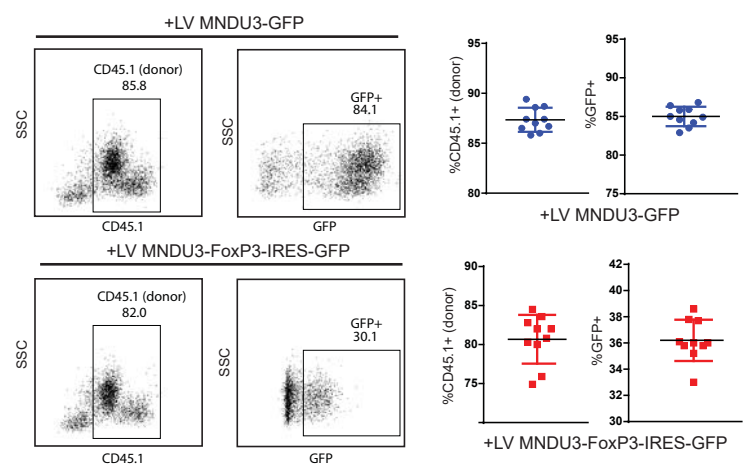
Supplemental Information

Lentiviral Gene Therapy in HSCs Restores

Lineage-Specific Foxp3 Expression and Suppresses

Autoimmunity in a Mouse Model of IPEX Syndrome

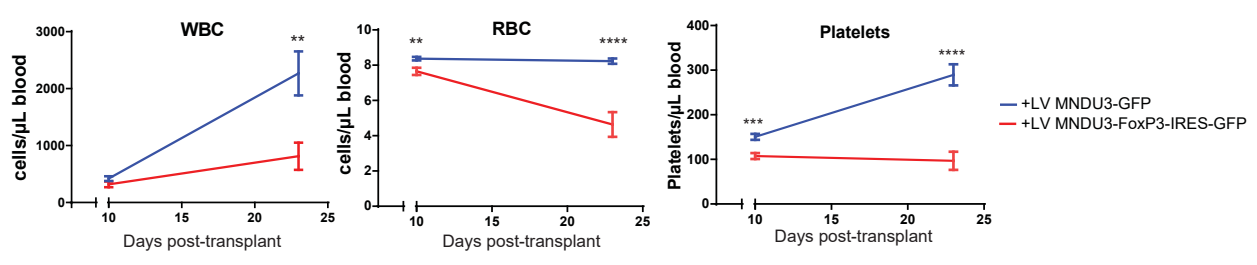Katelyn E. Masiuk, Jennifer Laborada, Maria Grazia Roncarolo, Roger P. Hollis, and Donald B. Kohn

A.

+LV MNDU3-GFP (control)

+LV MNDU3-FoxP3-IRES-GFP (constitutive FoxP3)

B.

+LV MNDU3-GFP

+LV MNDU3-FoxP3-IRES-GFP

C.

WBC

RBC

Platelets

— +LV MNDU3-GFP
— +LV MNDU3-FoxP3-IRES-GFP

D.

LV MND-GFP

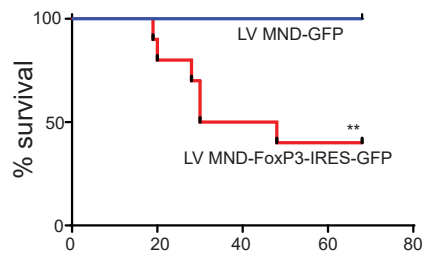LV MND-FoxP3-IRES-GFP
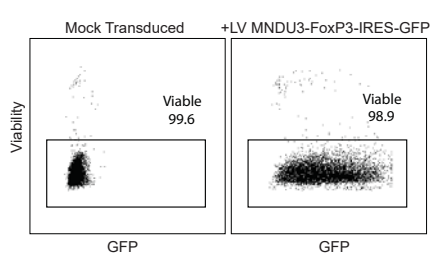
E.

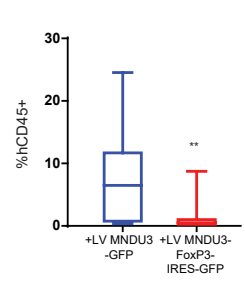Mock Transduced   +LV MNDU3-FoxP3-IRES-GFP

F.

Figure S1 (Corresponding to Figure 1) Ectopic FoxP3 expression from a constitutively active promotor is not acutely toxic to HSPC, but impairs proliferation/differentiation of engrafted HSPC

A. Murine lin- cells transduced with MNDU3-FoxP3-IRES-GFP show successful LV transduction and expression with no discernable effects on viability compared to control LV (MNDU3-GFP). Viability and GFP expression are shown at 3 days post transduction.

B. Lin- cells modified with MNDU3-FoxP3-IRES-GFP LV are capable of early engraftment and are readily detected in peripheral blood of transplant recipients at 7 days. FACS plots show donor (CD45.1) engraftment and GFP expression in donor cells. (n=10 mice/group)

C. The early post-transplant period (10-21 days) is marked by a rapid decline of red blood cell counts, and failure to reconstitute white blood cell and platelet counts in mice receiving lin- cells modified with LV MNDU3-FoxP3-IRES-GFP. Plots show white blood cell (WBC), red blood cell (RBC) and platelet counts in transplanted mice. (n = 10 mice per group)

D. Survival of mice in each group after transplant. N=10 mice per group

E. Human HSPC (CB CD34+ cells) transduced with MNDU3-FoxP3-IRES-GFP show successful LV transduction and expression with no discernable effects on viability compared to control LV (MNDU3-GFP). Viability and GFP expression are shown at 3 days post transduction.

F. NSG engraftment of hCD45+ cells in the peripheral blood is significantly impaired in mice receiving HSPC transduced with MNDU3-FoxP3-IRES-GFP compared to control LV. Peripheral blood engraftment of hCD45+ cells is expressed as a percentage of total hCD45+ + mCD45+ and was measured at 6-8 weeks post-transplant. Data represent mice humanized with CB CD34+ cells from 12 independent donors, n= 16-17 mice per group.

Data represent mean ± SD for (B), mean ± SEM for (C), and median ± IQR and range for (F). Data in (C) and (F) are analyzed using Student's t-test. Data in (D) are analyzed using log-rank (Mantel-Cox) test. *$p < 0.05$, **$p < 0.01$, ***$p < 0.001$.
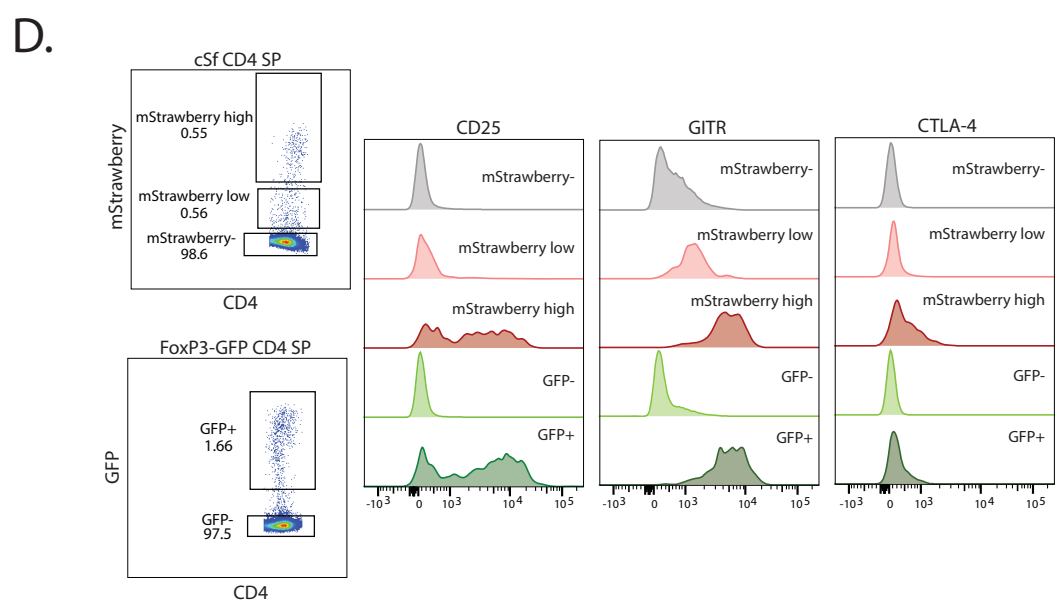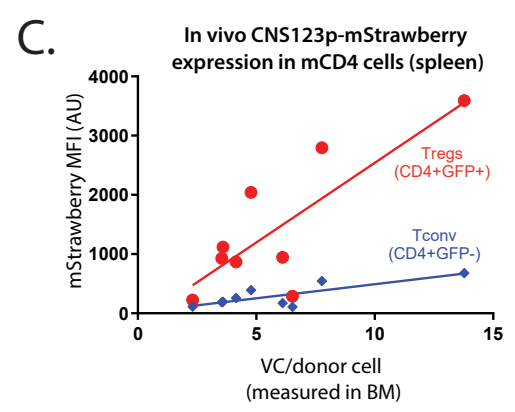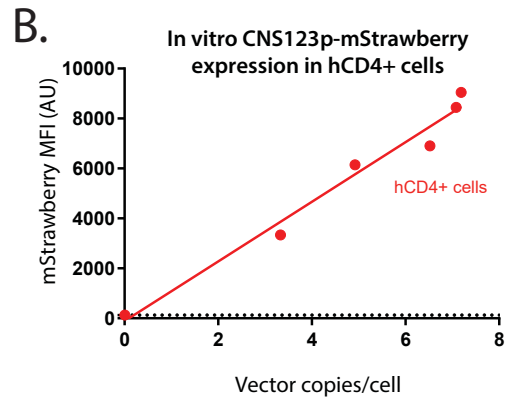
A. Gating for Spleen: Gating for BM: Gating for Thymus:

B. In vitro CNS123p-mStrawberry expression in hCD4+ cells

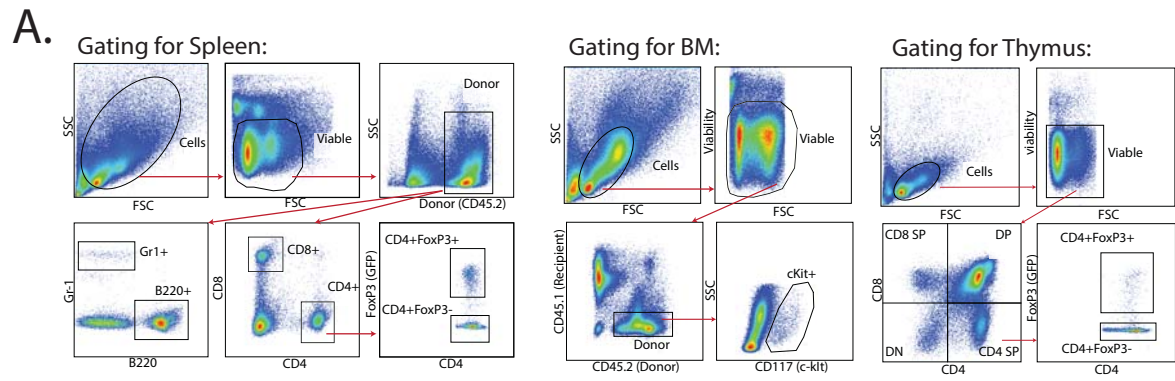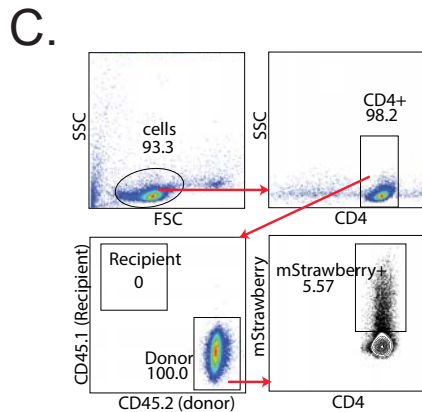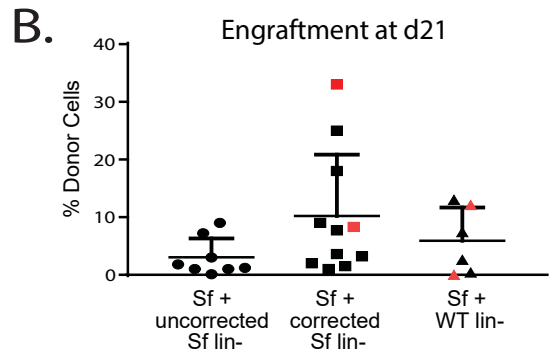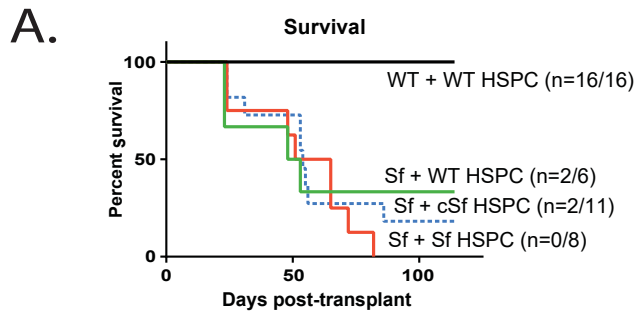C. In vivo CNS123p-mStrawberry expression in mCD4 cells (spleen)

D.

Figure S2 (Corresponding to Figure 1 and Figure 2): mStrawberry expression from the reporter LV (CNS123p-mStrawberry) shows heterogeneous expression which correlates with copy number

A. FACS gating is shown for each defined lineage analyzed for mStrawberry reporter LV expression (Figure 1E,F) Gating defines analyzed lineages in spleen (Gr1+, B220+, CD8+, CD4+FoxP3-, CD4+FoxP3+), Bone marrow (cKit+), and Thymus (DN, DP, CD8 SP, CD4+FoxP3-, CD4+FoxP3+)

B. Activated human CD4 cells were transduced with the FoxP3 reporter LV (CNS123pmStrawberry) and cultured for 11 days. A positive linear relationship is observed between LV expression (mStrawberry MFI, measured at d4) and vector copy number (measured at d11).

C. FoxP3-prom-GFP lin- cells were transduced with the FoxP3 reporter LV (CNS123pmStrawberry) and transplanted into WT recipients (Figure 1E,F). Data show a positive relationship between LV expression (mStrawberry MFI) and vector copy number per donor cell. A wide range of copy number/donor cells is seen amongst mice transplanted with the same bulk population of transduced cells, highlighting the wide range of LV transduction events amongst individual long term engrafting HSC (LT-HSC) within the bulk population of lin- cells. As only a small number of these LT-HSC engraft and repopulate the recipient mouse, a wide range of copy numbers/donor cells can be seen in recipient mice. Heterogeneity in expression per vector copy number is also apparent, and may be due to the different integration profiles of transduced HSC and subsequent changes in the epigenetic landscape as hematopoietic cells differentiate. Importantly, at each measured VCN, mStrawberry expression is brightest in the Treg lineage compared to all other lineages.

D. Corrected scurfy Treg surface markers levels in the thymus analyzed by level of mStrawberry (FoxP3) expression (Figure 2). CD25, GITR, and CTLA4 levels are highest in the "mStrawberryhigh" population, while the "mStrawberry-low" population does not express these markers. Treg surface marker expression levels are compared to GFP+ (FoxP3+ Tregs) and GFP- (FoxP3- Tconv) thymocytes from FoxP3-prom-GFP reporter cells.

A. Survival

Percent survival vs Days post-transplant

- WT + WT HSPC (n=16/16)
- Sf + WT HSPC (n=2/6)
- Sf + cSf HSPC (n=2/11)
- Sf + Sf HSPC (n=0/8)

B. Engraftment at d21

% Donor Cells

- Sf + uncorrected Sf lin-
- Sf + corrected Sf lin-
- Sf + WT lin-

C.

cells 93.3 (FSC vs SSC); CD4+ 98.2 (CD4 vs SSC); Recipient 0 / Donor 100.0 (CD45.2 donor vs CD45.1 Recipient); mStrawberry+ 5.57 (CD4 vs mStrawberry)

D.

Failed scurfy rescues (VCN<2, no poloxamer, low gene transfer)

Experiment Number	Litter	Mouse	Sex	Arm	CD4 cell dose	CD4 VCN	% mStrawberry+ of total CD4	Putative Treg Dose	% activated T cells (at 21d)
1		F1	M	Sf + cSf-CD4	2.60×10^7	1.4	2.69%	7×10^5	67%
1		F2	M	Sf + cSf-CD4	2.60×10^7	1.4	2.69%	7×10^5	85%
1		C1	M	Sf + Sf-CD4	-	-	-	-	90%
2		F2	M	Sf + cSf-CD4	40×10^7	1.78	2.76%	1.1×10^6	57%
2		C2	M	Sf + Sf-CD4	-	-	-	-	71%

Mice analyzed in Figure 3 (with poloxamer to improve gene transfer)

Experiment Number	Litter	Mouse	Sex	Arm	CD4 cell dose	CD4 VCN	% mStrawberry+ or %GFP+ of total CD4	Putative Treg Dose	% activated T cells (at 21d)
3		1	M	WT + PBS	-	-	-	-	10%
3		2	M	Sf + PBS	-	-	-	-	53%
3		3	M	Sf + Sf-CD4	8.0×10^6	7.47	10.80%	8.6×10^5	65%
3		4	M	Sf + cSf-CD4	1.8×10^7	3.25	5.45%	9.8×10^5	23%
3		5	M	Sf + WT-CD4	7.0×10^6	3.31	11.20%	7.8×10^5	12%
3		6	M	WT + PBS	-	-	-	-	8%
4		7	F	Sf + Sf-CD4	1.3×10^7	7.05	16.10%	2.1×10^6	75%
4		8	M	Sf + Sf-CD4	1.3×10^7	7.05	16.10%	2.1×10^6	72%
4		9	M	Sf + WT-CD4	1.3×10^7	5.56	10.10%	1.3×10^6	33%
4		10	F	Sf + WT-CD4	1.3×10^7	5.56	10.10%	1.3×10^6	15%
4		11	F	Sf + WT-CD4	1.3×10^7	5.56	10.10%	1.3×10^6	23%
4		12	F	Sf + Sf-CD4	1.3×10^7	7.05	16.10%	2.1×10^6	77%
4		13	F	Sf + PBS	-	-	-	-	75%
4		14	F	Sf + Sf-CD4	1.3×10^7	7.05	16.10%	2.1×10^6	72%
4		15	M	Sf + PBS	-	-	-	-	68%
4		16	M	Sf + PBS	-	-	-	-	75%
4		17	M	WT + PBS	-	-	-	-	13%
4		18	M	WT + PBS	-	-	-	-	8%
5		19	F	Sf + cSf-CD4	2.5×10^7	5.8	5.6%	1.4×10^6	29%
5		20	M	Sf + cSf-CD4	2.5×10^7	5.8	5.6%	1.4×10^6	20%
5		21	M	Sf + PBS	-	-	-	-	85%
5		22	F	Sf + PBS	-	-	-	-	76%

E.

% Activated T cells (CD44+CD62L-)

- Sf+ PBS / Sf+ cSf CD4 — No poloxamer cSf CD4 VCN<2
- Sf+ PBS / Sf+ cSf CD4 — +poloxamer cSf CD4 VCN>3

F.

%mStrawberry+ cells (within donor CD4+ gate) vs VCN/donor cell

estimated threshold for in vivo efficacy

G.

Sf mouse + Sf Tregs (mStrawberry only): mStrawberry+ 5.6%; FoxP3+ 0.3%

Sf mouse + cSf Tregs (FoxP3 cDNA + mStrawberry): mStrawberry+ 19.9%; FoxP3+ 13.6%
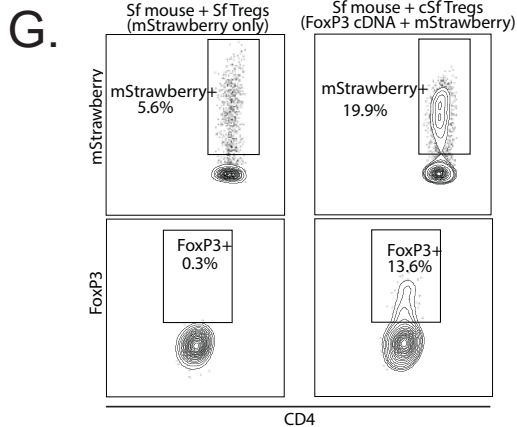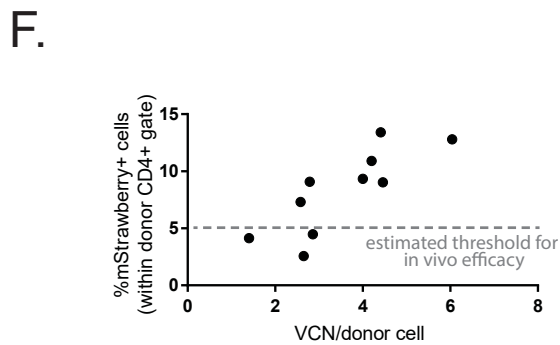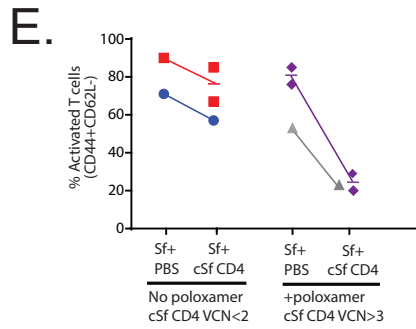
Figure S3: (corresponding to Figure 3): Assay for in vivo Treg function by HSPC transplantation and adoptive CD4 transfer to scurfy neonates

A. Survival curve in Scurfy (sf) or wild-type (WT) mice receiving HSPC transplant. Sf or WT neonates (d0-d1) were irradiated with 500 Rad followed by intrahepatic injection of LV-modified HSPC (lin- cells). Each pup received the total lin- cell dose purified from the femurs and tibia of 1 donor mouse (range 1E6 - 6E6 lin- cell/mouse). Scurfy lin- cells were transduced with the CNS123p-mStrawberry reporter LV (uncorrected scurfy HSPC "Sf HSPC") or the CNS123p-FoxP3-mStrawberry LV (corrected scurfy HSPC, "cSf HSPC"). WT lin- cells were transduced with the CNS123p-mStrawberry reporter LV (WT HSPC). Results represent pooled data from 9 transplanted litters (containing Sf and WT littermates) with 6-16 total mice per treatment group. Non surviving mice are mice that spontaneously died or were euthanized due to a moribund state as determined by a veterinarian blinded to the treatment groups. Differences between groups are n.s.

B. 21 day peripheral blood engraftment in Sf recipients of HSPC transplant. Percentages represent CD45.2+ donor cells as a percentage of total CD45+ (CD45.2 [donor] and F1 CD45.1/2 [recipient]) cells. Symbols marked in red represent engraftment in mice that survived to the end of the study (114 days).

C. Representative FACS analysis of magnetic bead purified donor (CD45.2+) CD4+ cells prior to adoptive transfer. Plots show enrichment of donor (CD45.2+) CD4+ cells with absence of contaminating CD45.1+ cells from transplant recipients or splenoctyes used for the initial rescue of scurfy HSPC donors.
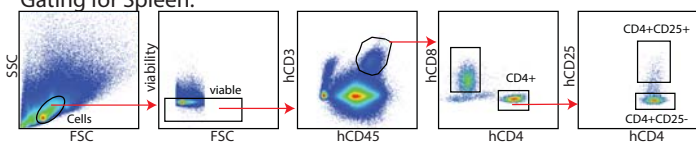
D. Characteristics of magnetically purified CD4 cell products used in adoptive transfer studies. For each distinct experiment number (#1-5), donor CD4 cells from each arm were magnetically purified from pooled spleens of transplant recipients, and single measurements of VCN and %GFP+/%mStrawberry+ (as a percentage of total CD4+ cells) were made for each cell product. The magnetically purified cells from each arm were injected into 1-3 scurfy neonates depending on the number of pups available and total cell number collected in order to achieve a target dose of ~1E6 putative Tregs/mouse. Distinct colors are used to show mice from the same litter. "Arm" defines genotype of injected neonate (Scurfy [Sf] or Wild-type [WT]) and the cell product injected (PBS = sham PBS injection, Sf-CD4 = uncorrected Scurfy CD4, cSf-CD4 = corrected scurfy CD4, WT-CD4 = Wild-type CD4).

E. Comparison of scurfy rescue efficacy before and after the addition of poloxamer F108 to the transduction protocol. Plot show activated T cells (measured as the percentage of CD4+CD44 +CD62L- cells in total CD4+ splenocytes) in untreated Sf controls and Sf mice injected with cSf Tregs under each transduction protocol (with and without poloxamer). Each distinct color/symbol represents control and treated mice from the same litter and experiment.
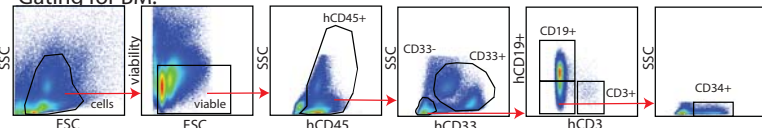
F. The relationship between VCN and mStrawberry is shown for a cohort of 10 mice transplanted with scurfy HSPC + LV CNS123p-FoxP3-mStrawberry (transduced with poloxamer F108). Cohort shows a wide range of variability in VCN with a trend towards higher mStrawberry expression with increasing VCN. Dashed line show estimated threshold for in vivo efficacy
(%mStrawberry >5%, based on adoptive transfer studies).

G. Comparison of mStrawberry expression and human FoxP3 protein expression. Left panel shows a scurfy mouse which received Sf-CD4 (mstrawberry only, no hFoxP3); right panel shows a scurfy mouse which received cSf-CD4 (mStrawberry + hFoxP3). FACS plots show the corresponding mStrawberry and hFoxP3 staining in CD4+ splenocytes.
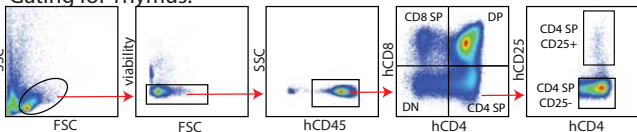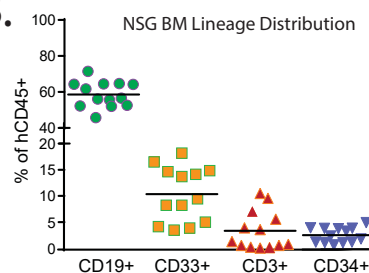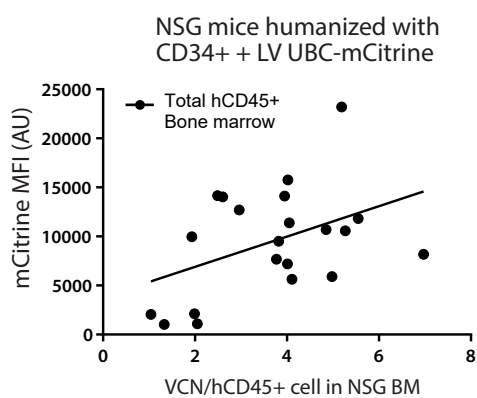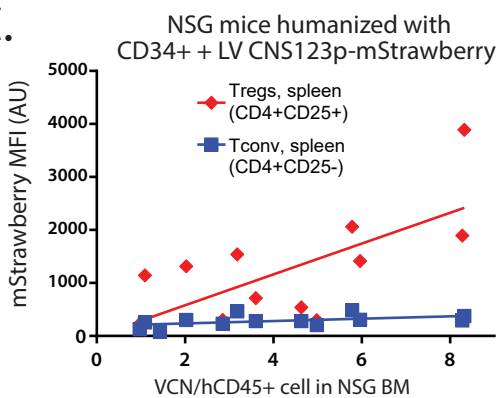
A. Gating for Spleen; Gating for BM; Gating for Thymus

B. NSG BM Lineage Distribution

C.
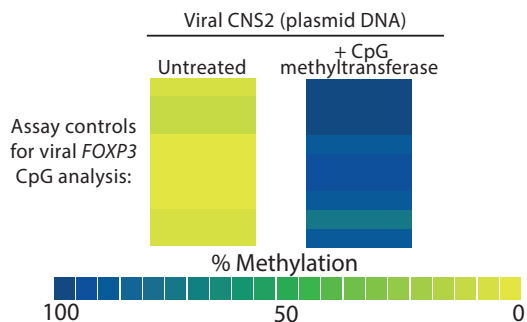NSG mice humanized with CD34+ + LV CNS123p-mStrawberry
- Tregs, spleen (CD4+CD25+)
- Tconv, spleen (CD4+CD25-)

NSG mice humanized with CD34+ + LV UBC-mCitrine
- Total hCD45+ Bone marrow

D.

NSG experiment #1
Female (XX) cord blood CD34+

CPG site	#42	#41	#40	#39	#38	#37	#36	#35	#34
Endogenous CNS2 (absolute methylation)									
Treg	94.1	64.6	65.8	54.1	64.0	60.1	56.2	55.0	53.5
Tconv	100.0	100.0	100.0	86.9	97.3	95.7	83.7	77.5	82.5
Endogenous CNS2 (Normalized for 2X chromosomes (x-50)/50)									
Treg	88.3	29.2	31.7	8.1	28.1	20.2	12.4	9.9	7.0
Tconv	100.0	100.0	100.0	73.9	94.6	91.4	67.4	54.9	65.1
Viral CNS2 (absolute methylation)									
Treg	10.5	3.1	3.8	0.0	3.5	0.0	0.0	0.0	0.0
Tconv	15.1	4.6	6.8	3.7	5.9	5.2	0.0	3.3	0.0

NSG experiment #2
Female (XX) cord blood CD34+

CPG site	#42	#41	#40	#39	#38	#37	#36	#35	#34
Endogenous CNS2 (absolute methylation)									
Treg	100.0	95.8	85.4	73.6	88.0	88.5	74.3	62.8	79.4
Tconv	100.0	98.9	99.2	84.1	95.1	91.1	78.9	75.0	86.1
Endogenous CNS2 (Normalized for 2X chromosomes (x-50)/50)									
Treg	100.0	91.6	70.9	47.1	76.0	77.0	48.6	25.7	58.8
Tconv	100.0	97.7	98.3	68.1	90.1	82.3	57.8	50.1	72.2
Viral CNS2 (absolute methylation)									
Treg	11.9	3.1	5.7	0.0	3.5	0.0	0.0	0.0	0.0
Tconv	12.3	2.8	5.4	0.0	3.7	3.3	0.0	0.0	0.0

E. Viral CNS2 (plasmid DNA)
Assay controls for viral FOXP3 CpG analysis: Untreated; + CpG methyltransferase
% Methylation — 100 ... 50 ... 0

F. Jurkat cells (Tconv-like, FoxP3-): Endogenous, Viral; MT-2 cells (Treg-like, FoxP3+): Endogenous, Viral
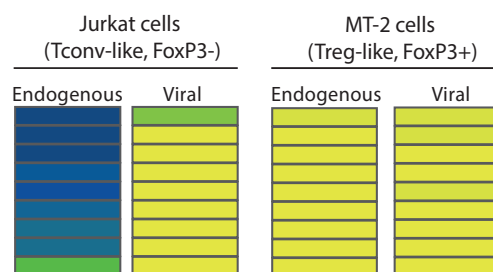
Figure S4 (corresponding to Figure 4): Analysis of reporter LV (CNS123p-mStrawberry) expression in NSG xenografts

A. Gating for lineages in humanized mice is shown for each defined population in the spleen (CD8+, CD4+CD25-, CD4+CD25+), bone marrow (CD33+, CD19+, CD3+, CD34 +), and thymus (DN, DP, CD8 SP, CD4+CD25-, CD4+CD25+) (Figure 4B,C)

B. Lineage distribution of engrafted human cells in NSG bone marrow (Figure 4 B,C). Percentages represent the relative contribution of each lineage as a percentage of total hCD45+ cells. Lineage distribution in this model is typical for humanized xenografts, with no mice showing abnormally high T cell percentages (xenogeneic graft vs host disease). n=13 mice pooled from 2 independent experiments.

C. Relationship between copy number and LV expression in NSG xenografts in vivo. Left plot shows positive relationship between in vivo mStrawberry expression (in splenic Tregs and
Tconv) and vector copy number per hCD45+ cell (measured in the bone marrow). mStrawberry expression is brightest in the Treg lineage at each measured copy number. Right plot shows data from Masiuk et al. 2017 in which NSG mice were humanized with bone marrow CD34+ cells transduced with a simple UBC-mCitrine LV. UBC-mCitrine data is shown to illustrate typical variability of LV expression in xenograft models.

D. Percentage of methylated reads at 9 CpG sites within FoxP3 CNS2 are shown for Treg and Tconv cells sorted from NSG mice humanized with CD34+ cells modified with LV CNS123p- FoxP3-mStrawberry (Figure 4E). Values are shown for 2 independent experiments using female cord blood CD34+ cells. Top row shows the absolute number of methylated reads for endogenous CNS2. Middle row shows normalized reads for endogenous CNS2 which accounts for a baseline 50% methylation of 2X chromosomes. Bottom row shows percentage of methylated reads in viral CNS2.

E. Assay controls for FoxP3 CNS2 methylation analysis (Figure 4E). Plasmid DNA encoding the CNS123p-FoxP3-mStrawberry LV genome was treated with CpG methyltransferase as a positive control while untreated LV plasmid was used as a negative control. Samples were analyzed for CpG methylation using pyrosequencing primers for the viral CNS2 site. Controls demonstrate the capacity of the pyrosequencing methylation assay to detect a full range of methylation at each CpG site with viral CNS2 primers.

F. Methylation analysis of endogenous and viral FoxP3 CNS2 in Jurkat and MT2 cells transduced with CNS123p-FoxP3-mStrawberry.